Effects of non-thermal food processing technologies on physicochemical properties of quinoa protein isolate dispersions

A thesis submitted in partial fulfilment of the requirement for the degree of Master of Food Technology

At Massey University, Auckland, New Zealand.

Lan Luo

2022

Abstract

The effects of high-pressure homogenisation (HPH) (0-50 MPa for 1 pass), sonication (14.4 W, 10 mL for 0-15 min), high hydrostatic pressure (HHP) (0-600 MPa for 15 min) and heat treatment (81 ± 2 °C for 30 min) on structural and physicochemical properties changes of quinoa protein isolate (QPI) dispersions were investigated in this thesis.

Firstly, the impacts of HPH on the physicochemical, microstructural, and rheological properties of QPI suspensions were studied. Individual protein bands were kept unchanged with HPH treatment up to 50 MPa, as revealed by sodium dodecyl sulfate-polyacrylamide gel electrophoresis (SDS-PAGE). After HPH treatment at 50 MPa, large protein aggregates were disrupted, and particle size was substantially reduced from ~8.2–0.5 μm. Concurrently, water solubility, emulsifying, and foaming capability were significantly enhanced. QPI molecules after HPH treatment became more flexible with increased surface hydrophobicity and adsorbed at the air-water and oil-water interfaces faster, resulting in a more rapid decrease of surface tension and interfacial tension. The secondary structure of QPI proteins was not significantly altered after HPH treatment as probed by Fourier transform infrared spectroscopy (FTIR). All QPI suspensions formed weak gels after thermal treatment (85 °C, 30 min), and HPH-treated QPI suspensions resulted in a stronger gel strength with a more compact and homogeneous protein network microstructure.

Secondly, 1% w/w QPI was exposed to sonication or HHP treatments at pH 5, pH 7, and pH 9. As revealed by SDS-PAGE, substantial amounts of 11S globulin participated in the formation of aggregates via the disulfide (S-S) bond under HHP, particularly at pH 7 and pH 9. Free sulfhydryl (SH) groups and surface hydrophobicity were increased after the sonication treatment, while an opposite trend was observed in HHP-treated samples. Finally, the

sonication treatment induced a significant improvement in the solubility and a reduction in particle sizes particularly at pH 7 and pH 9.

Lastly, the gelation of 10 w/w % QPI dispersions induced by HHP at three pHs (5, 7, and 9) was investigated. HHP was conducted at 20 °C for 15 min at 100, 250, 400, and 600 MPa. Thermally induced gelation (81 ± 2 °C, 30 min) was also conducted as a comparison to HHP. Both thermal and HHP (above 250 MPa) treatments can induce protein gelation, and the viscosity and elasticity of the gels increased with the increase in pressure levels. The gels formed either by heat or HHP treatment at pH 5 exhibited a stronger gel strength and a compact network structure than at pH 7 and 9. Confocal microscopy showed that HHP treatment formed a heterogenous and well-spanned network with large protein aggregates, while heat treatment resulted in a more homogeneous structure. SDS–PAGE revealed that QPI gels were formed by the denaturation and aggregation of 11S globulin.

These results showed that HPH and sonication had similar changes to the physicochemical, techno- functional, and microstructural properties of QPI suspensions, while HHP mainly induced protein gelation. Impacts of treatments are pH and concentration dependent. Based on the findings of this thesis, tailored properties of QPI could be achieved by selecting appropriate processing technologies.

Acknowledgements

There have been many people who have offered me help and support throughout my Master study. First, I would like to express my sincere gratitude to my supervisor, Dr Zhi Yang. He has provided me with the opportunity of studying this interesting topic, the advice and guidance throughout this study.

Many thanks to Professor Yacine Hemar (Shenzhen University, China) and Dr Lirong Cheng (Riddet Institute, Massey University) who provided me valuable advice and shared their experience on practical work.

I am sincerely grateful to many researchers and technicians for their assistance on laboratory use and equipment trainings, including Professor Marie Wong, Professor John Harrison, Dr Jon Palmer, Dr Noorzahan Begum, Negah Nikanjam, Arthur Xu, Rachel Liu, Jade Pope, Dr Yanyu He and PC Tong. I would like to express my gratitude to Ruth Brook for her kindly assistance.

I want to express my gratefulness to my family and my cat Milktea for their accompaniment and endless love. Many thanks to all my friends (Vina Zhang, Niki Wang, Sinong Wu, Charles Liang, Crystal Jiang, Skye Song, Summer Dawn Skelton, Jia Sun, Clarence Hu, Julia Yang and Alan Yu) who supported me throughout this hard time.

Table of Contents

List of tables

List of figures

List of abbreviations

ANS	8-Anilinonaphthalene-1-sulfonic acid
AE	Alkaline extraction followed by isoelectric precipitation
ANOVA	Analysis of variance
CD	Circular dichroism
*G**	Complex modulus
CLSM	Confocal laser scanning microscopy
GDL	D-(+)-Gluconic acid δ-lactone
DH	Degree of hydrolysis
S-S	Disulfide
DLS	Dynamic light scattering
DTNB	Ellman's reagent
EAI	Emulsifying activity index
ESI	Emulsifying stability index
FC	Foaming capacity
FS	Foaming stability
FTIR	Fourier transform infrared spectroscopy
GAE	Gallic acid equivalence
HHP	High hydrostatic pressure
HIUS	High intensity ultrasonication
HPH	High pressure homogenisation
pI	Isoelectric point
LSD	Least significance difference
LVR	Linear viscoelastic region
LC-MS	Liquid chromatography-Mass spectroscopy

G″	Loss modulus
N/A	Not applicable
OBC	Oil binding capacity
QE	Quercetin equivalence
QPI	Quinoa protein isolate
Q9, Q10, Q11	Quinoa protein isolates extracted at pH 9, 10 or 11.
SED	Salt extraction followed by dialysis
SEU	Salt extraction followed by ultrafiltration
SDS-PAGE	Sodium dodecyl sulfate-polyacrylamide gel electrophoresis
SPI	Soy protein isolate
SD	Standard deviation
G′	Storage modulus
SH	Sulfhydryl/Thiol
TGase	Transglutaminase
WHC	Water holding capacity
WPC	Whey protein concentrate
WPI	Whey protein isolate

1. Chapter 1: Introduction

1.1. Overview of the research

Protein is a fundamental part of people's daily diet and can help our body build muscle, skin, and organs (Schoenfeld & Aragon, 2018). Animal proteins such as dairy proteins (Xiong et al., 2020) and egg white protein (Chen et al., 2019) are critical in food formulations not only for their nutrients but also because of their excellent techno-functional properties that involve holding the three-dimensional structure of the food products. These techno-functional properties including gelation, foaming, and emulsifying properties, are generally better than those of plant proteins (Kornet et al., 2021; Sagis & Yang, 2022). However, plant-derived proteins have been increasingly studied and further gained more markets in recent years (Hopwood et al., 2020). The reason for consuming plant protein varies with personal preferences, cost, environmental concerns and ease of access. For example, compared to meat products, many plants require less time to mature with a lower cost. This makes plant proteins easier to access (Aschemann-Witzel et al., 2021).

However, most plant proteins such as amaranth and lentil proteins cannot provide all the essential amino acids required by a balanced diet (Day et al., 2022; Písaříková et al., 2005). For example, lentil and cornmeal proteins lack tryptophan, while most plants lack threonine (Day et al., 2022). It is particularly important to develop plant protein-based foods with a novel and versatile plant protein ingredient that can provide all the essential amino acids so that the consumers can enjoy their well-balanced nutritious diets. Quinoa (Chenopodium quinoa), with proteins consisting of all the nine essential amino acids, is a suitable food ingredient which can also provide nutrients such as unsaturated fatty acids and dietary fibre (Abugoch et al., 2008). These comprehensive nutrients make quinoa a superfood. As a food ingredient, quinoa protein

imparts many functionalities such as gelation when used in food formulations. In a previous study, it was found that the gelation properties of QPI could provide the suspension with a yoghurt-like texture after fermentation with a yoghurt starter at 42 °C for 12 h (Huang et al., 2022).

Physicochemical and techno-functional properties such as solubility, particle size, gelation, foaming, etc are critical properties for proteins used in food formulations, while most native plant proteins such as quinoa protein (López-Castejón et al., 2020), soy protein (Manassero et al., 2015; Tan et al., 2021) and pea protein (Chao et al., 2018) are inferior in these aspects. This would become a serious problem when applying QPI to food systems, so extensive studies have been conducted on modifications of QPI. However, most of them were focusing on chemical/biochemical modifications such as pH-shifting (Jiang et al., 2017) and enzymatic hydrolysis (Daliri et al., 2021; Galante et al., 2020). Many of these modifications are expensive, time-consuming, or not environmentally friendly which prevents them from wide applications in the food industry. On the other hand, physical modifications especially non-thermal processing technologies such as HPH, HIUS and HHP are environmentally friendly because no chemicals are needed. However, there are limited research on physical modifications of QPI. Therefore, this thesis will be focusing on effects of non-thermal processing technologies on physicochemical, techno-functional, and structural changes of QPI dispersions.

HPH is a physical processing method which is usually used in size reduction of particles in dispersions and preparation of emulsions. It was firstly used in milk processing, where the size of fat globules became homogeneous after homogenisation (Thiebaud et al., 2003). Nowadays, HPH has been widely used on different food systems such as plant protein suspensions and emulsions for size reduction, consistency improvement and functionality modifications (Cheng

et al., 2022; Guo et al., 2021; Yang et al., 2018). The operating principle of a high-pressure homogeniser is to pass the material with a large particle size through a small orifice with high pressure of up to 200 MPa (Dumont et al., 2018). When the protein dispersion passes through the orifice, the corresponding shear force will be generated to make the particles smaller and enable them to pass through the orifice. As mentioned before, the solubilities of plant proteins are relatively lower than animal proteins, therefore there have been many studies on the impact of HPH on the solubilities of plant proteins. However, there is no study on the effect of HPH on QPI, but a positive hypothesis may be made based on the HPH effects on other plant proteins such as amaranth protein isolate (Constantino & Garcia-Rojas, 2020).

HHP processing is a type of cold pasteurisation technique which is widely used in beverage processing. The advantage of HHP is to eliminate the bacteria in the food systems without causing nutrition loss or flavour change. HHP uses water or other fluids as the medium to apply pressure up to 600-1000 MPa and usually hold for a maximum 15-30 min. Bacteria will be killed during this process. Because of this characteristic, consumers prefer HHP fruit juice to heat-treated counterparts for more nutrients per serving. In addition, HHP has been also used to create protein gels and induce starch gelatinisation at room temperature. Heat treatments on QPI suspensions will also be investigated to compare with HHP treated QPI.

HIUS is another non-thermal processing technique that can alter the techno-functional properties of food ingredients. It produces high shear and creates cavitation when treating the ingredients. Typical effects of HIUS on QPI are reduction of particle sizes, enhancement of solubilities, increase of free SH groups, etc (Mir et al., 2019b; Vera et al., 2019). In the study of Mir et al. (2019b), 8% w/v QPI dispersions were sonicated at 20 kHz, 500 W and 25% amplitude for 5, 15, 25 and 35 min respectively. The gelling behaviour, emulsifying properties,

and water solubility were significantly improved after HIUS treatment for 35 min. However, to the best of our knowledge, there are limited studies on the comparison of HIUS and HHP on modifications of QPI dispersions at different pHs.

1.2. Research objectives

To investigate the physicochemical, techno-functional properties and structural changes of QPI dispersions as affected by HPH, HHP, HIUS and heat treatment.

1.3. Thesis structure

Chapter 1: Introduction (background of the research)

Chapter 2: Literature review

Chapter 3: Impact of high-pressure homogenization on physicochemical, structural, and rheological properties of quinoa protein isolates

Chapter 4: Impacts of sonication and high hydrostatic pressure on the structural and physicochemical properties of quinoa protein isolate dispersions at acidic, neutral and alkaline pHs

Chapter 5: Impact of high hydrostatic pressure on the gelation behaviour and microstructure of quinoa protein isolate dispersions

Chapter 6: Conclusion and future work

2. Chapter 2: Literature review

2.1. Quinoa

Plant proteins have been increasingly used in food formulations in recent years. One of the advantages of plant-based proteins is the higher conversion rate than animal proteins. They play an important role in vegetarians' daily diets to fulfil their needs for proteins. Some different nutritional information of different cereals is listed in **Table 1**. Among these cereals, quinoa seeds contain the highest content of protein, fat, and dietary fibre. The amino acid profile of quinoa protein is well-balanced and contains all nine essential amino acids required by the human diet. Quinoa protein contains 18.57% glutamic acid, 11.17% lysine, 10.9% arginine and 9.29% aspartic acid as the four dominant amino acids (Daliri et al., 2021).

Andean countries in South America are the source of quinoa. There are five main ecotypes of quinoa which are grown in Peru (Highlands), Bolivia (Yungas), Columbia (Inter-Andean valleys), Ecuador, Chile (Coastal/Lowlands) and Argentina (Salares) (Bazile et al., 2013). Because of its excellent nutritional value and high tolerance to saline stress (Schabes & Sigstad, 2005), the breeding and domestication of quinoa have been started from the 1990s to the 2000s globally and distributed throughout the world in 2013 (Bazile et al., 2013).

Table 1: Nutrition compositions of different seeds

Cereals	**Protein %**	**Fat %**	**Carbohydrates%**	**Ash %**	**Fibre %**	**References**
Quinoa	16.7	5.5	74.7	3.2	10.5	(Wright et al., 2002)
Rice	7.10	0.60	76.80	0.42	1.50	(Nascimento et al., 2014)
Wheat	14.13	1.56	82.00	0.63	1.49	(Collar & Angioloni, 2014)
Rye	10.21	1.06	73.26	0.93	8.94	
Buckwheat	15.17	2.93	65.00	1.94	6.74	
Amaranth	12.94	5.79	63.86	1.81	9.02	

As shown in **Table 2**, the macronutrient compositions of quinoa seeds differ with genotypes, which usually contain around 9.1-15.7% protein, 4.0-7.6% fat, 48.5-69.8% carbohydrates, and

8.8-14.1% dietary fibre (Nowak et al., 2016).

Table 2: Chemical composition of quinoa reported in different studies

Varieties of Quinoa	Protein %	Fat %	Carbohydrates %	Ash %	Fibre %	Reference
N/A*	16.5	6.3	69.0	3.8	3.8	(Kozioł, 1992)
Surumi	14.8	5.3	69.1	2.6	8.8	(Wright et al., 2002)
Canada	15.2	7.1	65.6	1.4	10.5	(Ogungbenle, 2003)
Red	15.35	7.5	59.2	3.05	2.45	(Bruin, 1964)
Yellow	15.95	6.15	58.1	3.65	3.1	
White	14.05	7.15	64.2	2.4	2.1	
Peru	12.5	8.5	60.0	3.7	1.92	(Dini et al., 1992)
Spanish	12.87	3.91	65.00	2.39	10.38	(Collar & Angioloni, 2014)
Argentina	12.10	6.31	57.20	2.01	10.40	(Nascimento et al., 2014)
Danish	16.2	5.7	54.3	3.73	19.5	(Pulvento et al., 2012)

*N/A: not applicable

2.2. Chemical compositions of quinoa

Although the content of individual macronutrients varies in quinoa from different origins, their composition remains nearly unchanged. For instance, the types of storage protein in the seeds of quinoa are the same from all origins. Detailed compositions of the protein, lipids, starch and antinutritional components will be described in the following sections.

2.2.1 Proteins

The proteins in quinoa seeds are mainly stored in the embryo to provide nutrients during growth (Capraro et al., 2020). The dominant storage proteins are 11S globulin (chenopodin) and 2S albumin which account for 37% and 35% of the total proteins, respectively (Brinegar & Goundan, 1993; Brinegar et al., 1996). The chenopodin is a globular protein with Mw of 320 kDa, consisting of 20-25 kDa basic polypeptides and 30-40 kDa acid subunits connected by disulfide bonds (Capraro et al., 2020). According to Brinegar and Goundan (1993), chenopodin is high in leucine (7.9%), isoleucine (4.9%), phenylalanine (4.0%) and tyrosine (2.9%) which

fulfils the essential amino acid requirements of adults (Rose et al., 1976). The 2S albumin has a molecular weight of 8-9 kDa under reducing conditions, which can be extracted by ammonium sulfate followed by centrifugation (Brinegar et al., 1996). The contents of cysteine, arginine and histidine (15.6%, 15.2 % and 7.6 %) in 2S albumin were found to be significant (Brinegar et al., 1996). Histidine and Arginine cannot be synthesised in the human body as essential amino acids (Tapiero et al., 2002; Brosnan & Brosnan, 2020). Because of the nutritional value, it is worth studying the physicochemical and techno-functional properties of quinoa proteins.

2.2.2 Lipids

Quinoa seeds contain ~8.59g total fat /100g dry weight which consists of ~11.56% saturated fatty acid and ~85.44% unsaturated fatty acids (Hager et al., 2012). Most lipids are stored in the embryo, which contains ~51% protein and ~49% fat (Ando et al., 2002). The total lipid content of quinoa seeds is relatively higher than other cereals such as wheat (~1.81%), rice (~0.9%), and buckwheat (~4.21%) (Hager et al., 2012). Moreover, the proportion of unsaturated fatty acid is also higher than in other cereals (around 60-80%). Quinoa seeds contain ~23.93% Oleic acid (18:1), ~52.68% Linoleic acid (18:2), ~4.60% α-Linolenic acid (18:3) and ~1.56% Eicosenoic (Gadoleic) acid (20:1) (Hager et al., 2012; Ruales et al., 2002). The unsaturated fatty acids in quinoa seeds are mainly essential fatty acids (ω-3 and ω-6) (Hager et al., 2012; Kaur et al., 2014).

2.2.3 Starch

Native starch molecules appear as granules of compact structures comprised of two types of polymers, amylose and amylopectin. The shape (spherical or ellipsoidal) and size of starch

granules vary from the source. Amylose is a linear chain of D-glucose linked via α (1→4) linkages and forms a helical structure, and usually occupies a lower proportion of the total starch. The structure of amylopectin is comprised of a large number of branches and forms a brush-like shape. Amylopectin usually does not form gels or forms weak gels upon heating but has a significant impact on the viscosity (Bello-Pérez & Paredes-López, 1994). The starch content of quinoa seed is ~48.88%, which is relatively lower than other cereals such as wheat (~68.06%), rice (~77.52%) and oat (~69.38%). Amylopectin is the dominant type of starch in quinoa seeds which accounts for ~95.38% (Hager et al., 2012).

2.2.4 Antinutritional components

Saponins, phytic acid and trypsin inhibitors are the major antinutritional factors found in quinoa seeds, but they can be easily reduced by, for example, washing and heat treatment (Ridout et al., 1991). Saponins (0.1-5%) is a bitter coating on the episperm of the quinoa seeds, which is also present in some legumes such as soybeans and peas (Kozioł, 1992). Saponins are toxic and can cause hemolysis of red blood cells, but they can be removed by washing with water or methanol (Kozioł, 1992). Besides, the toxicity of saponins is much lower in mammals than in cold-blooded animals. Nowadays, saponins are removed from food products mainly due to a bitter or astringent taste. Wet and dry methods are the two major ways for removing saponins, and both have their advantages and disadvantages. The wet method is typically used in a smaller scale of production by thoroughly washing the quinoa seeds with water several times, The benefit of the wet method is that the nutritional composition can be maintained after the washing but drying will be needed before further processing. The dry method is mostly employed in larger-scale production where the saponins are removed through heat treatments at 200 °C for 10 min or mechanical abrasion (Brady et al., 2007). However, this method will cause nutritional loss such as denaturation of proteins under heat treatment (Assatory et al.,

2019).

Phytic acid (1-3%) can act as a chelating agent to bind divalent cations such as minerals. It presents both in the episperm and the endosperm, which means only the phytic acid on the episperm can be easily removed by using the wet or dry methods as mentioned above. According to Kozioł (1992), the amount of phytic acid in quinoa seeds is similar to barley, corn, rice and wheat.

Trypsin inhibitors are widely found in the *Leguminosae* family and seeds of other plants such as soybeans, kidney beans and mung beans (Alam et al., 2015). They prevent the human body from utilising trypsin, which is important for protein digestion. The trypsin inhibitor activity is much higher in the hull (~6.5 units inhibited/ml of extract) of quinoa seeds than in the de-hulled seeds (~0.75 units inhibited/ml of extract) (Chauhan et al., 1992). Trypsin inhibitors can be destroyed after pre-soaking of quinoa seeds for 24 h followed by boiling in water for 30 mins (Alam et al., 2015).

2.2.5 Extraction methods of proteins from quinoa seeds

With the knowledge of the antinutritional components and undesired components (lipids and starch) in quinoa seeds, protein extraction methods could be developed. Various extraction methods will be reviewed in this section.

The extraction of plant protein can be generally categorised into wet-based and dry-based methods. The wet extraction methods include alkaline extraction followed by isoelectric precipitation (AE) and salt extraction followed by ultrafiltration or dialysis (SEU/SED) (Stone et al., 2015; Yang et al., 2021). The dry methods usually include grinding followed by air

classification or electrostatic separation (Assatory et al., 2019). Organic solvents such as hexane and petroleum ether are commonly used to defat the quinoa flour before starting the extraction procedure (Stone et al., 2015).

For quinoa seeds, the saponins need to be removed with water before the defatting. Previous studies (e.g., AE (López-Castejón et al., 2020) and SEU (Yang et al., 2021)) on extracting proteins from quinoa, faba bean and pea are listed in **Table 3** and **Table 4**. Briefly, these methods utilise salt or alkaline to extract the proteins into the aqueous phase and the supernatants containing proteins can be obtained after centrifugation (Elsohaimy et al., 2015; López-Castejón et al., 2020). For AE, the supernatant is adjusted to the isoelectric point of the protein where the solubility of the protein is minimum and precipitates from the solution (Boye et al., 2010). The suspension is then centrifuged, and the pellets containing proteins are collected for drying. Ultrafiltration is a type of membrane filtration, and the filtration was conducted under external pressure to drive the suspension passing through the membrane sizing from 5 to 50 kDa (Boye et al., 2010; Yang et al., 2021). Dialysis is similar to ultrafiltration but without applying pressure, and instead, the separation of molecules cross semi-permeable membranes is driven by different concentrations. Molecules tend to move from the higher concentration to the lower concentration to reach equilibrium. For SEU and SED, the pore size of the membrane used for ultrafiltration or dialysis can be selected to fit the targeted protein size.

Stone et al. (2015) compared the physicochemical and techno-functional properties of pea protein extracted by the AE and SED. It was reported that different extraction methods can cause differences in amino acid profiles and the total amount of amino acids in pea protein isolate (Stone et al., 2015). Moreover, AE usually produces proteins with higher surface

hydrophobicity, higher water holding capacity (WHC), lower solubility, lower foaming capacity (FC) and higher foaming stability (FS) compared to SED (Stone et al., 2015; Yang et al., 2021). Although the yield of protein extracted by SED (~19.2%) is higher than AE (~16.0%), the purity of protein extracted by SED (~76.1%) is lower than AE at ~83.3%. It is also a time-consuming process compared to AE. In general, AE is a more suitable extraction method to achieve high yield, purity and efficiency compared to SED.

Elsohaimy et al. (2015) studied the extraction condition of AE on quinoa protein, and found pH (5-10), stirring time (30-120 min) and NaCl concentration (0-1 M) significantly affect the extractability of QPI. The purity of protein increased with increasing pH, stirring time and NaCl concentration. At pH 4.5, the amount of protein precipitation is the highest among all other pH's which leads to the highest yield in protein.

Table 3: Studies on using the AE method for plant protein extractions

Protein	Yield %	Purity %	Highlights	References
Quinoa	N/A	82.11 (Q9*) 76.64 (Q11*)	Stronger emulsifying property for Q11.	(López-Castejón et al., 2020)
Quinoa	N/A	77.2 (Q9) 83.5 (Q11)	Lower solubility for Q11 than Q9 at pH above 5. Q11 showed no endotherm, and Q9 denatured at 98.1 °C with enthalpy 12.7 J/g.	(Abugoch et al., 2008)
Quinoa	N/A	88.74 (Q10*)	Studied different conditions of extraction (pH, NaCl and stirring time)	(Elsohaimy et al., 2015)
Faba bean	N/A	76 w/w dry weight	Solubilised at pH 7 results in 35% solubility at 1% concentration. HPH at 103 MPa improved solubility from 35% to 99%.	(Yang et al., 2018)
Pea	N/A	88.83	Compared with salt extraction, higher protein content and surface hydrophobicity.	(Yang et al., 2021)
Pea	N/A	88.94	The protein solution was dialysed with regenerated cellulose tubing for 96 h.	(Zhu et al., 2021)
Pea	62.6-76.7	83.3-86.9	Compared with SED, significantly higher yield, purity and surface hydrophobicity.	(Stone et al., 2015)

*Q9, Q10 and Q11 refer to QPI extracted at pH 9, 10 and 11.

Table 4: Studies on using salt extraction followed by ultrafiltration or dialysis for plant protein extractions

Protein	Yield %	Purity %	Methods and Outcomes	Reference
Flaxseed	N/A	10.9-32.6 in the supernatant	Highest protein content and solubility at 10 L/kg flour Na_3PO_4 and 0.8% NaCl. Without precipitation or filtration.	(Oomah et al., 1994)
Flaxseed	N/A	87.39	10 L/kg flour 50 mM Na_3PO_4 and 0.8% NaCl. Dialysed for 72 h.	(Karaca et al., 2011)
Canola	N/A	93.10	10 L/kg flour 0.05 M Tris-HCl and 0.1 M NaCl. Dialysed for 72 h.	(Karaca et al., 2011)
Pea	68.2-74.8	71.5-79.3	10 L/kg flour 0.1 M sodium phosphate buffer (pH 8.00) with 6.4% KCl. Dialysed for 72 h at 6-8 kDa cut-off.	(Stone et al., 2015)
Pea	N/A	86.76±0.14 (SED) 86.33±0.31 (SEU)	SED: 10 L/kg flour 0.1 M sodium phosphate buffer (pH 8.00) Dialysed for 5 days at 0.5-1 kDa cut-off. SEU: Passed through 5 kDa cut-off membrane ultrafiltration 5 times against distilled water.	(Yang et al., 2021)

Air classification and electrostatic separation are two common methods in dry extraction (Assatory et al., 2019). Air classification is based on the different particle sizes and densities of each component in the flour, and air induces centrifugal and gravitational forces to separate fine and coarse particles (Lundgren, 2011). the purity of protein increases when the particle size of the flour is cut smaller before classification, but the yield decreases at the same time Pelgrom et al. (2015). Using air classification can preserve the native protein structures and save energy (Assatory et al., 2019), but particles with similar density and particle size can hardly be separated (Tabtabaei et al., 2016). The purity of protein obtained is usually lower than the wet extraction methods. Although smaller particle sizes increase the purity to some extent, high milling speed can also induce damage to the starch fraction (Pelgrom et al., 2013).

Electrostatic separation is another dry extraction method based on the difference in dielectric properties of the components. For example, amino acids contain more ionisable groups than starch components (Tabtabaei et al., 2016). Similarly, the advantages of electrostatic separation are energy-saving and induces nearly no change in the structures of starch and proteins.

Moreover, it can also separate materials with similar densities and particle sizes. However, components with similar charges cannot be separated, which reduces the purity of the proteins. The other limitation is that the gravitational force can cause some particles to fall and settle down before being attracted by the electrodes, thus resulting in a low yield (Wang et al., 2015).

In general, the dry extractions are energy-saving, do not change the protein's native structure and no chemical reagents are required, leading to proteins with relatively low purity. They are more suitable for industrial productions due to the low cost, while wet methods are more suitable for fundamental research when pure proteins are required. In the wet extraction methods, salt and alkaline extractions are usually combined to maximise the yield of proteins (Elsohaimy et al., 2015; Oomah et al., 1994). Isoelectric precipitation is the most common method used for plant protein extractions, which is relatively faster and results in protein isolates with high purity (e.g., >80%).

Overall, it is worth applying QPI to various types of food products, for its excellent nutritional composition. However, many of the native plant proteins exhibit inferior techno-functional properties such as solubility, emulsifying and foaming properties compared to animal proteins (Jeske et al., 2018; Kang et al., 2022). These properties prevent the application of these native plant proteins as dairy alternatives. Therefore, studies on the impacts of various modification techniques on QPI are necessary to promote the use of QPI in the food industry. To avoid the adverse effects of heat treatment (Lima et al., 2014), non-thermal techniques will be focused on in this thesis.

2.2.6 Physical modifications

Physical modifying techniques such as HPH, HIUS, HHP, etc., have been extensively studied

on various plant proteins in recent years (Chao et al., 2018; Cheng et al., 2022; Gao et al., 2022). The impacts of every single treatment have been found differently on various protein sources and treatment conditions.

High pressure homogenisation

High pressure homogenisation is a physical technique to reduce particle size and improve the uniformity of dispersions with a pressure range from 10-200 MPa (Dumont et al., 2018). In the food industry, a two-stage homogeniser is commonly used. The homogenisation process can fit well in a food production line which is continuous and automatic. It is widely applied in milk and mayonnaise productions which produces uniform size distributions of fat droplets (Aganovic et al., 2018). The schematic diagram of a two-stage homogeniser is shown in **Figure 1**. The product flows through the inlet and passes the first stage where the droplet size is cut down by shear force driven by the high pressure up to 200 MPa. The second stage pressure is usually at 10 to 15% of the first stage to create a turbulent flow to improve the homogeneity of the product.

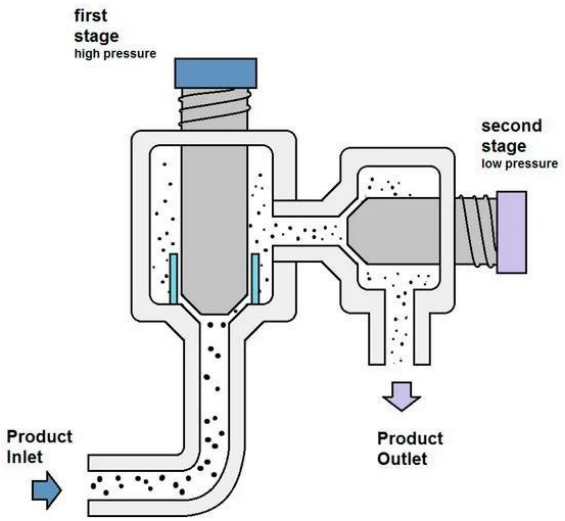

Figure 1. A schematic drawing of a two-stage high pressure homogeniser (Comuzzo & Calligaris, 2019, pp. 123).

Many studies have been carried out on the impact of HPH processing on the physicochemical properties of plant protein dispersions (Katzav et al., 2020; Tan et al., 2021). Recent studies on the effect of HPH on plant proteins are summarised in **Table 5**. In general, most studies found that HPH can reduce particle size, increase water solubility, improve emulsifying and foaming properties, and alter the tertiary and secondary structure of the plant proteins (Cheng et al., 2022; Saricaoglu et al., 2018). However, the primary structure of proteins was mostly not changed (Keerati-u-rai & Corredig, 2009).

Saricaoglu (2020) investigated the effect of HPH at 0-150 MPa on 4% lentil protein isolate at pH 9. The particle size of the lentil protein isolate was reduced dramatically from 98.73 μm to 12.62 μm with an increase in pressure from 0 to 150 MPa. The microscopic images showed that the shape of lentil protein particles is irregular and deformable before HPH. The large particles and flocculated small particles were unfolded and broken down to form smaller and uniform particles when the pressure in increased from 0 to 150 MPa. The result from SDS-PAGE under the reducing condition showed that there were no significant changes in protein patterns after the HPH treatment, indicating that HPH up to 150 MPa did not cause changes in the primary structure. However, HPH at 50-150 MPa induced the unfolding of lentil protein which enhanced the emulsifying and foaming properties. The emulsifying activity index (EAI) (100.22 m^2/g to 125.16 m^2/g), emulsifying stability index (ESI) (39.12 min to 226.34 min), FC (10.00% to 85.33%) and FS (4.29% to 66.63%) were continuously improved with increasing HPH pressure up to 100 MPa but reduced at 150 MPa. The solubility of lentil protein was first significantly increased with pressure up to 75 MPa and then decreased when the pressure was further increased to 100 and 150 MPa. Similar trends were found in the emulsifying and foaming properties, where both the emulsifying and foaming capacities and stabilities reached the maximum at 100 MPa.

A study by Cheng et al. (2022) investigated changes in the structural and physicochemical properties of 5% w/v pea protein isolate subjected to high pressure homogenisation at 60-240 MPa for one pass. The particle size and surface charge were found to be decreased, while the surface hydrophobicity, fluorescence intensity and free SH content were increased after the HPH treatment. This could be attributed to that the protein was partially denatured and unfolded when subjected to the HPH treatment. According to the FTIR results, the absorbance associated with -OH groups, amide I and amide II regions decreased after homogenisation which was associated with the formation of hydrogen bonds and unfolding of pea protein. By deconvoluting peaks in the amide I region (1600-1700 cm^{-1}), β-sheet and random coil contents were found to be increased with increasing pressure (above 60 MPa), while the α-helix content decreased.

Table 5: A summary of recent HPH studies of plant protein dispersions

Protein source, Concentration and Volume	Treatment Conditions	Highlights	References
Pea protein isolates **5% w/v**	60-240 MPa 1 pass Heat exchanger with cold water for cooling.	• The opacity of pea protein edible films was reduced from 7.39 A/mm to 4.82 A/mm with increasing pressure. • HPH improved the tensile strength (0.76 MPa to 1.33 MPa) and elongation at break (from 96% to 197%) of pea protein film at 240 MPa.	(Cheng et al., 2022)
Soy protein isolates **10% w/v**	50-150 MPa 2 passes 10 °C to 46.80 °C	• Particle size (from 367.1 nm to 104.7 nm) and solubility (from 55.14% to 84.13%) were modified the most at 100 MPa. • FC (from 161.11% to 205.97%) and FS (from 46.00% to 83.38%) increased with increasing pressure.	(Kang et al., 2022)
Pea protein isolates **2% w/w**	80 MPa 3 passes	• Particle size decreased from ~380 nm to ~80 nm after treatment. • Solubility increased from ~70% to ~80% at 80 MPa. • Improved EAI (from 68.56 m^2/g to 88.50 m^2/g), FC (from 15.00% to 24.33%) and FS (8.22% to 18.11%) were observed at 80 MPa.	(Zhao et al., 2022)
Kidney bean protein isolates **1% w/v**	30-120 MPa 1 pass pH 7 25 °C	• HPH at 30-60 MPa promoted the formation of soluble aggregates and enhanced the EAI (from 53.65 m^2/g to 161.90 m^2/g). • HPH at 90-120 MPa breaks protein aggregates and reduces the EAI (from 161.90 m^2/g at 60 MPa to 122.45 m^2/g).	(Guo et al., 2021)
Spirulina concentrate **5% w/v**	50-100 MPa pH 6.5 25 °C	• Decreased gelation temperature from ~67 °C to ~60 °C with increasing pressure at 100 MPa. • Increased solubility from ~65% to ~90% at 50 MPa, decreased to ~75% at 100 MPa.	(Lozober et al., 2021)
Lentil protein isolates **4% w/v**	25-150 MPa 1 pass	• Increased water solubility (from ~32% to ~47%) at 75 MPa, decreased to ~36% at 150 MPa.	(Saricaoglu, 2020)

	pH 9 RT*	• The highest EAI (126.16 m^2/g), ESI (226.34 min), FC (85.33%) and FS (66.63%) were achieved at 100 MPa.	
Hazelnut meal protein isolates **2% w/v**	25-150 MPa 1 pass pH 12 Start at RT, cooled down in an ice-water bath after HPH	• Solubility increased from ~77% before treatment to ~87% at 100 MPa. • The highest EAI (96.02 m^2/g), ESI (33.32 min), FC (90.00%) and FS (78.17%) were achieved at 100 MPa.	(Saricaoglu et al., 2018)
Faba bean protein isolates **1% w/v**	103-207 MPa 6 passes pH 7 Start at 22 °C, and cooled down in an ice-water bath after HPH	• Increased solubility from 35% to 99% at 103 MPa, with no significant change of solubility with further increasing pressure. • Increased FC from ~100% before treatment to ~250% at 207 MPa. • Decreased EAI (from ~27 m^2/g to ~19 m^2/g) and ESI (from ~40 min to ~17 min) from control to 207 MPa.	(Yang et al., 2018)
Peanut protein isolates	40-80 MPa 1 pass	• Improved EAI (24.4 m^2/g to 32.4 m^2/g) and FC (from 25% to 32%) at 80 MPa. • Reduced ESI (from 20.6 to 12.2) and FS (from 45.8% to 41.4%) with increasing pressure at 80 MPa.	(Dong et al., 2011)

*RT: Room temperature

High intensity ultrasonication

Another physical modification technique is HIUS which produces similar effects on the structure and properties of plant proteins compared with those treated with HPH (Cheng et al., 2022; Jiang et al., 2017). Ultrasound is the sound which exceeds the human hearing range (0.02 – 20 kHz). There are two types of ultrasound treatment: high frequency (above 100 kHz) with low intensity (below 1 W/cm^2), and low frequency (20 - 100 kHz) with high intensity (above 1 W/cm^2) (Soria & Villamiel, 2010). High-frequency ultrasound is a non-destructive technique extensively used for the determination of the structure and composition of the material (Izzetti et al., 2021). HIUS is a technique that can induce mechanical, physical and chemical/biochemical changes to a liquid sample. It produces an acoustic pressure to the medium which depends on time, frequency and amplitude (Patist & Bates, 2008). The effects of ultrasound on liquid systems are largely related to the cavitation phenomenon which is shown in **Figure 2** (O'Donnell et al., 2010; Soria & Villamiel, 2010). The ultrasound passed through the molecules of the medium via compression and rarefaction as a cycle. The rarefaction can introduce air bubbles from the gas nuclei existing in the medium. Although compressions exist in the cycle and can reduce the bubble size, the air bubbles still grow over several full cycles (Barbosa-Cánovas & Rodríguez, 2002). When the bubbles grow to a critical size, they become unstable and collapse. This produces high shear energy waves and turbulence in the cavitation zone which induce mechanical changes in the medium (Soria & Villamiel, 2010).

A

B

Figure 2: (A) Ultrasonic cavitation (Soria & Villamiel, 2010). (B) Schematic representation of ultrasonicator equipment (Malek et al., 2020).

The summary of recent research on the impact of HIUS on plant proteins is shown in **Table 6**. Previous studies have been conducted on plant proteins with HIUS treatments and found a decrease in particle size, an increase in water solubility, and unchanged primary structure. For example, Mir et al. (2019b) investigated the effect of HIUS on the structure and physicochemical properties of QPI at 500 W (acoustic energy determined: 43 W/cm^2) and 25% amplitude for 5, 15, 25 and 35 min using a frequency of 20 kHz. A change in the secondary structure of QPI has occurred after HIUS treatment where a decline of the wave number of the peak from 3000 to 3500 cm^{-1} has been observed in the FTIR analysis. This region correlates to the -OH groups of amino acids, and the decline in this region may be due to the formation of hydrogen bonds during the HIUS treatment. Mir et al. (2019b) also investigated the molecular structure by SDS-PAGE and found no significant changes in the protein profiles of QPI after the HIUS treatment. The increase in overall lane intensities at the longer treatment time indicated the higher solubility of QPI induced by HIUS. Furthermore, the turbidity decreased

with increasing the HIUS time. Structural characteristics of QPI also changed with the treatment time, and longer treatments led to more rough and irregular surfaces. The EAI, ESI, WHC and OBC all increased after the HIUS treatment, reaching maximum values at 25 min.

A study by Constantino and Garcia-Rojas (2020) evaluated the effect of various HIUS power (25-66 J/cm^3) and time (15 and 30 min) on the protein's structure and physicochemical properties of amaranth protein isolate (10%) at pH 7. The temperature of samples was kept at 3.0 ± 1 °C in an ice bath during the HIUS treatment. There were no significant changes observed in the molecular weight distribution of amaranth protein after the HIUS treatment as revealed by SDS-PAGE. The particle size was reduced after the treatment, which leads to higher solubilities and enhanced emulsifying properties.

Table 6: A summary of previous HIUS studies on plant protein-based systems

Protein source, Concentration and Volume	Treatment Conditions	Highlights	Reference
Amaranth protein isolates 3% w/v	750 W 50% amplitude 10 min pH 7 Ice bath	• Decreased particle size from ~1200 nm to ~500 nm after treatment. • Increased solubility from ~40% to ~65% after treatment. • Increased FC (from 236.7% to 293.0%) and FS (69.1% to 83.3%) significantly after treatment.	(Figueroa-González et al., 2022)
Pea protein isolates 10% w/v 25 mL	11.14-31.34 W/cm^2 3s/2s 5, 10, 20 min pH 7 < 30 °C	• Highest solubility (79.92%) at 31.34 W/cm for 20 min. • Decreased EAI by 5 times (~140 m^2/g to ~30 m^2/g) at 31.34 W/cm^2 for 20 min. • Highest ESI (from ~17% to ~33%) at 11.14 W/cm^2 for 5 min. • Highest FS (from ~40% to ~80%) at 31.34 W/cm^2 for 20 min.	(Gao et al., 2022)
Amaranth protein isolates 10% 20 mL	25-66 J/cm^3 15, 30 min pH 7 3 °C	• Increased solubility the most (from ~25% to ~70%) at 35 J/cm^3 for 15 min. • Highest EAI (from 136.95 m^2/g to 146.96 m^2/g) and ESI (from 17.87 min to 28.12 min) at 50 J/cm^3 for 30 min.	(Constantino & Garcia-Rojas, 2020)
Gluten protein isolates 3% w/v	67 W/L 28, 28-40, 28-40-80 kHz 10s/5s 10 min 30 °C	• Particle size was minimised from 197.93 nm to 110.15 nm after triple-frequency treatment. • WHC (from ~1.2 g/g to ~1.4 g/g), oil binding capacity (OBC) (from ~0.6 g/g to ~1.6 g/g) and solubility (~10% to ~40%) maximised after triple-frequency treatment.	(Zhang et al., 2020)
Album protein isolates 8% 87 mL	125 W 5 min rest between samples 5, 15, 25, 35 min pH 7 10 °C	• Minimised particle size from ~250 μm to ~130 μm at 25 min. • Increased solubility the most from ~68% to ~94% at 25 min. • FC (from ~32% to ~75%) and FS (from ~92% to ~100%) enhanced the most at 25 min.	(Mir et al., 2019a)
Quinoa extract 47.2% 250 mL	39 W 1s/5s, 10s/10s, 5s/1s 5- 30 min	• Increased particle size the most from 37.78 μm to 47.29 μm at 5s/1s for 5 min (soluble aggregates formed).	(Vera et al., 2019)

	pH 8 20 ℃	• Solubility increased the most at 5s/1s for 5 min (from 2.33% to 3.93%).	
Quinoa protein isolates **8% w/v**	43 W/cm^2 5, 15, 25, 35 min	• EAI (from~60% to ~100%) and ESI (from ~50% to ~90%) increased the most at 25 min. • Increased WHC (from ~144% to ~168%) the most at 25 min. • Increased OBC (from ~96% to ~132%) the most at 25 min.	(Mir et al., 2019b)
Pea protein isolates **5% w/w** **15 mL**	22-48 W/cm^2 5s/2s 30 min pH 7	• Reduced particle size from ~210 nm to ~140 nm at 22 W/cm^2 and continued to drop to ~130 nm until 48 W/cm^2. • FC (from ~150% to ~200%) and FS (from ~60% to ~ 75%) increased with rising power level.	(Xiong et al., 2018)
Pea protein isolates **3%**	68 W/ 100 mL 5 min pH 7 < 35 ℃	• Decreased particle size from 206.9 nm to 75.3 nm after treatment. • Increased solubility by 7-folds from 8.17% to 55.80% after treatment.	(Jiang et al., 2017)
Soybean glycinin **1% w/v** **20 mL**	80 W 5s/1s 5, 20, 40 min pH 7 RT	• Particle size minimised (from ~220 nm to ~50 nm) after 40 min HIUS treatment. • Solubility maximised (from ~87% to ~95%) after 40 min HIUS treatment.	(Zhou et al., 2016)
Black bean protein isolates **10% w/v** **100 mL**	150, 300, 450 W 4s/2s 12, 24 min pH 7 < 2 ℃	• Increased solubility with increasing power and time, reached the peak (~50%) at 300 W for 24 min. • Particle size increased with increasing power and time and reached the peak (~75 nm) at 450 W for 24 min.	(Jiang et al., 2014)

High hydrostatic pressure processing

HHP is a cold pasteurisation method which has been extensively employed in the food industry (Chen et al., 2015; Porretta et al., 1995). Applying HHP processing to food products can kill the bacteria and enhance the nutritional value without changing the original colour and other beneficial components such as antioxidants (Chen et al., 2015; Huang et al., 2020). There are mainly two types of high-pressure processing: direct compression and indirect compression as shown in **Figure 3**. Direct pressurisation uses pistons to apply pressure directly to the product, while indirect pressurisation utilises the pressurised fluid such as water to indirectly apply pressure. When applying pressure, the temperature will rise ~ 3 °C per 100 MPa, and vice versa (Yordanov & Angelova, 2010). The pressure used in most food applications usually does not exceed 1000 MPa, while the pressure range is selected based on the sensitivity of the material to pressure and the desired effects after pressurisation.

Although their names are similar, HPH and HHP have several differences from mechanism to output. HPH usually set pressure below 200 MPa, while the pressure level of HHP can be up to 600 MPa (Lomelí-Martín et al., 2021). Apart from the pressure range, the main difference between HPH and HHP is that in HPH processing, the shear is the major force that breaks down the particle size to ~0.2 μm (Lai et al., 2022). While in HHP, the hydrostatic pressure is the major force that compresses the product towards the centre. Another difference between HPH and HHP is the sample requirements and pretreatments. The samples for HPH need to be a suspension and require a premix to reduce the particle size before entering the homogeniser, while both solid and liquid samples can be treated with HHP with no requirement of particle sizes.

Figure 3: A schematic drawing of direct pressurisation (left) and indirect pressurisation (right) for HHP (Yordanov & Angelova, 2010).

HHP has been extensively used for the modification of physicochemical properties of plant proteins, and some of the recent studies are listed in **Table 7**. It has been found that major impacts of HHP processing on plant proteins were the formation of large aggregates, alterations of proteins' secondary and tertiary structures, and changes in the physicochemical and techno-functional properties. For example, Tan et al. (2021) studied the effect of HHP on the structure and emulsifying properties of 4% w/v soy protein isolates at 200 or 400 MPa for 10 min at pH 7. After HHP treatments, the solubility of protein was increased with pressure levels, while the particle size was reduced. Both free SH groups and surface hydrophobicity were increased, indicating the unfolding of the protein structure, and exposure of hydrophobic groups and SH groups. For the protein secondary structure, α-helix and random coil contents were increased and the β-sheet content was decreased after the HHP treatment. The emulsifying activity and stability of soy protein isolate increased from 12.70 ± 0.28 m^2/g and 21.80 ± 0.07 min to 18.59 ± 0.09 m^2/g and 24.41 ± 0.61 min, respectively after the HHP treatment at 400 MPa.

Zhou et al. (2022) investigated the effect of HHP at 100-500 MPa on the structures and physicochemical properties of 1% w/v buckwheat protein isolate for 10-30 min at pH 3 and 7.

The fluorescence intensity and surface hydrophobicity were found to be increased with pressurization time and pressure levels but decreased with pH increased from 3.0 to 7.0. These results indicated that the buckwheat protein was partially denatured and aggregated after the HHP treatment. The secondary structure of buckwheat protein was changed as well. The α-helix and β-turn contents decreased while β-sheet and random coil contents increased after the HHP treatment. The HHP treatment also led to increased solubility, emulsifying activity, emulsifying stability, foaming capacity and foaming stability.

Table 7: A summary of previous studies of HHP treatment on plant protein systems

Protein source, Concentration and Volume	Treatment conditions	Highlights	References
Buckwheat protein isolates **1% w/v**	100-500 MPa 10-30 min pH 3 and 7 25 ℃	• Increased solubility (from ~40% to ~90%), EAI (from ~50 m^2/g to ~80 m^2/g), ESI (from ~27% to ~42%) and FC (from~60% to ~85%) at 500 MPa for 30 min at pH 7. • HHP at 500 MPa at pH 3 (~50%) showed higher FS than at pH 7 (~40%).	(Zhou et al., 2022)
Cowpea protein isolates **7.5-13.5 % w/w**	400-600 MPa 5 min pH 7 20 ℃	• 12.0-13.5% cowpea protein formed gels at 400 and 600 MPa, hardness increased (from 0.10 N to 0.15 N) at 600 MPa. • WHC was improved (from 98.25% to 99.07%) with 13.5% protein at 600 MPa.	(Peyrano et al., 2021)
Soy protein isolates **4% w/v**	200-400 MPa pH 3, 7 and 11 10 min	• Increased EAI (17.77 m^2/g to 29.57 m^2/g) and ESI (26.8 min to 35.06 min) with rising pressure from 200 MPa to 400 MPa at all pH levels. • Particle size decreased (30.62 μm to 23.68 μm) with increasing pressure levels at all pH levels. • Samples treated at pH 11 had the highest solubility (~65%) and smallest particle sizes (23.68 μm) at all pressure levels compared with pH 3 and 7.	(Tan et al., 2021)
Potato protein isolates **10 %** **0.5-5 mL**	300-500 MPa 30 min pH 3 and 7 < 40 ℃	• Only formed gels at pH 3 for all pressure levels. • Gel hardness increased (from ~0.25 N to ~0.6 N) at 500 MPa at pH 3. • WHC increased the most (from ~10% to ~30%) at 500 MPa at pH 3.	(Katzav et al., 2020)
Kidney bean protein isolates **20 % w/w** **25 mL**	200-600 MPa 15 min 20-26 ℃	• FC (from 76.7% to 44.6%) and FS (from 54.5% to 40.5%) decreased at 0-600 MPa. • EAI (from 24.2 m^2/g to 40.4 m^2/g) and ESI (from 68.3 min to 142.3 min) increased at 200 and 400 MPa and dropped to 33.9 m^2/g and 80.8 min at 600 MPa. • WHC increases from 2.07 to 2.56 g/g at 25 °C with increasing pressure.	(Ahmed et al., 2018)
Pea protein isolates **1% w/v** **250 mL**	200-600 MPa 5 min pH 7 From 23 ℃,	• Decreased ESI (from ~98% to ~60%) at 0-600 MPa. • Demoted the FC (from ~75% to ~65%) at 0-600 MPa.	(Chao et al., 2018)
Cowpea protein isolates **1 % w/v**	200-600 MPa 5 min pH 7	• HHP improved WHC (0.95 g/g to 1.66 g/g) at 0-600 MPa. • Decreased solubility (from 93.6% to 87.5%) at 200 MPa and increased to 92.1% at 600 MPa.	(Peyrano et al., 2016)

	20-38 ℃		
Sweet potato protein isolates **1 % w/v** **50 mL**	200-600 MPa 15 min pH 3, 6 and 9 25 ℃	• Improved EAI (from ~90 m^2/g to ~150 m^2/g) with increasing pH at 600 MPa. • Decreased ESI (from ~47 m^2/g to ~24 m^2/g) with increasing pH at 600 MPa. • The smaller particle size at pH 3 (2.21 μm) compared to pH 6 (6.16 μm) and 9 (6.24 μm) at 600 MPa.	(Khan et al., 2015)
Soy protein isolates **1% w/v**	HHP: 600 MPa 10 min pH 5.9, 6.4 and 7.8 20-33.5 ℃	• Solubility increased by ~5% after HHP at all pH levels. • Maximum solubility (~87%) achieved at pH 8.0 with 600 MPa HHP treatment.	(Manassero et al., 2015)
Arachin (peanut) protein isolates **1 % w/v**	200-600 MPa 20 min pH 7.5 25 ℃	• Highest EAI (~150 m^2/g) was found under 300 MPa HHP treatment. • ESI first increased at 200 MPa (from ~80 min to ~90 min) and dropped to ~50 min under 600 MPa treatment. • Solubility dropped remarkably from ~90% to ~2% at 600 MPa.	(Zhao et al., 2015)
Peanut protein isolates **5 % w/v**	50-200 MPa 5 min 25 ℃	• Gradually increases the WHC (from ~2.2% to ~2.8%) and OBC (~2.25% to ~2.8%) at 0-200 MPa. • Maximum gel hardness (~170 g) at 100 MPa.	(He et al., 2014)
Amaranth protein isolates **1, 5 and 10 %**	200-600 MPa 5 min pH 7 < 33.5 ℃	• HHP decreased the solubility at all three protein concentrations (from~100% to ~40%) at 0-600 MPa. • HHP at all pressure levels induced the breakdown of soluble aggregates and the formation of insoluble aggregates.	(Condés et al., 2012)

2.2.7 Chemical modifications

Apart from the physical modification techniques, some chemical modifications have also been studied and found to have different influences on protein structures and techno-functional properties. These chemical modifications typically include reactions with chemical agents, Maillard reactions and pH alterations, which will be discussed in the following sections (Zink et al., 2016).

pH shifting

The pH of a globular protein is vital to its physicochemical and techno-functional properties (Tan et al., 2021). When the pH is close to the isoelectric point (pI) of the protein, the net surface charge becomes zero which reduces electrical repulsions and leads to the aggregation of protein molecules. As a result, the solubility of the globular protein is usually minimum at its pI. In contrast, when the pH of a globular protein is far away from its pI, electrical repulsion appears and prevents the molecules from attracting each other. Therefore, protein-water interactions are promoted, leading to a higher solubility.

pH shifting is a chemical method to modify plant and animal proteins. Briefly, adjust the pH of the protein solution to an extreme pH, either acidic or alkaline, to induce protein unfolding (Jiang et al., 2017). The pH is then adjusted back to neutral (pH 7) and some refolding of protein structure occurred. Typical effects of alkaline pH-shifting are improved solubility, increased free SH groups and surface hydrophobicity (Jiang et al., 2017). Both acidic and alkaline pH-shifting can induce changes on protein's secondary structure (Figueroa-González et al., 2022).

Maillard reaction

Maillard reaction is a non-enzymatic browning method to alter the protein's native structure and change the techno-functional properties of proteins. It occurs between the protein molecules and reducing sugars under the heat treatment. Browning happens during and after the reactions. It has been found that the enhancement of fish gelatin's antioxidant properties was achieved after the Maillard reaction at 90-130 °C with glucose (Kchaou et al., 2019). Other typical changes of Maillard reaction on proteins are primary structure, emulsifying and foaming properties (Teng et al., 2021).

2.2.8 Biochemical modifications

Biotransformation using enzymes and fermentation has been extensively used in modification of food proteins (Zink et al., 2016). Enzymes can induce hydrolytic reactions such as splitting peptide bonds, redox reactions, and crosslinking. Enzymatic hydrolysis, transglutaminase (TGase) crosslinking and fermentation will be reviewed in the following sections.

Enzymatic hydrolysis

Enzymatic hydrolysis is a biochemical method for modifying a protein's structure and properties. The typical effect of enzymatic hydrolysis is the breakdown of proteins into polypeptides with smaller molecular weights (Galante et al., 2020). After breaking down the high molecular weight polypeptides, more hydrophobic groups are exposed. This conformational change may lead to better physicochemical and techno-functional properties such as solubility, emulsifying and foaming properties (Daliri et al., 2021). Hydrolysed proteins with smaller peptides also make them easier for human digestion.

TGase crosslinking

TGase has been extensively used for crosslinking of proteins (Escamilla-García et al., 2019; Song & Zhao, 2014). Inter- and intra-molecular linkages could be formed between glutamine and lysine residues of the proteins, which can alter the techno-functional properties of proteins (DeJong & Koppelman, 2002). Typically crosslinking proteins leads to enhancement of water and oil binding capacities, emulsifying and foaming properties, and alterations of tertiary structures (Shen et al., 2022; Song & Zhao, 2014).

Fermentation

Fermentation is usually used in grain processing in order to decompose the structure of cell walls and help release soluble components such as phenolic compounds and flavonoids (Zhang et al., 2021). In the study performed by Zhang et al. (2021), Lactobacillus acidophilus (NCIB1899), Lactobacillus casei (CRL 431), and Lactobacillus paracasei (LP33) were cultured in the MRS broth at 37 °C for 30 h and mixed at a ratio of 1:1:1 before being used for inoculation with 2% v/v quinoa protein hydrolysate. During the fermentation, the temperature was maintained at 37 °C for 35 h, followed by sterilisation at 70 °C for 10 min. Thereafter, the content of total phenolic compounds was increased from ~186.8 to ~256.5 mg gallic acid equivalence (GAE)/100 g DW. The total flavonoid content was increased from ~248.9 to ~312.6 mg quercetin equivalence (QE)/100 g DW, and the total antioxidant activity was increased from ~363.0 to ~473.4 µmol TE/g DW. Generally, fermentation does not alter the chemical composition but breaks down the protein molecules to peptides and free amino acids (Rocchetti et al., 2019).

2.2.9 Characterisation of physicochemical properties and structural changes of proteins

After each treatment, the changes in protein structures and physicochemical properties are characterised by using different methods. The structural changes are determined by SDS-PAGE (primary structure), circular dichroism (CD)/FTIR (secondary structure) and surface hydrophobicity and free SH groups (tertiary structure). The methods to probe the changes in techno-functional properties such as solubility, gelation, emulsifying and foaming properties, will be also reviewed in the following sections.

Solubility

Solubility is a critical physicochemical property of proteins which relates to the hydrophilic-hydrophobic balance of the protein and its interaction with solvents. Most plant proteins have low water solubilities, which limit their applications in beverages (Sen & Kahveci, 2020). Thus, modifications of plant proteins to improve their solubilities are necessary for their applications in beverage formulations. The pH affects the solubility of plant globular proteins, and the solubility of QPI is minimum around the pI (~ 4.5) (Steffolani et al., 2016)). This is because of the reduced surface charges of the protein molecules at pI which leads to the reduction of electrostatic repulsions (Manassero et al., 2015; Zhou et al., 2022). Meanwhile, the hydrophobic groups tend to approach each other due to the dominance of hydrophobic interactions.

There are several methods for measuring the solubility of a protein such as gravimetrical (Barr, 2000) and Bradford methods (Bradford, 1976). To analyse the solubility gravimetrically, an excess amount of the protein is added to the solvent and allowing the protein to solubilise. Afterwards, the supernatant after centrifugation is dried and the weight of the resulting solute is measured. The calculation is shown in Equation (1).

$$\text{Protein solubility (\%)} = \frac{\text{Protein weight in supernatant}}{\text{Total protein weight}} \times 100\% \quad (1)$$

The Bradford method utilises Coomassie Brilliant Blue to bind proteins in the supernatant obtained from centrifugation and the absorbance at 595 nm was measured (Bradford & Thodos, 1966). Bovine gamma-globulin at different concentrations was used to produce a standard curve for calculations (absorbance versus protein concentration).

Previous studies on plant protein solubilities as affected by HPH, HIUS and HHP treatments are listed in **Table 8**. Many studies have found an increase in solubility after HPH (Saricaoglu, 2020; Saricaoglu et al., 2018) and HIUS (Jiang et al., 2017; Mir et al., 2019b) treatments due to the decrease in particle sizes. However, prolonged treatments at extreme conditions such as pressures above 150 MPa could lead to the formation of aggregates which decreases the solubility. For example, Saricaoglu et al. (2018) studied the effect of HPH up to 150 MPa on 2% hazelnut meal protein isolate dispersions at pH 12. The solubility of hazelnut meal protein was enhanced from ~77% to ~88% with the pressure increasing up to 100 MPa, while slightly decreased to ~86% at 150 MPa (Saricaoglu et al., 2018). At 150 MPa, inner hydrophobic amino acids were exposed, thus promoting hydrophobic interactions between protein molecules. This could lead to the formation of protein aggregates. The solubility of 10% amaranth protein isolate increased with increasing power and treatment time under HIUS (25-66 J/cm^3 for 15-30 min) treated. The highest solubility (~70%) of amaranth protein isolate was observed at 66 J/cm^3 for 30 min (Constantino & Garcia-Rojas, 2020). Similarly, the increase in solubility after HIUS treatments could be the result of particle size reduction (Constantino & Garcia-Rojas, 2020).

Meanwhile, several studies have been performed to study the influences of HHP on the solubility of plant proteins such as pea protein (Chao et al., 2018), buckwheat (Zhou et al., 2022) and soy protein (Tan et al., 2021)). Chao et al. (2018) found that the solubility of 1% pea protein isolate was decreased from ~27% to ~25% after HHP treatment at 200-600 MPa for 5 min at pH 7 with minor differences among samples treated at different pressure levels. The authors found that HHP treatments in the range of 200-600 MPa induced the formation of insoluble aggregates due to the unfolding of protein and the dominance of hydrophobic interactions. However, Tan et al. (2021) found an increase in the solubility (from ~22% to ~35%) of 4% soy protein isolate after HHP treatment at 400 MPa for 10 min. It has been suggested that HHP induced the formation of soluble aggregates from soy protein molecules. Based on these studies, the impact of HHP on the solubility of proteins is dependent on protein sources, pressure levels, and treatment time.

Table 8: Changes in solubilities of plant protein dispersions after HPH, HIUS and HHP treatments

Protein or source	Conc. (%)	Type	Treatment conditions	Solubility	Reference
Lentil protein isolate (pH 9)	4	HPH	0-150 MPa 1 pass RT	Increased from ~32% (non-treated) to ~46% after 75 MPa treatment, and then decreased to ~36% at 150 MPa	(Saricaoglu, 2020)
Hazelnut meal protein isolate (pH 12)	2	HPH	0-150 MPa 1 pass RT	Increased from ~77% to ~88% when pressure increased from 25 to 100 MPa, slightly decreased to ~86% at 150 MPa	(Saricaoglu et al., 2018)
Amaranth protein isolate (pH 7)	10	HIUS	25-66 J/cm^3 15-30 min 3.0 ±1 ℃	Solubility increased from ~25% to ~70% after HIUS treatment (66 J/cm^3) for 30 min.	(Constantino & Garcia-Rojas, 2020)
Quinoa protein concentrate	47.2	HIUS	39 W 5-30 min 1s/5s, 10s/10s, 5s/1s	Improved after all HIUS treatments. The highest solubility was achieved at a pause time of 1s/5s (3.85%) at 30 min, and lowest at 10s/10s (3.26%) at 30 min.	(Vera et al., 2019)
Quinoa protein isolate	8	HIUS	43 W/cm^2 5-35 min 25 ℃	Increased with increasing treatment time (observed by SDS-PAGE).	(Mir et al., 2019b)
Buckwheat 13S globulin (pH 3, 7)	1	HHP	100-500 MPa 10-30 min	Increased from ~70% to ~93% after 500 MPa for 30 min at pH 7. Increased from~40% to ~63% after 500 MPa treatment for 30 min at pH 3.	(Zhou et al., 2022)
Soy protein isolate (pH 7)	4	HHP	200, 400 MPa 10 min	Increased from ~22% to ~35% after 400 MPa for 10 min.	(Tan et al., 2021)
Pea protein isolate	1	HHP	200-600 MPa 5 min	Decreased from ~27% to 25% at 200-600 MPa at pH 7, with no significant changes of solubility among treated samples at different pressure levels.	(Chao et al., 2018)
Soybean protein isolate (pH 5.9-8.0)	1	HHP	600 MPa 10 min	Increased from ~70% to ~80% at 600 MPa for 10 min. Highest at pH 8.0 (~87%), lowest at pH 5.9 (~42%) at 600 MPa for 10 min	(Manassero et al., 2015)

Particle sizes

The particle size of proteins in solution is strongly related to the solubility, where smaller particles often lead to better solubility (Vera et al., 2019). This is because smaller particles at the same concentrations expose a larger surface area to the solvent. However, large particles

do not necessarily result in poor solubilities. For example, Jiang et al. (2014) applied HIUS at 150-450 W for 12-24 min on 10% w/v black-bean protein isolate dispersions. Soluble aggregates (~37 to ~75 μm) were formed with higher solubility, which could be due to the unfolding of protein and increased protein-water interaction (Jiang et al., 2014).

There are two common methods to measure the particle size of protein isolates, namely microscopy (Ahmed et al., 2018) and light scattering (Constantino & Garcia-Rojas, 2020). The advantage of measuring particle size by microscopy is the ease of distinguishing aggregates and single particles. However, the particle size distribution obtained from microscopic analysis is sometimes considered not bulk representative and it is also time-consuming (Maguire et al., 2018). Another commonly used method is dynamic light scattering, in which a laser beam with a fixed scattering angle is scattered by particles and scattering intensities are collected by a detector. This technique provides a quick analysis with a particle size smaller than 10 μm.

Some recent studies on the impact of non-thermal processing on the particle size of plant proteins are listed in **Table 9**. The typical change in the particle size of protein dispersions subjected to HPH is decreasing because of the shear force when passing through the homogeniser (Kang et al., 2022; Saricaoglu, 2020). Several studies on quinoa and other plant proteins have also found decreases in particle size after HIUS treatments (Mir et al., 2019b; Vera et al., 2019). However, prolonged HPH and HIUS treatments can induce protein aggregation due to increased hydrophobic interactions resulting from the exposure of hydrophobic groups.

For example, Cheng et al. (2022) found the particle size of 5% pea protein isolate dispersions decreased from ~170 nm to ~147 nm after being subjected to HPH treatment at 120 MPa, while decreased to ~153 nm at 240 MPa. The continuously increasing surface hydrophobicity led to

stronger hydrophobic interactions and formation of aggregates. However, Figueroa-González et al. (2022) found the particle size of 3% amaranth protein decreased from ~1200 nm (untreated) to ~500 nm after HIUS treated at 50% amplitude (130 W maximum) for 10 min due to cavitation and shear force that break the non-covalent bonds.

The effect of HHP on the particle size of plant protein dispersions varied with species of proteins, the concentration of proteins, pressure levels and treatment time. For instance, Tan et al. (2021) applied HHP at 200-400 MPa for 10 min on 4% soy protein isolate dispersions and found a decreasing trend in particle size (from ~73 nm to ~36 nm) with increasing pressure levels. The authors suggested that the pressure of up to 400 MPa can disrupt the larger aggregates, thus resulting in smaller particle sizes. However, Zhao (2019) found an increase in particle size of 10% sweet potato protein from ~249.45 nm to ~270.20 nm after HHP at 550 MPa. A possible reason could be the unfolding of protein that led to formation of larger aggregates due to hydrophobic interactions.

Table 9: Effect of HPH, HIUS and HHP treatments on particle sizes of plant protein dispersions

Protein or source	Conc. (%)	Type	Treatment conditions	Particle size	Reference
Pea protein isolate	5	HPH	60-240 MPa 1 pass	Decreased from ~170 nm to ~147 nm at 120 MPa, increased to ~153 nm at 180 MPa.	(Cheng et al., 2022)
Soy 11S globulin	10	HPH	50-150 MPa 2 passes	Decreased from ~367.1 nm to ~104.7 nm at 100 MPa. Slightly increased to ~127.9 nm at 150 MPa.	(Kang et al., 2022)
Lentil protein isolate (pH 9)	4	HPH	25-150 MPa 1 pass RT	Gradually decreased with increasing pressure level. Decreased from ~98.73 μm to ~12.62 μm at 150 MPa.	(Saricaoglu, 2020)
Hazelnut meal protein isolate (pH 12)	2	HPH	0-150 MPa 1 pass RT	Gradually decreased with increasing pressure level. Decreased from ~203.92 μm to ~58.91 μm at 150 MPa.	(Saricaoglu et al., 2018)
Amaranth protein isolate (pH 7)	10	HIUS	25-66 J/cm^3 15-30 min 3.0 °C	Increased from ~414.40 nm to ~478.67 nm at 25 J/cm^3 15 min, decreased at all other conditions. Minimal size at 29 J/cm^3 30 min (~38.96 nm).	(Constantino & Garcia-Rojas, 2020)
Quinoa extract	47.2	HIUS	39 W 5-30 min 1s/5s, 10s/10s, 5s/1s	Increased from ~37.78 nm to ~45.76 nm after 30 min HIUS. Highest with a pause time of 5s/1s at ~45.76 nm, and lowest with 1s/5s at ~39.97 nm.	(Vera et al., 2019)
Soy protein isolate (pH 7)	4	HHP	200-400 MPa 10 min	Gradually decreased from ~73 μm to ~36 μm at 400 MPa.	(Tan et al., 2021)
Lentil protein isolate (pH 7.6)	5	HHP	300-600 MPa 15 min 20-26 °C	Increased from ~81.2-259 μm to ~75.5-293 μm at 300 MPa.	(Ahmed et al., 2019)
Sweet potato protein isolate	10	HHP	0.1-600 MPa 30 min 25 °C	Increased from ~249.45 nm to ~270.20 nm at 550 MPa.	(Zhao, 2019)

Gelation properties

Gelation properties of globular protein have huge impacts on the texture of many food products such as sausages (Iwasaki et al., 2006), tofu (Zhao et al., 2020) and yoghurt (Karaman & Ozcan, 2021). Various processing treatments such as heat treatment (Nicolai & Chassenieux, 2019;

Zheng et al., 2022) and pressurisation (Peyrano et al., 2021; Zhao et al., 2018b) have been extensively used to form plant protein gels in recent years. Generally, plant proteins were found to have inferior gelation properties compared to dairy and other animal proteins (Kornet et al., 2021; Silva et al., 2019). Thus, studies on modifying the gelation properties of plant proteins are required to promote the use of plant proteins as dairy/meat alternatives in the food industry.

The gelation properties can be evaluated by a rheometer using small and large deformation oscillatory rheological measurements. G' and G'' are two parameters that represent the elastic and viscous response of the sample when subjected to different frequencies, temperatures and stress/strain (MacDonald et al., 1969). Frequency sweep, a small oscillatory deformation method, is to keep the strain amplitude at a low, constant value and study the G' and G'' as a function of frequency. For gelled samples, G' and G'' are weakly dependent on the frequency with G' being at least ten times larger than G'' in the entire frequency range. The benefit of this technique is that the measurement is non-destructive to samples. Whereas the strain sweep, a large oscillatory deformation method for gel characterisations, is to keep the frequency and temperature constant and study the G' and G'' with increasing stress or strain amplitudes (MacDonald et al., 1969).

Physical modifications such as HPH and HIUS have been also used to alter the gelation properties of plant proteins (Khatkar et al., 2020; Sun et al., 2022), while HHP was typically used to produce protein gels as an alternative to heat-induced gelation (Peyrano et al., 2021). In the case of HPH and HIUS, the treated plant proteins generally exhibited better gel characteristics than the native proteins. For example, Lozober et al. (2021) found that HPH (50 and 100 MPa) on 5% w/v spirulina protein isolate dispersions resulted in a 3-fold increase in storage modulus (G'). In another study by Li et al. (2020), the impact of HIUS treatment at 0-

450 W for 12 and 24 min (4s/2s) on 10% w/v black bean protein isolate was investigated. The gel strength of black bean protein gel was considerably enhanced after HIUS treatments (2-folds) at 300 W for 24 min (Li et al., 2020). The authors suggested that the HIUS treatment may facilitate the exposure of the hydrophobic amino acid groups of proteins, resulting in increasing protein-protein interactions and gel formations (Li et al., 2020; Tan et al., 2014).

In the case of HHP-induced gelation, various plant proteins have been investigated including soybean proteins (Speroni et al., 2009), potato proteins (Katzav et al., 2020), and cowpea proteins (Peyrano et al., 2021), to name a few. Two studies on potato protein and cowpea protein will be compared below (Katzav et al., 2020; Peyrano et al., 2021). Katzav et al. (2020) compared effects of thermal treatment (45-90 °C for 30 min) and HHP treatment (300-500 MPa for 30 min) on gelation of 10% potato protein isolate at pH 3 and 7. It was reported that all samples treated at pH 3 exhibited higher gel strength than the ones treated at pH 7 because at pH 3 the electrostatic repulsion is at minimum leading to enhancement of hydrophobic interactions (Katzav et al., 2020). Another finding is that the HHP induced gels were less stable compared to heat-induced gels at both pH 3 and 7, suggesting the vitality of heat on protein unfold and aggregations (Katzav et al., 2020). In the study of Peyrano et al. (2021) on 7.5-13.5% (w/w) cowpea protein, their findings agreed with Katzav et al. (2020) that the gel strength increased with rising pressures (400 to 600 MPa), while the gel is still weaker than the heat-treated samples (70-90 °C for 20 min).

Emulsifying and foaming properties

Emulsifying and foaming properties of globular proteins are critical for their applications in food formulations. They are directly related to the quality and shelf life of some food products

such as whipped cream (Sajedi et al., 2014) and mayonnaise (Patist & Bates, 2008). However, many plant proteins such as pea protein (Qamar et al., 2019) and rice protein (Romero et al., 2012) exhibit inferior interfacial properties compared to animal proteins, which prevent them from applying in food formulations. Therefore, various non-thermal processing techniques such as HIUS, HPH, and HHP have been used to improve the emulsifying and foaming properties of plant proteins.

To evaluate the emulsifying and foaming properties of a protein as affected by processing or modification, their capacities and stabilities need to be determined. The EAI of a protein is determined by measuring the absorbance of the sample at 500 nm. The calculation is shown in Equation (2) (Pearce & Kinsella, 1978). The ESI can be calculated by Equation (3) with the determination of the absorbance at 500 nm at the initial and final time points (Pearce & Kinsella, 1978).

$$\text{EAI } (m^2/g) = \frac{2 \times 2.303 \times A_i \times DF}{1 \times c \times \varphi \times L} \qquad (2)$$

$$\text{ESI (min)} = \frac{A_i \times \Delta t}{A_i - A_f} \qquad (3)$$

Where A_i and A_f are the absorbances of samples at the initial and final time after treatment at 500 nm, DF represents the dilution factor, c is the initial protein concentration (g/mL), φ is the oil volume fraction and L is the length of the cuvette.

Recent studies on the impact of HPH, HIUS and HHP treatments on the emulsifying properties are shown in **Table 10**. Generally, HPH and HIUS can enhance the ESI of plant proteins, which might be due to the decrease in particle size and improvement in solubility (Constantino &

Garcia-Rojas, 2020). However, a decrease in ESI also occurred in some cases because of the aggregate formation and solubility reduction induced by extreme conditions (e.g., HPH at 150 MPa) (Dong et al., 2011; Saricaoglu et al., 2018).

For example, Saricaoglu et al. (2018) studied the effect of HPH at 0-150 MPa for 1 pass on the emulsifying properties of 2% hazelnut meal protein. They found that the EAI increased from 87.79 m^2/g to 96.02 m^2/g from 0 to 100 MPa and slightly decreased to 93.20 m^2/g at 150 MPa (Saricaoglu et al., 2018). The ESI had a similar trend as EAI which increased from 12.47 min to 33.32 min at 0-100 MPa and further decreased to 29.99 min at 150 MPa (Saricaoglu et al., 2018). The authors suggested that HPH up to 100 MPa could induce the partial unfolding of proteins, which exposes more hydrophobic groups and leads to better emulsifying properties (Saricaoglu et al., 2018). While HPH at 150 MPa might induce further unfolding of proteins, leading to aggregation and solubility reduction, thus reducing the EAI and ESI (Saricaoglu et al., 2018). Similarly, Constantino and Garcia-Rojas (2020) applied HIUS at 25-66 J/cm^3 for 15-30 min to 10% amaranth protein isolate. Both EAI (from 136.95 m^2/g to 158.64 m^2/g) and ESI (from 17.87 min to 28.12 min) increased with increasing in HIUS power and treatment time (Constantino & Garcia-Rojas, 2020). These results suggested that both HPH and HIUS can improve the emulsifying properties of plant proteins at mild treatment conditions (e.g., HPH at 100 MPa).

Same as HPH and HIUS, the effect of HHP on the emulsifying properties of plant protein is also dependent on the processing conditions. Ahmed et al. (2018) investigated the impact of HHP (200-600 MPa for 15 min) on the physicochemical properties of 20 % kidney bean protein isolate. Both EAI (from 24.2 m^2/g to 40.4 m^2/g) and ESI (from 68.3 min to 142.3 min) were enhanced at 400 MPa but decreased to 33.9 m^2/g and 80.8 min, respectively at 600 MPa. The

improvement of the emulsifying properties was due to the partially unfolding of globular proteins which increased the surface area of the protein molecules for adsorption. The exposed hydrophobic amino acids also enhanced the interactions between protein molecules. However, the weakening of emulsifying properties occurring at 600 MPa could be due to the decrease in interactions between protein molecules which limited the formation of strong interfacial membranes (Ahmed et al., 2018; Chao et al., 2018). Thus, HHP treatment under mild conditions (e.g., ~400 MPa for 15 min) might improve the emulsifying properties of plant protein dispersions.

Table 10: Changes in EAI and ESI of plant protein dispersions after HIUS, HPH and HHP treatments

Protein	Treatment	Treatment conditions	EAI	ESI	Reference
Lentil protein isolate 4% (pH 9)	HPH	0-150 MPa 1 pass RT	Increased from 100.22 m^2/g to 125.16 m^2/g at 100 MPa. Decreased to 106.63 m^2/g at 150 MPa.	Increased from 39.12 min to 226.34 min at 100 MPa. Decreased to 138.07 min at 150 MPa.	(Saricaoglu, 2020)
Hazelnut meal protein isolate 2% (pH 12)	HPH	0-150 MPa 1 pass RT	Increased from 87.79 m^2/g to 96.02 m^2/g at 100 MPa. Decreased to 93.20 m^2/g at 150 MPa.	Increased from 12.47 min to 33.32 min at 100 MPa. Decreased to 29.99 min at 150 MPa.	(Saricaoglu et al., 2018)
Peanut protein isolate	HPH	0-80 MPa	Increased from 24.4 m^2/g to 32.4 m^2/g at 80 MPa.	Decreased from 20.6 min to 12.2 min at 80 MPa.	(Dong et al., 2011)
Pea protein isolate 10% (pH 7)	HIUS	200-500 W 5-20 min 3s/2s <30 °C	Decreased from ~140 m^2/g to ~30 m^2/g at 500 W for 5-20 min.	Increased the most from ~17% to ~28% with 10 min HIUS at 500 W. No significant change with 20 min HIUS at all power levels.	(Gao et al., 2022)
Amaranth protein isolate 10%	HIUS	25-66 J/cm^3 15-30 min 3.0 °C	Increased with pressure and time from 136.95 m^2/g to 158.64 m^2/g at 66 J/cm^3 for 30 min.	Increased the most at 50 J/cm^3 for 30 min, from 17.87 min to 28.12 min.	(Constantino & Garcia-Rojas, 2020)
Buckwheat 13S globulin 1% (pH 3, 7)	HHP	100-500 MPa 10-30 min	Increased with pressure and time (from ~72 m^2/g to ~83 m^2/g). EAI at pH 7 is higher than pH 3 (~67 m^2/g).	ESI at pH 3 increased with pressure and time (from ~27% to ~38%). Increased from ~36% to ~46% at 100 MPa at pH 7 and decreased gradually to ~41% at 500 MPa.	(Zhou et al., 2022)
Lentil protein isolate 5% (pH 7.6)	HHP	300 MPa 15 min 20-26 °C	Increased from 85.44 m^2/g to 111.37 m^2/g at 300 MPa.	Decreased from 20.27 min to 16.38 min at 300 MPa.	(Ahmed et al., 2019)
Kidney bean protein isolate 20%	HHP	200-600 MPa 15 min	Increased from 24.2 m^2/g to 40.4 m^2/g at 400 MPa. Decreased to 33.9 m^2/g at 600 MPa.	Increased from 68.3 min to 142.3 min at 400 MPa. Decreased to 80.8 min at 600 MPa.	(Ahmed et al., 2018)
Pea protein isolate 1% (pH 3, 5, 7)	HHP	200-600 MPa 5 min	N/A	Decreased with pressure at pH 3 and 5. Increased to ~100% at 400 MPa at pH 7, then decreased to ~85% at 600 MPa.	(Chao et al., 2018)

Foam is a two-phase system in which air is surrounded by a liquid phase forming a cohesive interfacial film. The foaming properties are critical for the application of proteins in food formulations as they might affect the mouthfeel of the products (Sato et al., 2022). Foaming capacity (FC) and stability (FS) are two critical parameters that indicate the foaming property of the protein. The FC and FS can be calculated using Equation (4) and Equation (5).

$$FC=\frac{V_b-V_a}{V_a}\times 100\% \qquad (4)$$

where Vb and Va indicate the volume of foam after mixing and the volume of the original protein solution, respectively.

$$FS=\frac{V_{30}}{V_0}\times 100\% \qquad (5)$$

where V_0 and V_{30} represent the initial volume of foam after mixing and the volume of foam after storage for 30 min, respectively.

Generally, the foaming properties of plant proteins are inferior compared to animal proteins such as egg white protein (Saricaoglu, 2020; Van der Plancken et al., 2007). Several studies have been conducted on the foaming capabilities of plant protein dispersions as affected by non-thermal processing techniques, which are listed in **Table 11**. In most cases, the FC and FS were increased after the HIUS and HPH treatment (Figueroa-González et al., 2022; Saricaoglu, 2020).

For example, Kang et al. (2022) investigated the effect of HPH at 50-150 MPa on the foaming properties of 10% soy 11S globulin. Both FC (from 161.11% to 205.97%) and FS (from 46.00% to 83.38%) were enhanced at 150 MPa due to the decrease in particle size and increase in surface hydrophobicity after HPH treatment (Kang et al., 2022). Similarly, Xiong et al. (2018)

studied the impact of HIUS at 22-48 W/cm^2 for 30 min (5s on/2s off) on 5% pea protein isolate. The FC was improved from ~150% to ~200% at 48 W/cm^2, and the FS was improved from ~59% to ~73%. A possible explanation suggested by the author was the partial denaturation of pea protein isolate leading to faster adsorption at the air-water interface.

However, previous studies found various effects of HHP on the foaming properties of plant proteins. For example, Chao et al. (2018) investigated the impact of HHP at 200-600 MPa on 1% pea protein isolate dispersion. The FC of the pea protein isolate did not change (~38%) with the pressure, while the FS decreased from ~58% to ~38% at 600 MPa (Chao et al., 2018). It could be due to the formation of aggregates during HHP treatments, which could weaken the interfacial membranes (Chao et al., 2018). On the contrary, Zhou et al. (2022) found that FC (from ~83% to ~87%) and FS (from ~40% to ~50%) of 1% buckwheat 13S globulin increased after HHP (100-500 MPa for 10-30 min) treatment. In this case, the authors suggested that HHP treatment enhanced the solubility, where only the soluble fractions of protein are involved in foam formation (Zhou et al., 2022). Based on these studies, the effect of HHP on the foaming properties of plant proteins varied with different protein sources, pressure levels and treatment times.

Table 11: Changes in foaming capacity and stability of plant protein dispersions after HIUS, HPH and HHP treatments

Protein isolates	Conc. (%)	Treatment	Treatment conditions	FC	FS	Reference
Soy 11S globulin	10	HPH	50-150 MPa 2 passes	Increased from 161.11% to 205.97% at 150 MPa.	Increased from 46.00% to 83.38% at 150 MPa.	(Kang et al., 2022)
Lentil (pH 9)	4	HPH	0-150 MPa 1 pass RT	Increased from 10.00% to 85.33% at 100 MPa. Decreased to 66.63% at 150 MPa	Increased from 4.29% to 66.63% at 100 MPa. Decreased to 40.38% at 150 MPa	(Saricaoglu, 2020)
Hazelnut meal (pH 12)	2	HPH	0-150 MPa 1 pass RT	Increased from 40.67% to 90.00% at 100 MPa. Decreased to 70.17% at 150 MPa	Increased from 22.83% to 78.17% at 100 MPa. Decreased to 73.67% at 150 MPa	(Saricaoglu et al., 2018)
Amaranth (pH 7)	3	HIUS	750 W 50% amplitude 10 min	Increased from 236.7% to 293.0% after 10 min HIUS.	Increased from 60.6% to 66.1% after 10 min HIUS.	(Figueroa-González et al., 2022)
Pea (pH 7)	10	HIUS	200-500W 5-20 min 3s/2s <30 °C	Decreased from ~100% to ~90% at 500 W. Increased with time	Increased from ~40% to ~80% at 500 W. Increased with time	(Gao et al., 2022)
Pea	5	HIUS	22-48 W/cm^2 30 min 5s/2s Ice bath	Gradually increased from ~150% to ~200% at 48 W/cm^2.	Gradually increased from ~59% to ~73% at 48 W/cm^2.	(Xiong et al., 2018)
Buckwheat 13S globulin (pH 3, 7)	1	HHP	100-500 MPa 10-30 min	Increased from ~82.5% to ~90% at 200 MPa and fell back at 500 MPa at pH 7. Increased from ~58% to ~80% at 500 MPa at pH 3.	Increased from ~30% to ~38% at 500 MPa at pH 7. Increased from ~41% to ~50% at 500 MPa at pH 3.	(Zhou et al., 2022)
Lentil (pH 7.6)	5	HHP	300MPa 15 min 20-26 ˚C	Decreased from 86.02% to 81.43% at 300 MPa.	Increased from 60.21% to 62.85% at 300 MPa.	(Ahmed et al., 2019)
Kidney bean	20, 25	HHP	200-600 MPa 15 min	Decreased from 76.7% to 44.6% at 600 MPa.	Decreased from 54.5% to 40.5% at 600 MPa.	(Ahmed et al., 2018)

Primary structure

The primary structure of a globular protein is the polymerisation of different amino acids linked by peptide bonds (Barbhuiya et al., 2021). The amino acids are linked linearly one by one. Most amino acids have non-polar side chains, such as alanine, valine and leucine which contain bulky side chains and they are hydrophobic (Volkenstein, 1965). A relatively smaller group of polar amino acids such as tyrosine and glycine can form hydrogen bonds. There are also several acidic (negatively charged: aspartate and glutamate) and basic (positively charged: arginine, lysine, and histidine) amino acids which can form ionic bonds (Volkenstein, 1965).

The primary structure of a protein can be analysed by mainly two methods, SDS-PAGE and Liquid chromatography-mass spectrometry (LC-MS), both based on molecular weight. LC-MS analysis can provide the amino acid profile by breakdown the protein into smaller peptides using trifluoroacetic acid and acetonitrile, dissolving the samples into the mobile phase, followed by separating the peptides by the molecular weight (Visser et al., 1991). On the other hand, SDS-PAGE is mainly utilized for identification of polypeptides in proteins (Laemmli, 1970). The addition of SDS and heat treatment help disrupt the tertiary and secondary structure of protein samples (Laemmli, 1970). To break down disulfide bonds, a reducing agent such as β-mercaptoethanol is usually added (Shen et al., 2021). Then the samples are loaded onto a polyacrylamide gel and separated based on the molecular weight of the polypeptides during electrophoresis. By comparing the results from the reducing and non-reducing SDS-PAGE, information about disulfide bonds can be obtained (Jiang et al., 2017).

The effect of physical modifications (HPH, HIUS and HHP) on the primary structure of plant proteins have been studied (Kornet et al., 2021; Zhao et al., 2022). Due to the physical nature

of these modifications, the molecular weight distributions were usually maintained. Some studies found an increase in the overall band intensity after treatments, which can be attributed to the improvement of protein solubility (Gao et al., 2022; Mir et al., 2019a).

Secondary structure

After forming the polypeptide backbone, the hydrogen atoms in N-H groups and oxygen atoms in C=O groups appear to have positive and negative charges due to electron exchanges through ionic bonds (Figueroa-González et al., 2022). These atoms approach each other because of electrostatic attractions. As a result, the position of the amino acids backbone is altered and formed different secondary structures such as α-helix, β-sheet, β-turn and random coil (Figueroa-González et al., 2022). The hydrogen atoms in the N-H group and oxygen atoms in the C=O group can form the α-helix through hydrogen bonding, which is a right-hand helix conformation. Whereas β-sheet conformation is composed of β-strands, in which several pairs of hydrogen-bonded oxygen and hydrogen atoms hold the backbone into pleated sheets (Ahn et al., 2017). β-turn is defined by four consecutive amino acids and formed by a hydrogen bond between the first and last amino acids (Ahn et al., 2017). Random coil refers to disordered amino acid orientations (Ahn et al., 2017).

Conformational changes in proteins are related to the changes in physicochemical and techno-functional properties. CD and FTIR are two common techniques for probing the secondary structures of proteins. When analysing the FTIR spectra, the region at ~1632 cm^{-1} relates to the C=O vibration (amide I), and the regions at ~1526 cm^{-1} and ~1235 cm^{-1} correspond to the CN stretching and NH bending in amide II and III, respectively (Ahmed et al., 2019; Cheng et al., 2022). The deconvolution of the amide I region can be used to determine the secondary

structure components of a protein. The specific regions of α-helix, β-sheet, β-turn and random coil are in ranges of 1654-1658 cm^{-1}, 1624-1642 cm^{-1}, 1666-1688 cm^{-1} and 1646-1650 cm^{-1}, respectively (Yang et al., 2015).

Some recent studies on the impact of HPH, HIUS and HHP treatments on the secondary structure changes of plant proteins are listed in **Table 12**. Secondary structures of proteins were changed after the treatments, which were dependent on the protein source, treatment type and treatment conditions. For example, Cheng et al. (2022) found that the α-helix and β-turn contents of 5% pea protein isolate were decreased after HPH treatments at 60-240 MPa, while the β-sheet and random coil contents were increased. The authors found a positive correlation between the content of β-sheet and the tensile strength of the film formed by pea protein isolate (Cheng et al., 2022).

A study by Vera et al. (2019) showed different conformational changes among quinoa protein extract when HIUS treated at various pause (on/off) times (10s/10s, 5s/1s and 1s/5s). They found that the changes in β-sheet, α-helix and random coil contents of 10s/10s and 5s/1s with increasing HIUS time are similar to each other. Under these two HIUS conditions, the β-sheet content decreased from ~32% to ~23% at 5-20 min and then increased to ~27% at 30 min. The α-helix content increased from ~15% to ~24% at 5-20 min and decreased to ~16% at 30 min. The content of random coil under 10s/10s and 5s/1s decreased by ~4% after 30 min HIUS. While for samples under 1s/5s HIUS, the α-helix content increased from ~15% to ~25% at 5-30 min, and the β-sheet content decreased gradually from ~32% to ~23% at 5-30 min. The β-turn content increased slightly from ~22% to ~24% at 5-30 min. The random coil content decreased from ~32% to ~28% at 5-30 min.

Khan et al. (2015) studied the effect of HHP on sweet potato proteins at pH 3, 6 and 9, and changes in protein secondary structures varied at different pHs. At pH 3 and 6, the α-helix and β-turn contents decreased after treatment, while the β-sheet and random coil contents increased. At pH 9, the α-helix and β-sheet contents decreased, and the β-turn and random coil contents increased after treatment. However, Zhao (2019) found that at pH 3, the α-helix and random coil contents increased but β-sheet and β-turn contents decreased. The β-sheet, β-turn and random coil contents increased at pH 6, while the α-helix content decreased. At pH 9, the random coil content increased with the decrease of α-helix, β-sheet, and β-turn contents. These studies indicated that the conformational changes of protein after HPH, HIUS and HHP were related to the protein source, treatment type and treatment conditions (e.g., time and pH).

Table 12: Changes in protein secondary structure after HPH, HIUS and HHP treatments (↑ stands for increasing, ↓ stands for decreasing, = means no significant changes)

Protein or source	Conc. (%)	Type	Treatment conditions	α-helix	β-sheet	β-turn	Random Coil	Reference
Quinoa extract	47.2	HIUS	39 W 5-30 min 1s/5s	↑	↓	↑	↓	(Vera et al., 2019)
			10s/10s	↑5-20 min ↓30 min	↓5-20 min ↑30 min	0	↓10-30 min	
			5s/1s	↑5-20 min ↓30 min	↓5-20 min ↑30 min	=	↓10-30 min	
Amaranth protein isolate (pH 7)	3	HIUS	750 W 50% amplitude 10 min	↓	↑	↑	↑	(Figueroa-González et al., 2022)
Pea protein isolate (pH 7)	10	HIUS	11.14-31.34 W/cm^2 5-20 min 3s/2s <30 °C	↓with power ↑with time ↓↓16.89 W/cm^2 20 min	↓with power ↑with time	↓	Only appears at 31.34 W/cm^2 ↓with time	(Gao et al., 2022)
Zein protein isolate (Corn)	1	HPH	50-150 MPa 1 pass	↓50 MPa ↑75-150 MPa	↑50 MPa ↓75-150 MPa	↓75 MPa ↑all other	↑50 MPa ↓75-150 MPa	(Sun et al., 2016)
Pea protein isolate	5	HPH	60-240 MPa 1 pass	↓	↑	↓60 MPa = 120-240 MPa	↑	(Cheng et al., 2022)
Sweet potato protein isolate (pH 3)	1	HHP	200-600 MPa	↓all pressure ↓↓200 MPa	↑all pressure ↑↑200 MPa	↓↓200 MPa = 400 MPa ↓600 MPa	↑200 MPa ↓400, 600 MPa	(Khan et al., 2015)
Sweet potato protein isolate (pH 6)				↓200, 400 MPa ↑600 MPa	↑200, 400 MPa ↓600 MPa	↓200 MPa ↓↓400 MPa ↑600 MPa	↑200, 400 MPa = 600 MPa	
Sweet potato protein isolate (pH 9)				↓200, 600 MPa ↑400 MPa	↑200 MPa ↓400, 600 MPa	↓200 MPa ↑400 MPa = 600 MPa	↓200 MPa ↑400, 600 MPa	
Soy protein isolate (pH 7)	4	HHP	200, 400 MPa 10 min	↑	↓	↑	↑	(Tan et al., 2021)
Buckwheat 13S globulin (pH 3, 7)	1	HHP	100-500 MPa 10-30 min	↓	↑	↓	↑	(Zhou et al., 2022)

Sweet potato protein isolate (pH 3)	4	HHP	250-550 MPa 30 min	↑	↓	↓	↑	(Zhao, 2019)
Sweet potato protein isolate (pH 6)				↓	↑	↑	↑	
Sweet potato protein isolate (pH 9)				↓	↓250, 400 MPa ↑550 MPa	↑250 MPa ↓400, 550 MPa	↑250, 400 MPa ↓550 MPa	

Tertiary structure

The 11S globulin of quinoa is a globular protein containing hydrophobic amino acids surrounded by hydrophilic amino acids (Brinegar & Goundan, 1993). These amino acids can form polypeptides that are connected each other through different types of bonds and interactions. The tertiary structure of a globular protein is usually stabilised by disulfide bonds, hydrophilic interactions, hydrophobic interactions, hydrogen bonds and ionic bonds (Gao et al., 2022). Disulfide bonds are covalent bonds, which are formed between a pair of SH groups side chains of two cysteine residues (Gao et al., 2022). In the case of hydrophilic and hydrophobic interactions, the hydrophilic amino acids tend to interact with the aqueous phase, while the hydrophobic amino acids approach each other. For hydrogen bonds, interactions form between a negatively charged donor O and a positively charged acceptor H in another amino acid by electrostatic force (Fang et al., 2021). Ionic bonds, also known as salt bridges, are formed with atoms having opposite charges due to electrostatic attractions (Bader & Henneker, 1965). The changes in protein tertiary structure can be investigated by determining the contributions of these interactions.

The surface hydrophobicity of proteins is strongly related to the conformational changes in the protein structure (Cheng et al., 2022). The aromatic amino acids of a protein usually have hydrophobic side chains which are buried inside the native protein (Daliri et al., 2021). When the treatments such as HPH, HIUS and HHP are applied, the protein unfolds leading to the exposure of hydrophobic side chains to the surface of proteins (Peyrano et al., 2021). As a result, the surface hydrophobicity of protein increases. 8-Anilinonaphthalene-1-sulfonic acid (ANS) is a fluorescence probe that is commonly used in determining the surface hydrophobicity of a protein. It binds to the hydrophobic region of a protein as a fluorescent dye

and the fluorescence intensity can be determined by a spectrofluorometer from 400 nm to 600 nm emission wavelength and the excitation at 365 nm (Jiang et al., 2009; Zhou et al., 2016). Previous studies on plant protein tertiary structural changes as induced by these three treatments are listed in **Table 13**. Typically, HPH, HIUS and HHP treatments under mild conditions induced an increase in surface hydrophobicity (Cheng et al., 2022; Fang et al., 2021; Tan et al., 2021), while higher pressure or power levels might cause aggregations which reduce the surface hydrophobicity (Kang et al., 2022; Khan et al., 2015).

For example, Kang et al. (2022) found that the surface hydrophobicity of 10% soy 11S globulin was increased after HPH treatment with increasing pressure from 55.29 to 70.41 at 100 MPa, while increased to 59.29 at 150 MPa. The authors suggested that the particle size was decreased at 50-100 MPa, thus exposing the hydrophobic amino acids and increasing the surface hydrophobicity. However, HPH at 150 MPa could induce aggregation because of the increase in hydrophobic interactions. Fang et al. (2021) studied 0.1% w/v soy protein subjected to HIUS treatment at 540 W for 5 min at pH 7 and found an increase in surface hydrophobicity after treatment. It could be due to the decrease in particle size and the unfolding of protein under HIUS treatments. In the case of HHP, Khan et al. (2015) found that the surface hydrophobicity of 1% (w/v) sweet potato protein decreased from ~142 to ~128 at 200-600 MPa for 15 min. This could be due to protein aggregation induced by hydrophobic interactions (Khan et al., 2015).

Table 13: Changes in protein surface hydrophobicity after HPH, HIUS and HHP treatments

Protein or source	Conc. (%)	Type	Treatment conditions	Surface hydrophobicity	References
Pea protein isolate	5	HPH	60-240 MPa 1 pass Heat exchanger for cooling	Increased from ~10 to ~50 at 240 MPa.	(Cheng et al., 2022)
Soy 11S globulin	10	HPH	50-150 MPa 2 passes	Increased from 55.29 to 70.41 at 100 MPa. Decreased to 59.29 at 150 MPa.	(Kang et al., 2022)
Pea protein isolate (pH 7)	10	HIUS	11.14, 16.89, 31.34 W/cm^2 5-20 min 3s/2s <30 ℃	Decreased from ~2800 to ~800 at 31.34 W/cm^2.	(Gao et al., 2022)
Soy protein isolate (pH 7)	0.1	HIUS	540 W 5 min Ice bath	Increased from ~9.5 to ~12 after treatment.	(Fang et al., 2021)
Quinoa extract	47.2	HIUS	39 W 5-30 min 1s/5s	Increased at 5 min	(Vera et al., 2019)
			10s/10s	Increased, highest at 5 and 20 min	
			5s/1s	Increased at 5 and 20 min	
Buckwheat 13S globulin (pH 3, 7)	1	HHP	100-500 MPa 10-30 min	Increased from ~3000 to ~6000 at 500 MPa at pH 3. No significant changes at pH 7 (~800)	(Zhou et al., 2022)
Soy protein isolate (pH 7)	4	HHP	200, 400 MPa 10 min	Increased from ~30000 to ~45000 at 400 MPa.	(Tan et al., 2021)
Cowpea protein isolate (pH 7)	1	HHP	200-600 MPa 5 min 20-38 ℃	Increased from 1356 to 3450 at 600 MPa.	(Peyrano et al., 2016)
Sweet potato protein isolate	1	HHP	200-600 MPa 15 min 25 ℃	Decreased from ~142 to ~128 at 600 MPa.	(Khan et al., 2015)

The content of free SH groups is another parameter to reflect the tertiary structural changes of a protein. By measuring the difference in free SH contents before and after treatments, the changes in disulfide bonds can be determined. Three factors that affect the formation of S-S bonds are the physical accessibility of the cysteine side chains, the pH and the redox environment. The formation of disulfide bonds usually occurs in alkaline and oxidising conditions rather than acidic and reducing conditions. Physical treatments such as HPH and HIUS under mild conditions usually induce an increase in free SH content, while HHP

treatments can reduce the content of the free SH (Cheng et al., 2022; Constantino & Garcia-Rojas, 2020; Zhou et al., 2022). Previous studies on the changes in SH groups as affected by HIUS, HHP, and HPH are listed in **Table 14**. For example, Cheng et al. (2022) found that HPH at 60-240 MPa (single pass) on 5% pea protein isolate dispersion can cause the free SH content to increase from ~35 μmol/g to ~45 μmol/g with increasing pressure. The authors suggested that this could be due to the unfolding of protein after HPH treatment (Cheng et al., 2022). In the case of HIUS, Constantino and Garcia-Rojas (2020) investigated the effect of various power (30-90% amplitude or 25-66 J/cm^3) and time (15-30 min) on 20 mL 10% Amaranth protein isolate dispersion at 3 °C. The free SH content was found to be gradually increased from ~7 to ~11.5 μmoL/g soluble protein at 50 J/cm^3 (60% amplitude) for 30 min but fell back to ~9 μmoL/g at 66 J/cm^3 (90% amplitude) for 30 min. The authors suggested that during HIUS treatment, the disrupted force induced a partial unfolding of the protein tertiary structure, while the generation of hydrogen peroxide could reduce the free SH content under prolonged HIUS treatments (Constantino & Garcia-Rojas, 2020). The hydrogen peroxide generated in the HIUS treatment might oxidise the free SH groups, thus decreasing the content of free SH group (Constantino & Garcia-Rojas, 2020; Zhu et al., 2018).

However, another study on 1% buckwheat 13S globulin under HHP indicated that the free SH group decreased at both pH 3 (from~10 μmol/g to ~5 μmol/g) and pH 7 (from~2 μmol/g to ~1 μmol/g) after the HHP treatment at 100-500 MPa (Zhou et al., 2022). They suggested that the HHP treatment induced the formation of disulfide bonds and caused the protein to unfold, while an alkaline environment would further decrease the free SH content (Zhou et al., 2022).

Table 14: Effect of HPH, HIUS and HHP treatments on free SH groups of plant protein dispersions

Protein or source	Conc. (%)	Type	Treatment conditions	Free SH groups (µmol/g soluble protein)	References
Pea protein isolate	5	HPH	60-240 MPa 1 pass Heat exchanger for cooling	Gradually increased from ~35 to ~45 at 240 MPa.	(Cheng et al., 2022)
Soy 11S globulin	10	HPH	50-150 MPa 2 passes	Increased from 5.14 to 6.90 at 50 MPa. Decreased to 5.97 at 150 MPa.	(Kang et al., 2022)
Amaranth protein isolate (pH 7)	3	HIUS	750 W 50% amplitude 10 min	Decreased from ~9 to ~7 at 750 W for 10 min.	(Figueroa-González et al., 2022)
Soy protein isolate (pH 7)	0.1	HIUS	540 W 5 min Ice bath	Decreased from ~13.2 to ~12.5 at 540 W for 5 min.	(Fang et al., 2021)
Amaranth protein isolate (pH 7)	10	HIUS	25-66 J/cm^3 15-30 min 3.0 ±1˚C	Increased from ~7 to ~11.5 at 50 J/cm^3 for 30 min. Decreased to ~9.5 at 66 J/cm^3 for 30 min.	(Constantino & Garcia-Rojas, 2020)
Buckwheat 13S globulin (pH 3, 7)	1	HHP	100-500 MPa 10-30 min pH 3 and 7	Decreased from ~10 to ~5 at 500 MPa at pH 3. Decreased from ~2 to ~1 at 500 MPa at pH 7.	(Zhou et al., 2022)
Soy protein isolate (pH 7)	4	HHP	200, 400 MPa 10 min	Increased from ~2.25 to ~2.75 at 400 MPa.	(Tan et al., 2021)
Sweet potato protein isolate	4	HHP	250-550 MPa 30 min	Increased from 2.85 to 3.14 at 400 MPa. Decreased to 3.03 at 550 MPa.	(Zhao, 2019)
Peanut protein isolate	5	HHP	50-200 MPa 5 min 25 ± 2 ˚C	No significant changes from 50 to 100 MPa, maintained at ~4. Decreased to ~2 at 200 MPa.	(He et al., 2014)

In general, this literature review summarised the background information on quinoa proteins, including chemical compositions of quinoa seeds, quinoa proteins extraction methods, modification methods, and characterisation methods. Some studies have been conducted on plant proteins subjected to non-thermal processing technologies but most of them focused on soy, pea, and faba bean protein isolates. Systematic investigations and comparisons of three non-thermal processing techniques namely HHP, HPH, and HIUS on the physio-chemical,

microstructural, and techno-functional properties of QPI dispersion were limited.

The major objectives of this thesis are:

1. To investigate the impact of HPH processing on physicochemical, rheological properties, and microstructural characteristics of the QPI suspensions.
2. To compare the effect of HHP treatment (100, 250, 400, and 600 MPa) and thermal treatment (81 ± 2 °C, 30 min) on the protein aggregation, flow behaviour, viscoelasticity, and microstructural characteristics of QPI dispersions at pH 5, 7, and 9.
3. To compare the effect of HIUS and HHP on microstructural characteristics and physicochemical properties of diluted (1% w/w) QPI dispersions at pH 5, 7, and 9.

3. Chapter 3: Impact of high-pressure homogenization on physico-chemical, structural, and rheological properties of quinoa protein isolates*

Keywords: Quinoa protein isolate; High pressure homogenisation; Viscoelasticity; Interfacial properties; Microstructures

3.1. Introduction

A possible solution to accommodating the rapid growth in world population and alleviating greenhouse gas emission is markedly increasing the consumption of plant-based foods. Significant efforts have been devoted to fabricating plant-derived food products such as meat-analogues and dairy-alternatives (Dekkers et al., 2018; Mäkinen et al., 2016; McClements et al., 2019). The global and local food manufacturers and consumers are increasingly demanding that their proteins come from a sustainable source. Plant proteins, such as quinoa protein, appear as promising candidates (Dakhili et al., 2019). Quinoa (*Chenopodium quinoa* Willd.) is a pseudocereal that originates from South America and recently becomes one of the emerging protein sources having an excellent well-balanced essential amino acid profile and bioactive peptides (Abugoch et al., 2008; Shen et al., 2021). Generally, the quinoa seed contains higher contents of protein (12–23%w/w), lipids (4–6%w/w), and lower content of starch (55–60%w/w) compared to other major cereals (e.g. rice, barley, and wheat) (Contreras-Jimenez et al., 2019; Dakhili et al., 2019; Wood et al., 1993). Quinoa proteins co-exist with lipid, fibre and saponin in the embryonic tissue while starch is mainly stored in the perisperm (Ando et al., 2002; Dakhili et al., 2019; Prego et al., 1998). In addition, quinoa proteins are also health-promoting food ingredients. Peptides derived from quinoa globulins are able to inhibit digestion of dietary carbohydrates and reduce the risk of type II diabetes as revealed by a recent *in vitro* simulated gastrointestinal digestion study (Vilcacundo et al., 2017). Depending on variety, quinoa has a protein content in a range of 12–23%, which is mainly composed of two protein fractions-11 S globulin (50–60 kDa) and 2S albumin (< 15 kDa) (Kaspchak et al., 2017). The globulin and albumin account for around 37% and 35% of the total proteins in quinoa and both of them are stabilised through disulphide bonds (Brinegar & Goundan, 1993; Brinegar et al., 1996).

Compared to animal and dairy proteins, plant proteins show inferior techno-functional

properties such as poor solubility (Day et al., 2022). Therefore, in order to fulfil the potential of plant protein applications in the food industry, their techno-functional properties including solubility, gelation, foaming and emulsifying capabilities must be improved (Abugoch et al., 2008). Recently, many modification approaches have been developed and they generally fell into three categories including chemical reaction (i.e. glycosylation, acylation, succinylation, deamidation, pH-manipulation, and phosphorylation) (Nasrabadi et al., 2021), biochemical modifications (fermentation and enzymatic hydrolysis) (Panyam & Kilara, 1996) and physical processing (i.e. thermal treatment and extrusion cooking) (Brishti et al., 2021). Most of these methods are time consuming, high-cost, and energy intensive, which limit their wide and prompt applications in the food industry (Akharume et al., 2021).

In recent years, non-thermal processing technologies, such as high pressure homogenisation (HPH) have received massive attention from both industry and academia and have been applied extensively to modify the molecular structures, physico-chemical properties, and techno-functionalities of food biopolymers (Levy et al., 2021; Lullien-Pellerin & Balny, 2002). Most of studies focused on starch, dairy, and animal-derived proteins (Dissanayake & Vasiljevic, 2009; Mirmoghtadaie et al., 2016). HPH typically reaches pressure levels in a range of 50–200 MPa and has found many important applications in food industry such as improving emulsion and beverage stability, reducing particle size, and stabilising proteins in dispersions (Levy et al., 2021). During the HPH process, a continuous flowing fluid or suspension are pushed through a narrow gap, which lead to high turbulence and shear stress (dos Santos Aguilar et al., 2018). Those effects can lead to the modification of the physico-chemical properties of plant proteins such as particle disruption and improvement of gelation and emulsification properties. Recently, some studies have investigated the effect of HPH processing on plant proteins including faba bean proteins (Yang et al., 2018), kidney bean proteins (Guo et al., 2021), potato

proteins (Hu et al., 2021; Levy et al., 2021), pea proteins (Melchior et al., 2022), and lentil proteins (Saricaoglu, 2020). Those studies suggested that HPH processing can induce significant modifications of physico-chemical and techno-functional properties of plant proteins such as improvement of solubility, foaming, gelling and emulsifying properties, and reduction in particle size. However, to the best of our knowledge, there is no information about applying HPH on the modifications of physico-chemical, structural, and rheological properties of quinoa protein isolates. Therefore, the main focus of this study is to investigate the impact of HPH processing on physico-chemical, rheological properties, and microstructural characteristics of the QPI suspensions. Moreover, the effect of HPH processing on the QPI gel formation was also studied as thermally induced gelation is considered as one of the most critical attributes of plant proteins and plays important roles in many food and pharmaceutical applications (Luo et al., 2021; Yang et al., 2022b). We believe that the knowledge gained from this study will lay a foundation for future HPH applications in other emerging protein-based system such as rapeseed, hemp seed, and algae proteins.

3.2. Materials and methods

3.2.1. Materials

Quinoa seeds were kindly donated by Kiwi Quinoa Inc. (Taihape, New Zealand). According to the supplier, the quinoa seeds used for protein extractions contain 17.5% w/w protein, 4.5% w/w fat, 64.0%w/w sugar, and 11.0w/w dietary fibre based on the dry weight. All chemicals including SDS, HCl, NaOH, petroleum ether, isopropanol, acetic acid, low viscosity mineral oil (M5904), Ellman's reagent (5′, 5-dithiobis (2-nitrobenzoic acid), DTNB), 8-anilino-1-naphthalene sulphonate (ANS), gallic acid, Folin-Ciocalteu reagent, methanol, and sodium azide were purchased from Sigma-Aldrich (St. Louis, MO, USA) and they were of analytical

grade. Soy bean oil was purchased from a local supermarket (New World, Albany) in Auckland, New Zealand. The 4× Laemmli sample buffer, β-mercaptoethanol, 10× Tris/Glycine/SDS running buffer, Coomassie Brilliant Blue R-250 staining solution, and Bradford Protein Assay Kit were purchased from Bio-Rad (Hercules, CA, USA). Milli-*Q* water was used in all the sample preparations.

3.2.2. Extraction of quinoa protein isolate (QPI)

The QPI was prepared according to the method of Kaspchak et al. (2017) with slight modifications. Firstly, a bench-top coffee grinder (Breville, New Zealand) was used to ground quinoa seeds into flour, and the flour was passed through a 500-micron sieve to remove any large particles. Then, the fat in the quinoa was removed by mixing the quinoa flour with petroleum ether (1:10 (w/v)) and the suspension were kept magnetically stirring for 5 h at 22 °C in a fume hood. The defatted quinoa flour was obtained by gravity sedimentation after repeating the twice of the defatting procedure. Afterwards, it was dried on a plastic tray for 2 days in a fume hood. Then the defatted quinoa flour (200 g) was mixed with 2 L of NaCl (0.5 M) for 2 h and the pH was adjusted to 8 with 1 M NaOH. The extracted proteins in the supernatant were separated from insoluble components by centrifugation of the suspension at 20,000g for 30 min at 22 °C using a Sigma centrifuge (3-18KS, Osterode am Harz, Germany). Afterwards, the pH of the supernatants was adjusted to the isoelectric point of quinoa proteins, 4.5 using 1 M HCl in order to recover the proteins. The protein precipitation at pH 4.5 lasted for 2 h before centrifuging again under the same condition to obtain protein precipitates. The pellets were thoroughly washed with Milli-*Q* water for five times followed by centrifugation. The residual NaCl concentration in the washing solutions were monitored by determining the electric conductivity using an EC metre (HI98304, HANNA instruments, UK). The NaCl concentration in the final washing solution was below 1 mM. After this, the protein pellets were redispersed

in Milli-*Q* water containing 0.02% w/w sodium azide to prevent growth of microorganism and the suspension was kept under magnetically stirring overnight. The pH was adjusted back to 7 using 1 M NaOH. Finally, a freeze dryer (Labconco, MO, USA) was used to lyophilise the protein solutions to the QPI powder for five days before grinding them using a mortar and pestle. The QPI powder was stored in a desiccator before further use. The QPI powder contained 91.6%w/w protein, 2.9%w/w fat, 2.8%w/w ash, and 2.7%w/w moisture as determined by the Nutrition Laboratory of Massey University (Palmerston North, New Zealand).

3.2.3. High pressure homogenisation treatment of the QPI suspensions

5% w/w QPI suspension was prepared by dispersing 5 g of QPI powder to 95 g of Milli-*Q* water. The QPI suspension was kept under magnetically stirring for 24 h at 20 °C to allow fully hydration. During the hydration, the pH was regularly checked and maintained at pH 7 using 1 M NaOH or 1 M HCl. Subsequently, the QPI suspension (~200 mL) was subjected to the HPH treatment using a high-pressure homogeniser (APV 2000, SPX Flow Technology, Rosista GmbH, Germany) at three pressures of 10 MPa, 30 MPa, and 50 MPa, respectively for 5 passes. The maximum temperature of the HPH treated QPI suspension was 33 °C, which is far below the denaturation temperature of QPI (75–85 °C) (Abugoch et al., 2008; Shen et al., 2021). The QPI suspension without undergoing HPH treatment was regarded as a control.

3.2.4. Sodium dodecyl sulphate polyacrylamide gel electrophoresis (SDS-PAGE)

SDS-PAGE under reducing and non-reducing conditions were conducted to characterise the protein profiles of the QPI before and after HPH treatments (Laemmli, 1970). In the case of reducing SDS-PAGE, 20 µL of 0.15% QPI was mixed with 6 µL of Laemmli sample buffer

(4×, Bio-Rad, USA) and 0.8 µL of a reducing agent β-mercaptoethanol at room temperature. Thereafter, the sample was boiled for 10 min. For non-reducing SDS-PAGE, β-mercaptoethanol was replaced by Milli-Q water while other procedures remain the same. After that, 10 µL of the sample was carefully loaded on the well of a commercial Mini-protein TGX (Tris/Glycine) precast gel (Cat.# 4561083, Bio-Rad, USA) consisting of 4% stacking gel and 15% resolving gel. The electrophoresis was conducted at a constant 150 V using a PowerPac Basic (Bio-Rad, USA) in a running buffer prepared by the dilution of 10× Tris/Glycine/SDS running buffer (Bio-Rad, USA). Once the electrophoresis was completed, the gel was carefully removed from the electrophoresis tank and stained with Coomassie Brilliant Blue R-250 staining solution (Bio-Rad, USA). Afterwards, the gel was destained with a destaining solution containing 10% isopropanol/glacial acid solution under mild shaking. The destaining solution was changed every 3 h for 3–4 times until the gel background became clear. For protein bands identification, a protein molecular weight marker (Precision Plus Protein Dual Xtra Standards) (Catalog # 161-0377, Bio-Rad, USA) with a Mw range of 10–250 kDa was used. The gels were visualised by a ChemiDoc XRS imaging system (Bio-Rad, MO, USA).

3.2.5. Fourier transform infrared spectroscopy (FTIR)

Various HPH treated QPI suspensions were freeze dried and milled with a mortar and pestle to obtain fine powders. FTIR spectra was recorded with a compact ATR FTIR spectrometer (ALPHA II, Bruker, Germany). The range of scan was set between 4000 and 500 cm^{-1} at 4 cm^{-1} resolutions. The background scan was conducted prior to each sample measurement. At least duplicate measurements with 64 scans were averaged before baseline subtraction and smoothing.

3.2.6. Determination of free sulfhydryl (SH) groups, absorbance at 280 nm, and

surface hydrophobicity

Contents of free SH groups of all the QPI samples were determined using Ellman's reagent (DTNB) in accordance with Beveridge et al. (1974) and Shen et al. (2017). Absorbance at 280 nm was determined according to the methods of Melchior et al. (2022) and with slight modifications. All QPI dispersions (5% w/w) were centrifuged at 1500g for 15 min at 22 °C using a benchtop centrifuge (Thermofisher 3000, USA). The supernatant was collected, diluted with Milli-Q water, and the absorbance of protein solutions at 280 nm was determined by a UV-Vis spectrophotometer (Shimadzu 2000, Japan). Surface hydrophobicity was determined according to Zuo et al. (2022) with some modifications. The 8-anilino-1-naphthalene sulphonate (ANS) was used as a fluorescence probe. QPI dispersions were diluted to the concentrations of 12.5, 25, 50, 100, and 200 μg/mL with 10 mM Tris-HCl buffer (pH 7.0) separately. Afterwards, 50 μL of 8.0 mM ANS solution was mixed with 3 mL of each QPI solution for a 20 min reaction at 20 °C in the dark. Fluorescence measurements were recorded at 470 nm (emission) and 390 nm (excitation) with slit widths of 5 nm on a Shimadzu RF-6000 fluorescence spectrophotometer (Shimadzu, Kyoto, Japan). Fluorescence intensities (background subtracted) were plotted versus QPI concentrations, and the initial slope obtained from the linear regression analysis was regarded as the index of surface hydrophobicity (Kato & Nakai, 1980). QPI samples without adding the ANS were treated as the background.

3.2.7. Images acquisition of QPI dispersions

To examine sedimentation of various QPI suspensions, all the samples right after the HPH treatment were left on the bench for 5 h at room temperature (~20 °C) and photographs were taken.

3.2.8. Determination of particle size distributions using static light scattering

Static light scattering (Mastersizer 2000, Malvern Instruments, Worcestershire, UK) was used to determine the particle size distributions of QPI particles subjected to HPH treatments at different pressures. Refractive indices of QPI particles and water were 1.456 and 1.33, respectively (Shen et al., 2021). In the case of emulsion oil droplet size, the refractive indices used for soy oil and the dispersant were 1.47 and 1.33, respectively (Mackie et al., 2000). The volume mean diameter ($D[3,4]=\sum n_i d_i^4/n\, d^3$) was used to represent the mean particle diameter for QPI particles and oil droplets. The reported D[3,4] value is averaged from three measurements on duplicate samples at room temperature (~20 °C).

3.2.9. Determination of the protein solubility

Solubility of QPI before and after HPH treatments was determined according to the method by Yang et al. (2018) with slight modifications. Briefly, the QPI dispersions (5%w/w) were centrifuged at 1500g for 15 min at 22 °C using a benchtop centrifuge (Thermofisher 3000, MO, USA). Thereafter, the supernatant was carefully pipetted and the soluble protein concentration in the supernatant was determined using a Bradford Protein Assay Kit (Bio-Rad, USA) using gamma-globulin as the standard. A UV-Vis spectrophotometer (Shimadzu 2000, Kyoto, Japan) was used to determine the absorbance of protein solutions at 595 nm. The solubility was calculated as the percentage of the original protein concentrations in the QPI suspension before centrifugation.

3.2.10.Confocal laser scanning microscopy (CLSM)

CLSM was used to probe microstructural characteristics of the QPI suspensions before and after HPH treatments and the gels obtained after thermal treatments. Firstly, the QPI suspensions were mixed with several drops of 1% Fast Green dye (Sigma Aldrich, USA) and

then vortex mixed for 10 s at 20 °C. Afterwards, the protein-dye mixture was pipetted into a glass slide with a cavity and was covered by a coverslip. Nail polish was used to seal the coverslip to prevent water evaporation (Wang et al., 2019). In the case of gel samples, the slides with samples were incubated in an oven (Thermofisher, USA) at 85 °C for 30 min. Then, a confocal laser scanning microscope (Leica TCS SP5, Leica Microsystems) equipped with an oil immersion objective lens (100×) was employed to observe the microstructures of QPI solutions and the corresponding gels at a wavelength of 630 nm. All the images were processed with Image J software (NIH, MD, USA).

3.2.11.Rheological properties

The QPI gel formation was induced by a thermal treatment (85 °C, 30 min) and their small and large deformation viscoelasticity was characterised by a rotational stress-controlled rheometer (DHR-3, TA instruments, New Castle, DE, USA) equipped with a stainless-steel parallel plate geometry (diameter 40 mm, gap 1 mm). Various 5% w/w QPI suspensions before and after HPH treatments were added with NaCl powder to achieve the final NaCl concentration of 100 mM. The ionic strength of all samples was fixed at 100 mM in order to promote gelation of QPI dispersions by diminishing electrostatic repulsions between protein molecules (Yang et al., 2022b). The mixture was kept under magnetically stirring for 2 h at 20 °C and pH was check and adjusted to 7 using 1 M NaOH or 1 M HCl.

Aliquots of QPI suspension were carefully transferred into the bottom plate using a 3 mL plastic dropper. The sample was then carefully trimmed, and low viscosity mineral oil (M 5904, Sigma Aldrich, USA) was added around the edge of the sample to prevent evaporation. The rheological measurements were carried out in the following steps: (1) a temperature sweep was conducted by heating the samples from 25 to 85 °C at 1 °C/min, maintaining at 85 °C for 30

min, and decreasing from 85 to 25 °C, this step was used to initiate the gel formation; (2) after this step, a frequency sweep measurement was conducted at a constant strain 1% with the frequency varying from 0.01 to 100 Hz; (3) in the end, a strain sweep was performed with frequency fixed at 1 Hz, and the strain amplitude varied from 0.1% to 1000%. Both frequency and strain sweep measurements were conducted at 25 °C and all rheological measurements were repeated at least twice.

3.2.12.Determination of interfacial tension and surface tension

The time evolution of oil-water interfacial tension and air-water surface tension of the QPI samples (0.01 mg/mL) was monitored using a Thea Felx Plus optical tensiometer (Biolin Scientific Instruments, Västra Frölunda, Sweden) based on the pendant drop method as suggested by Yang et al. (2018) with slight modifications. For oil-water interfacial tension, a QPI suspension droplet with a fixed volume (5 µL) was generated by the stainless-steel syringe tip and the droplet was immersed in soy oil in a disposal cuvette. In the case of air-water surface tension, soy oil was replaced by an empty cuvette covered with parafilm while other procedures remained the same. The evolution of interfacial tension and surface tension was monitored for 10,000 s and 3500 s, respectively and the results were calculated and processed automatically with One Attention Software (Biolin Scientific Instruments, Västra Frölunda, Sweden).

3.2.13.Determination of emulsifying and foaming properties

Emulsions stabilised by both untreated and HPH treated QPI suspensions were prepared by mixing 2 mL of 1% QPI suspensions with 8 mL of soy oil using a rotor-stator homogeniser (T10 basic, IKA, Germany) with a 10 mm probe (S10N-10G, IKA, Germany) for 1 min at 10,000 rpm. Emulsifying activity index (EAI) of QPI suspensions were determined according

to the method by Saricaoglu (2020) with slight modifications. Briefly, each fresh emulsion (50 µL) was mixed with 5 mL of 0.1% SDS solution. The absorption of the diluted emulsion at 500 nm was determined using a UV-Vis Spectrophotometer (Shimadzu 2000, Japan). The following equation was used to calculate the EAI (Yang et al., 2018):

$$\text{EAI } (m^2/g) = \frac{2 \times 2.303 \times A \times DF}{1 \times c \times \varphi \times L} \qquad (6)$$

Where A is the absorbance at 500 nm, DF represents the dilution factor (10), c is the initial protein concentration (g/mL), φ is the oil volume fraction (0.25) and L is length of the cuvette (1 cm). Three measurements were conducted for duplicated QPI suspensions.

Foaming properties (capacity and stability) of both untreated and HPH treated QPI suspensions were determined according to a previous method (Wang et al., 2010) with some modifications. 10 mL of 1% QPI suspension was transferred to a 15 mL glass graduated cylinder before homogenising for 15,000 rpm for 5 min using a rotor-stator homogeniser (T10 basic, IKA, Germany). Three measurements were performed for duplicated QPI suspensions. The following equations were used to calculate the foaming capacity (FC) and foaming stability (FS). All the measurements were performed at 20 °C.

$$FC = (V_b - V_a)/V_a \times 100\% \qquad (7)$$

where V_b and V_a indicate the volume of foam after mixing and the volume of original protein solution, respectively.

$$FS = V_{30}/V_0 \times 100\% \qquad (8)$$

where V_0 and V_{30} represent the initial volume of foam after mixing and the volume of foam after storage for 30 min, respectively.

3.2.14.Statistical analyses

All the measurements were carried out in triplicate or duplicate, and the results are represented as mean ± standard deviations (SD). SPSS software (v 21.0, Chicago, USA) was used to conduct Analysis of Variance (ANOVA) suing the Least Significance Difference (LSD) test for mean comparison.

3.3. Results and discussion

3.3.1. Structural characterisations

Protein profiles revealed by SDS-PAGE

The impact of HPH treatments on protein profiles of QPI was characterised by both non-reducing and reducing SDS-PAGE (**Figure 4**). QPI exhibits complex protein profiles, consisting predominantly of 11S globulin (45–55 kDa) and 2S albumin (< 15 kDa) (Brinegar & Goundan, 1993; Brinegar et al., 1996). Similar QPI protein profiles were also observed in previous studies of QPI obtained by alkaline extraction (Ruiz et al., 2016; Shen et al., 2021; Yang et al., 2022b). Apparently, HPH treatments up to 50 MPa did not result in prominent changes in protein profiles of QPI and all individual protein bands were preserved. This is consistent with few previous HPH studies which reported that HPH treatments do not induce the disruption of constituting protein molecules in several plant proteins such as lentil, and hazelnut meal proteins (Saricaoglu, 2020; Saricaoglu et al., 2018). Under non-reducing conditions, an appearance of intense and smeared protein bands can be identified in the top loading wells of the gels, which is indicative of the presence of large protein aggregates with molecular weight larger than 250 kDa (Mäkinen et al., 2016). In the presence of the reducing

agent β-mercaptoethanol, those large protein aggregates bands disappeared, accompanied by the appearance of intense bands located at ~28–30 kDa and ~22–25 kDa. Those small molecule bands were assigned as acidic and alkaline subunits, respectively, which formed the 11S globulin (~55 kDa) through disulphide bonds (Shen et al., 2021). Protein bands located at ~10–15 kDa were assigned as 2S albumin (Brinegar et al., 1996).

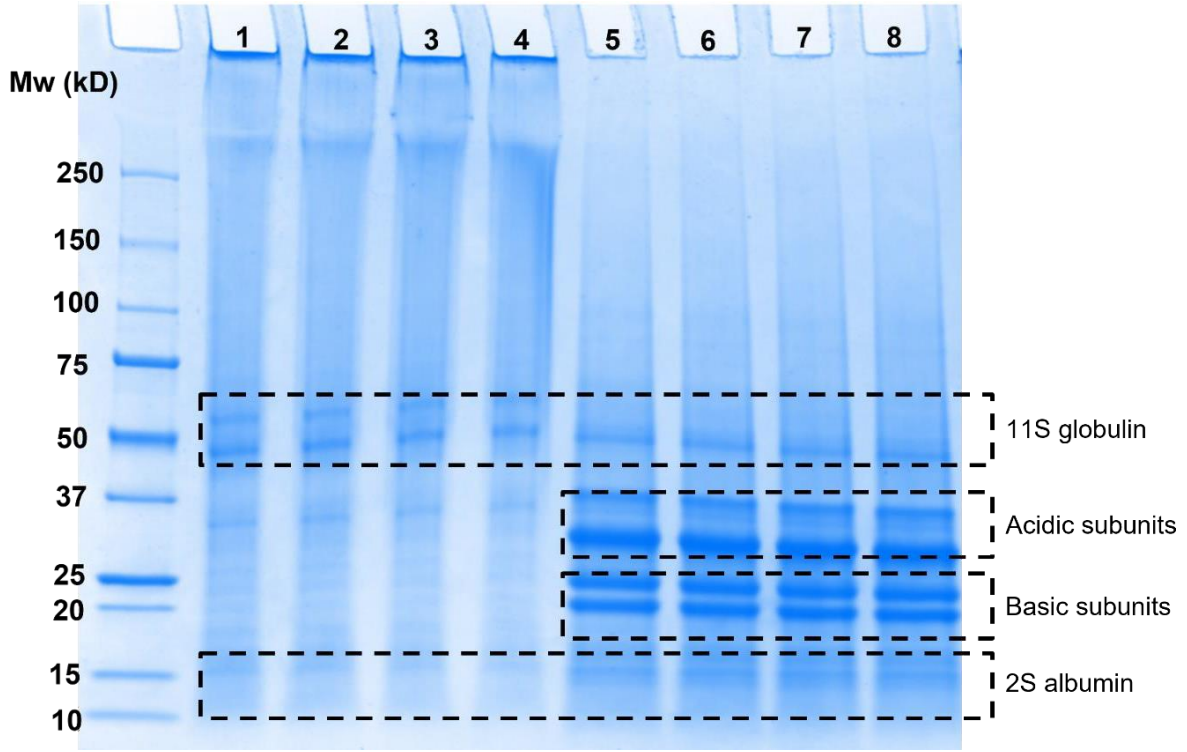

Figure 4: SDS-PAGE profiles of untreated and HPH treated QPI under non-reducing and reducing conditions. Lanes 1–4: non-reducing; Lanes 5–8: reducing. Lanes 1 and 5: non-treated; Lanes 2 and 6: 10 MPa; Lanes 3 and 7: 30 MPa; Lanes 4 and 8: 50 MPa. Mw: Molecular weight standards. The name of the proteins were labelled in correspondence of the bands.

Fourier transform infrared spectroscopy (FTIR) analysis

In order to investigate the impact of HPH treatment on the secondary structure of QPI proteins, FTIR spectra were recorded for all QPI powders as shown in **Figure 5**. The overall FTIR profile including the absorption peak position and their relative intensities were in accordance with previous reports on quinoa proteins (Drzewiecki et al., 2018; Wang et al., 2020). For all the QPI powders, major absorption bands were observed at 3290 cm−1, 1646 cm−1, 1516 cm−1,

and 1230 cm−1, which were assigned as OH-stretching, amide I, amide II, and amide III bands, respectively (Vera et al., 2019; Wang et al., 2020). There was no difference in peaks position among different HPH treated and nontreated QPI samples, indicating HPH treatments did not induce significant alterations on the secondary structure of quinoa proteins. Similar observations were also found in previous FTIR studies on high-pressure microfluidization treated potato protein isolates (Hu et al., 2021) and high hydrostatic pressure treated kidney bean protein isolates (Ahmed et al., 2018).

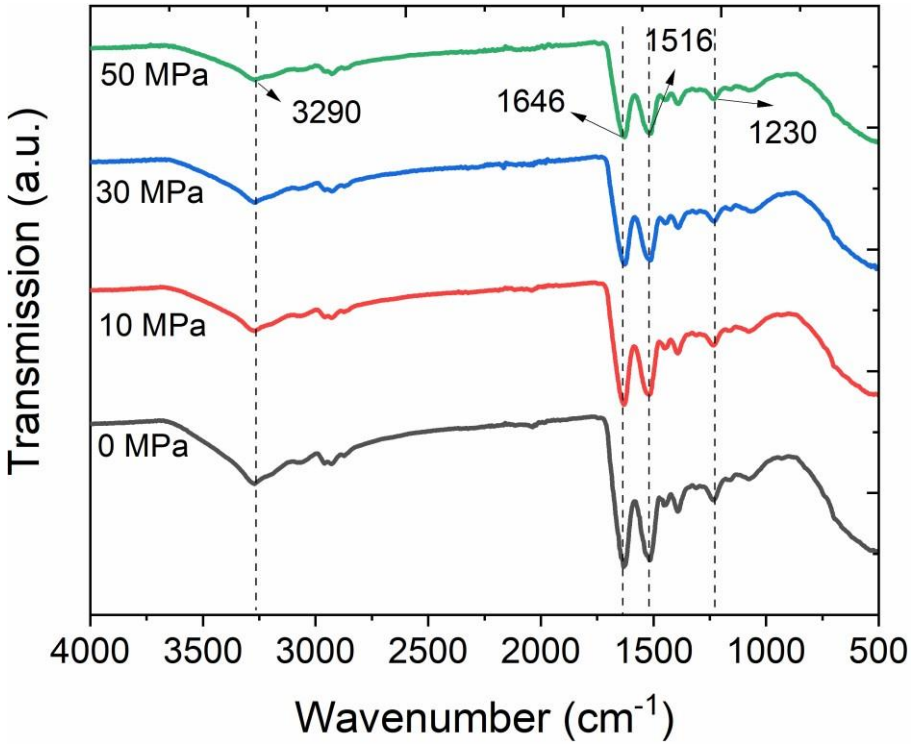

Figure 5: FTIR spectra of untreated and HPH treated QPI powders. The FTIR patterns are vertically shifted for clarity.

Free sulfhydryl (SH) groups content, absorbance at 280 nm, and surface hydrophobicity

Free sulfhydryl (SH) groups, absorbance at 280 nm, and surface hydrophobicity of proteins were determined (**Table 15**) to further probe HPH-induced structural modifications of quinoa proteins. Contents of SH groups increased significantly with increasing pressure. This implies that the SH groups originally buried inside of the protein are increasingly exposed due to large

shear forces and cavitation effects induced by HPH (Levy et al., 2021; Melchior et al., 2022). A similar trend was also observed for the absorbance at 280 nm (**Table 15**). This could be attributed to either an increase in the concentration of soluble proteins and/or an exposure of tyrosine and tryptophan residues on the surface of proteins (Antosiewicz & Shugar, 2016; Melchior et al., 2022). The similar behaviour was reported in previous HPH studies on pea proteins (Melchior et al., 2022) and soy proteins (Fayaz et al., 2019). The surface hydrophobicity of proteins is critical for their stability, conformation, and emulsifying capability (Kato & Nakai, 1980). Compared to the untreated sample, **Table 15** shows that the surface hydrophobicity of HPH treated samples was higher at 30 MPa and 50 MPa. This indicates that HPH treatments induce a certain degree of protein unfolding, which lead to exposure of hydrophobic groups originally buried inside of the protein (Jiang et al., 2014; Yang et al., 2018).

Table 15: Content of free sulfhydryl (SH) groups, absorbance at 280 nm, and surface hydrophobicity of HPH-treated quinoa protein dispersions.

Pressure (MPa)	Free SH groups ($\mu molL^{-1}g^{-1}$)	Absorbance at 280 nm	Surface hydrophobicity (a.u.)
0	7.4 ± 0.1 ^{d}	0.41 ± 0.01 ^{c}	20205 ± 120 ^{c}
10	8.5 ± 0.1 ^{c}	0.44 ± 0.01 ^{c}	21059 ± 150 ^{c}
30	14.6 ± 0.2 ^{b}	0.54± 0.03 ^{b}	23126 ± 150 ^{b}
50	21.4 ± 0.2 ^{a}	0.68± 0.04 ^{a}	26470 ± 160 ^{a}

Results are the average of duplicates. Different superscript letters in the same column represent significant differences based on the SPSS LSD test ($p < 0.05$).

3.3.2. Physico-chemical properties characterisations

Particle size distributions

The impact of HPH treatments on the particle size D[4,3] and particle size distributions of QPI suspensions are shown in **Figure 6**A. Non-treated QPI suspensions display a bimodal distribution with two main peaks at ~2×10^{-1} µm and ~8.6 µm. The presence of large aggregates

in the range of ~0.06–100 μm in the reconstituted QPI suspensions was also reported in a previous study (Shen et al., 2021). Previous research has suggested that the alkaline extraction followed by precipitation at the isoelectric point could promote the formation of aggregates through hydrophobic interactions between globulins (Yang & Sagis, 2021). The extent of protein aggregation and particle size distributions are highly dependent on quinoa seed varieties, reconstitution conditions such as stirring speed and time, extraction procedures, and drying methods (Ruiz et al., 2016). For example, spray-dried QPI powders exhibited a median particle size of ~8 μm, while freeze-dried and vacuum-dried QPI powder showed a much larger median particle size of ~50 μm (Shen et al., 2021). This bimodal particle size distribution was also observed in water reconstituted plant protein ingredients such as rice proteins (Zhang et al., 2018) and faba bean proteins (Yang et al., 2018). In the case of QPI solutions, different sizes of aggregates respond differently to HPH treatment. Larger aggregates (~8.6 μm) are relatively easier to be broken down, while the smaller aggregates (~0.2 μm) are more resistant towards HPH treatment. Interactions between protein and protein, and protein and phenolic compounds could contribute to the formation of those large protein aggregates (Dakhili et al., 2019). Indeed, the total phenolic compound content was determined as ~230 mg GAE (gallic acid equivalent) per 100 of dry QPI sample. The decrease in the peak of large particle size population accompanied with the increased peak of small particle size population was also reported in the HPH treated faba bean proteins (Yang et al., 2018), pea proteins (Melchior et al., 2022; Zhao et al., 2022), and potato proteins (Levy et al., 2021).

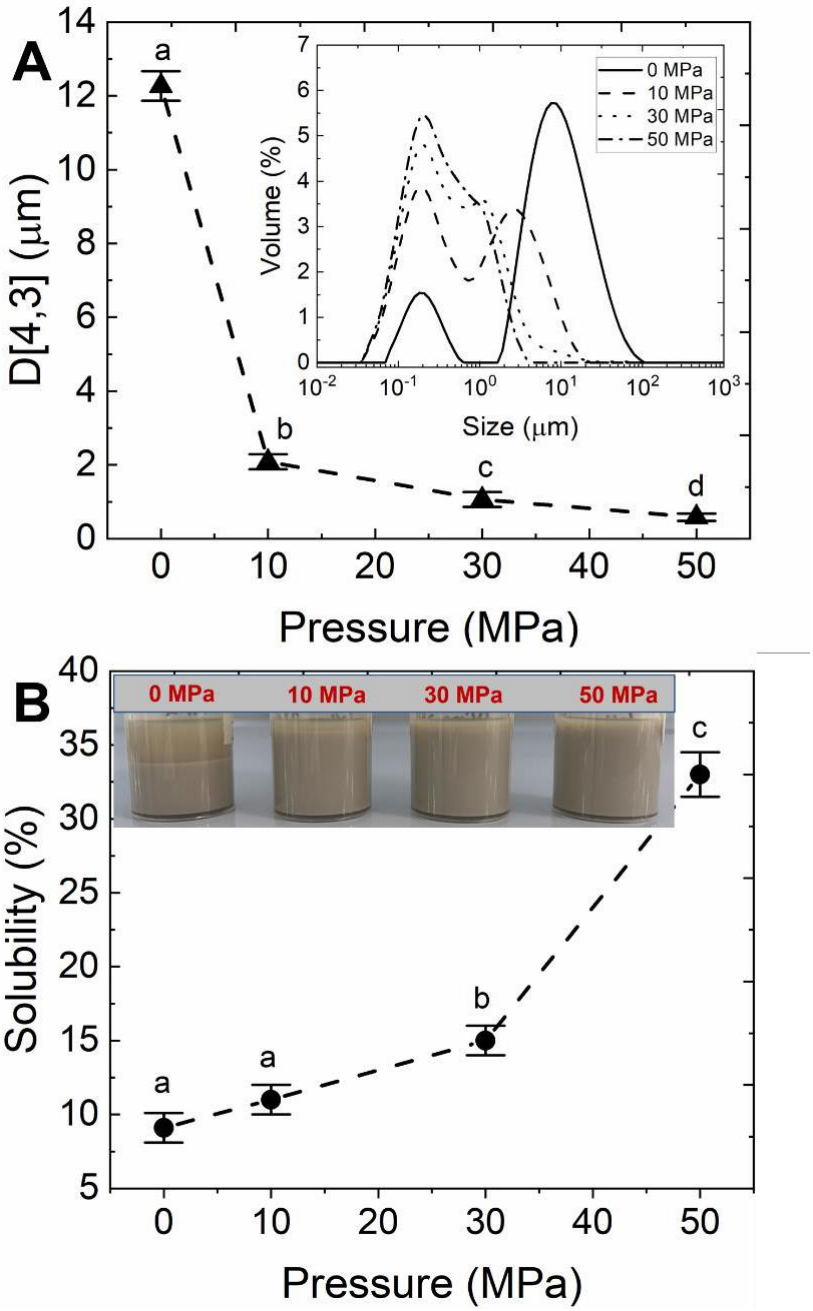

Figure 6: (A) Particle size as a function of High pressure homogenisation (HPH) treatment pressures for 5 w/w% QPI suspensions. Inset, particle size distribution of untreated and HPH treated QPI suspensions. (B) Solubility as a function of HPH treatment pressures for 5 w/w% QPI suspensions. Inset, visual appearances of QPI suspensions. Error bars represent standard deviations.

After 10 MPa treatment, the relative abundance of large size population was significantly decreased and shifted toward smaller sizes (~3.0 μm). The position of small size peak remained unchanged while its relative abundance was increased. Further HPH treatments at 50 MPa led to a nearly monomodal distributions where only a peak is observed around ~0.2 μm with a faint

shoulder around ~0.8 µm, and the disappearing of the larger size peak. The volume mean diameter D[4,3] is plotted as a function of the HPH treatment pressure (**Figure 6**) to better represent the particle size reduction induced by the HPH treatment. It can be observed that the D[4,3] value decreased sharply from 12 to 2 µm when the pressure increased from ambient to 10 MPa. This significant reduction in size is expected as the larger particles were easier to disrupt as mentioned above. A similar behaviour was reported in previous HPH studies on lentil protein (Saricaoglu, 2020) and hazelnut meal protein (Saricaoglu et al., 2018) (this can be easily observed by plotting the values presented in Table 2 in their manuscripts). The particle size D[4,3] was further decreased from ~2 µm to ~0.6 µm with the pressure increased from 10 MPa to 50 MPa. This limiting size could correspond to the small dense protein aggregates that cannot be broken down under the current HPH treatment conditions. Saricaoglu (2020) reported that HPH treatments (50 MPa, one pass) induced a decreased in D[4,3] from ~99 µm to ~20 µm of lentil protein dispersions, while the same group found that a two folds reduction in D[4,3] of hazelnut meal protein dispersions under the same HPH conditions (Saricaoglu et al., 2018). The extent of particle size reduction by HPH treatments could be related to the aggregation nature and deformability of protein particles and HPH processing conditions. Confocal laser scanning microscopy was used to confirm the particle size analysis. Micrographs (**Figure 7**) show that lager protein aggregates progressively transformed to fine and homogenous protein particles, which is in accordance with the particle size results.

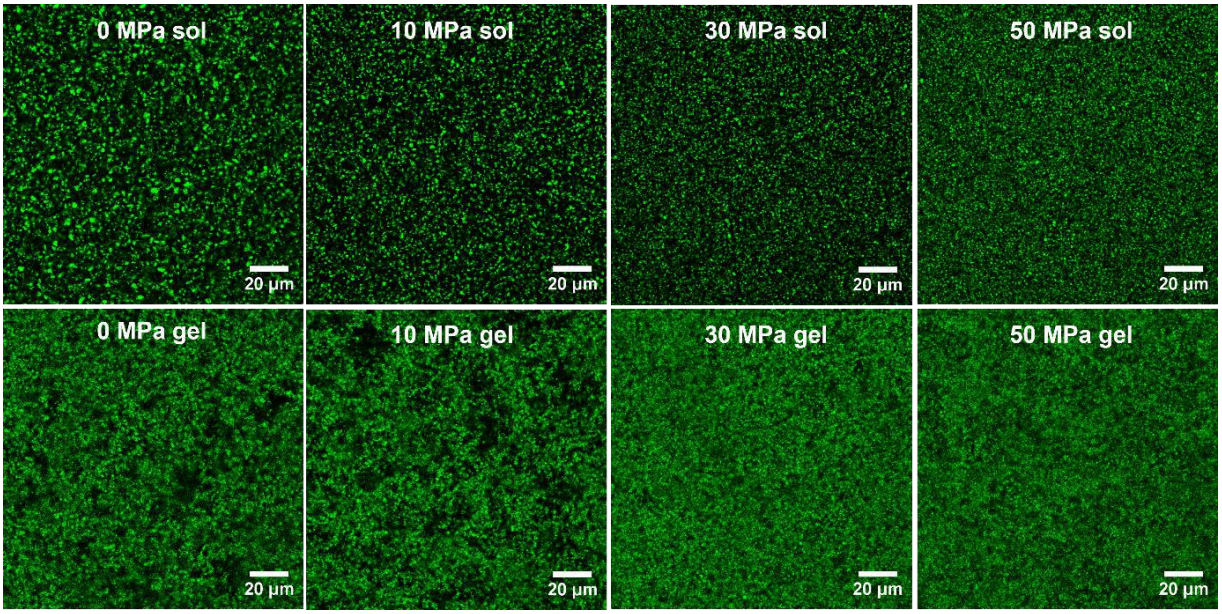

Figure 7: Confocal laser scanning microscopy images of various untreated and HPH treated QPI suspensions and their corresponding gels. The gels were formed by heating at 85 °C for 30 min.

3.3.3. Techno-functional properties of HPH treated QPI dispersions

Solubility

Solubility measurements (**Figure 6**B) indicate that the HPH treatments particularly at 30 and 50 MPa dramatically promoted the solubility of QPI suspensions. The solubility improved nearly six folds from ~9% to ~33% at 50 MPa. The improvement of solubility could be explained by the reduction of protein particle size (**Figure 6**A). Large protein particles have a lower solubility because of their rapid sedimentation under gravity. This is also reflected in the photographs shown in **Figure 6**B (inset): the non-treated QPI suspension were prone to sediment due to gravity while its 50 MPa treated counterpart exhibited a relatively good colloidal stability over a prolonged storage at room temperature (~5 h). The improvement of solubility was identified in previous studies on plant proteins, and again, it is related to the nature of proteins, protein extraction methods, solubility determination methods (e.g. centrifugation force and time), and HPH processing parameters. For example, Yang et al. (2018) reported that the solubility of 1%

faba bean protein increased from 35% to 98% after the HPH treatment at ~210 MPa. In another study working on lentil proteins, Saricaoglu (2020) reported that the solubility increased from ~32% to ~38% at 50 MPa (1 pass). According to a recent study of Melchior et al. (2022), the solubility of pea protein dispersions was only slightly increased from ~22% to ~26% at 70 MPa (1 pass).

Small and large deformation viscoelasticity

Small and large deformation oscillatory rheology was performed to understand the heat induced gel formation characteristics as affected by HPH treatments. The frequency sweep and strain sweep results are shown in **Figure 8**A and B, respectively. The frequency sweep measurement was performed at 1% strain, which is in the Linear Viscoelastic Region (LVR). For all the QPI samples, elastic modulus G' is almost 10 folds larger than loss modulus G'' in the entire frequency range, and both G' and G'' are only slightly increased with the increase of frequency. In addition, the low values of G' (less than 100 Pa) were observed for all QPI gels, which was due to low protein content used in the gelation study (Yang et al., 2022b). All these observations indicated that all QPI gels are weak gels (Wang et al., 2019). Similar dynamic viscoelastic behaviour had been reported in QPI gels that are formed by heat treatment (Shen et al., 2021). It has been suggested that non-covalent bonds such as hydrophobic interactions, hydrogen bond, and electrostatic attractions (Sun & Arntfield, 2010) as well as covalent (disulphide) bonds (Luo et al., 2021; Mession et al., 2013) are mainly responsible for the formation of most thermally induced plant protein gels. To better compare the gel strength of various QPI gels, the complex modulus at 1 Hz, $G^* = (G'^2 + G''^2)^{1/2}$ is plotted for all the QPI gels (**Figure 8**A inset). The value of G^* is increased from ~12 Pa to ~20 Pa when the QPI suspensions were HPH treated at 50 MPa. The improvement of gel strength could be attributed to greater solubility

and smaller particle size at 50 MPa, which facilitated protein interactions and aggregation during the heating process to from gel networks (Ruiz et al., 2016; Shen et al., 2021). Similar results were reported in previous studies on the gel formed by the HPH treated soy milk (Cruz et al., 2009), potato proteins (Levy et al., 2021) and soy protein stabilised emulsion gels (Bi et al., 2020).

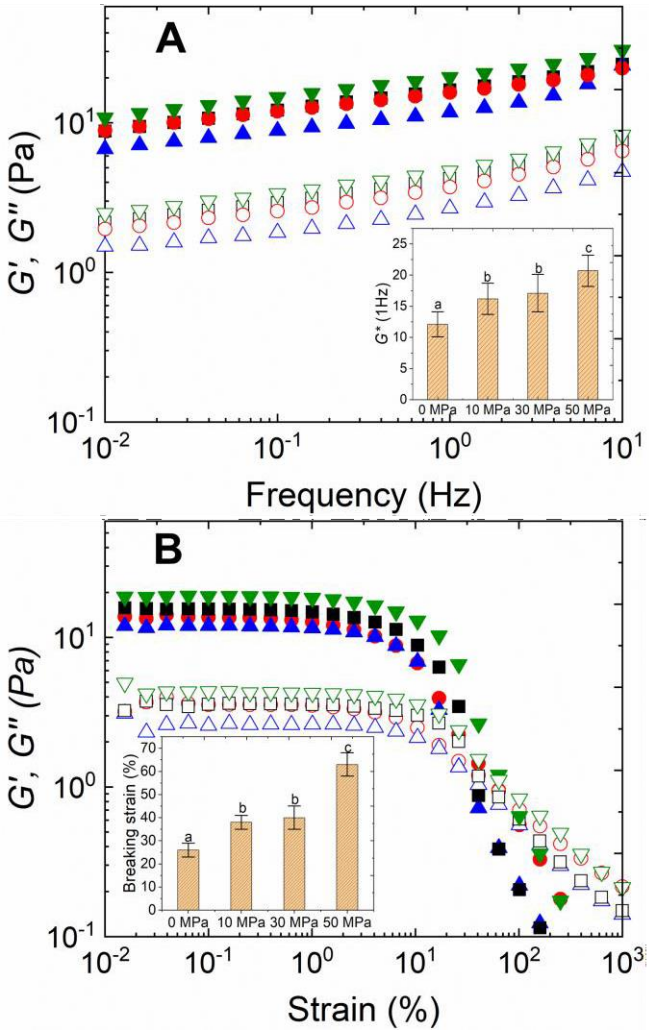

Figure 8: The dependence of frequency (A) and strain amplitude (B) on G' (solid symbols) and G'' (open symbols) for untreated and HPH treated QPI suspensions (5 wt%) in the presence of 100 mM NaCl measured at 25 °C. (A) inset: Complex modulus G^* (1 Hz) of various QPI gels; (B) inset: Breaking strain (%) of various QPI gels. (0 MPa (▲), 10 MPa (●), 30 MPa (■), 50 MPa (▼)).

Large deformation rheological behaviours of various QPI gels are demonstrated in **Figure 8**B

by plotting G' and G'' versus the applied strain amplitude. Qualitatively, all the QPI gels displayed a similar strain-depending behaviour: G' was greater than G'' and both G' and G'' were independent of strain amplitude until reaching the end of LVR. Beyond the critical strain point, G' and G'' started to decrease markedly until reaching a cross-over point where $G' = G''$. The corresponding strain and stress at the cross-over point are defined as breaking strain and breaking stress, respectively. When the strain amplitude was further increased, G'' began to dominate G', which suggested the gel structure was broken down and the sample started to flow (Yang et al., 2015). To compare the large deformation rheological characteristics among the different QPI gels, the breaking strain for the different samples is shown in **Figure 8**B inset. The value of breaking strain was progressively increased from ~25% at 0 MPa to 60% at 50 MPa, which suggested that the QPI gel at 50 MPa were more resistant toward rearrangement and fracture under large oscillatory deformation. Briefly, the variation of breaking strain with HPH treatment pressures followed a similar trend as G^*. The greater the HPH treatment pressures, the higher values of G^* and breaking strain. This indicated the large deformation rheological behaviours correlated well with the small deformation viscoelastic properties.

The microstructures of all the QPI gels were characterised by CLSM and micrographs are displayed in **Figure 7**. The protein stained by Fast Green appeared as green, while the serum voids were shown as black. It can be observed that in all QPI gels, interconnected protein networks were formed. A large porosity can be identified in the 0 MPa and 10 MPa samples, while finer, denser, and more homogenous protein networks can be seen in the 30 MPa and 50 MPa samples. This might explain the greater mechanical strength of QPI gels at 30 MPa and 50 MPa as revealed by the rheological investigations. Generally, the microstructural characteristics of the QPI gels are in good agreement with their rheological properties.

Foaming capabilities and surface tension

The foaming capacity and foaming stability of the QPI suspensions before and after HPH treatments at the same concentration of 1% are shown in **Figure 9**A. Both the foaming capability and stability were steadily increased with the increase in HPH treatment pressures. The foaming capacity of 50 MPa treated QPI was nearly two folds higher than that of untreated QPI. HPH treatments induced a significant increase of foaming stability from ~60% at 0 MPa to ~80% at 50 MPa. This indicated that the HPH treatment could significantly promote the foaming capacity and stability of QPI, which was in accordance with previous studies on faba bean proteins (Yang et al., 2018), hazelnut meal proteins (Saricaoglu et al., 2018), pea proteins (Zhao et al., 2022), and potato proteins (Hu et al., 2021). In order to better understand the foaming behaviour of the QPI suspension as affected by HPH treatments, the surface tension between water-air surface was determined and the results are shown in **Figure 9**B. The evolution of surface tension with time provided information on the kinetics of protein diffusion, absorption to the interface and the subsequent structural rearrangement (MacRitchie, 1989). At the first ~15 s, a lag (plateau) phase was observed for all the QPI samples indicating limited QPI protein molecules diffused from the aqueous phase to the interface (**Figure 9**B inset). However, HPH treatment could reduce the lag time. The lag time was progressively decreased from ~14 s at 0 MPa to ~4 s at 50 MPa. Similar results were also found in faba bean proteins (Yang et al., 2018), and the reduced lag time could be due to the smaller particle size in the HPH treated QPI suspensions (Rullier et al., 2008). As revealed by the particle size, the large aggregates (~8 μm) were disrupted and dissociated into sub-micron supramolecular aggregates under HPH treatments, which were subsequently able to diffuse to the interface at a faster rate.

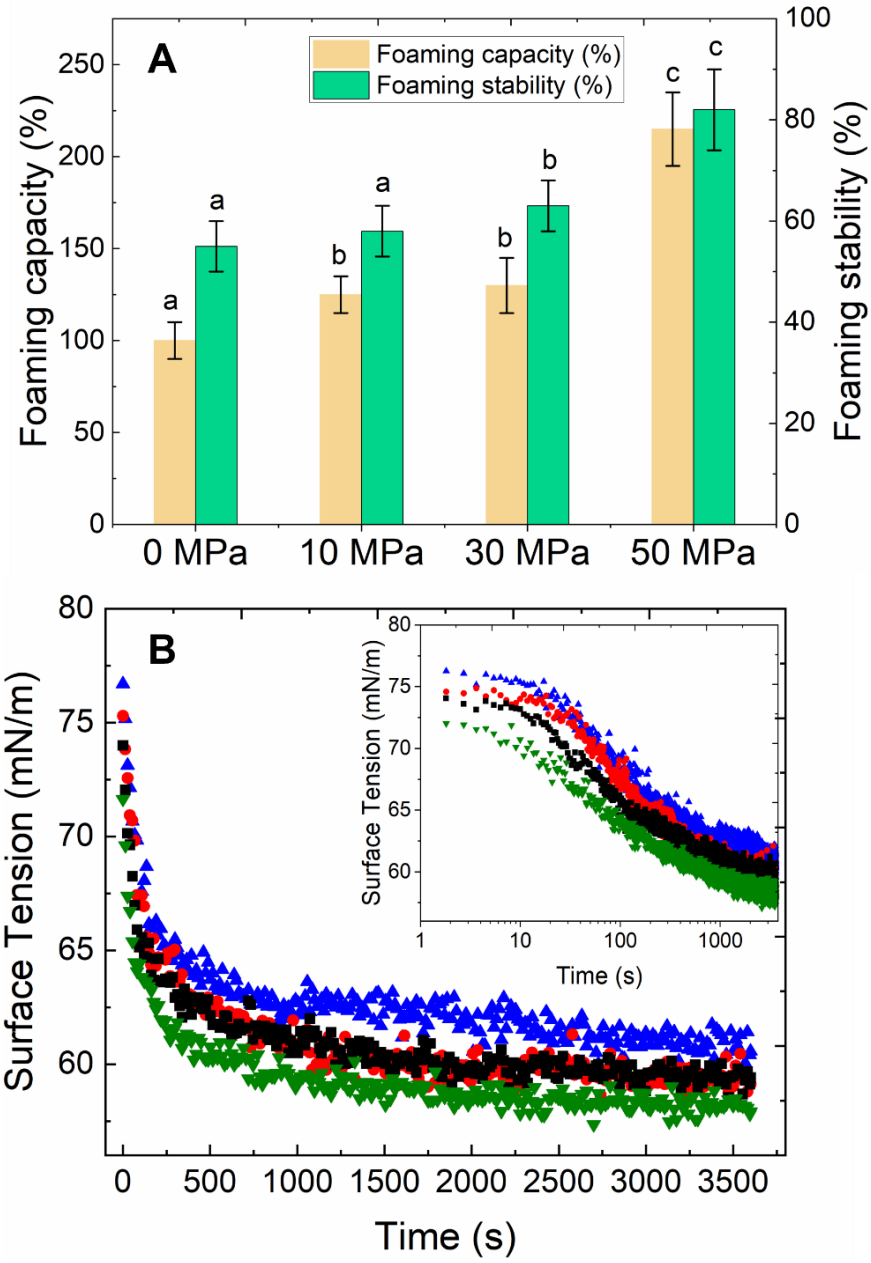

Figure 9: (A) Foaming capacity and foaming stability of untreated and HPH treated QPI suspensions (1%). (B) Time evolution of the surface tension for the adsorption of QPI (0.01 mg/mL) with different HPH treatment pressures at the air-water interface. The inset is used to estimate the lag time. (0 MPa (▲), 10 MPa (●), 30 MPa (■), 50 MPa (▼)).

Beyond the lag phase, the surface tension of all the QPI samples exhibited a shape decrease up to ~500 s. This could be explained by the rapid diffusion and absorption of QPI protein molecules to the interface (Xiong et al., 2018). When the time was further increased, the decrease of surface tension became much slower and almost reached a plateau at ~3500 s. The

final surface tension after ~1 h absorption was slightly decreased from ~62 mN/m at 0 MPa to ~57 mN/m at 50 MPa. Comparable final (plateau) surface tension values were reported in previous studies on various dairy and plant proteins when using the same protein concentration (0.01 mg/mL) and the same pH (pH = 7). For examples, surface tensions of faba bean proteins, peas proteins, green pea proteins, and chickpea proteins were reported as 55 mN/m, 47–52 mN/m, 47–54 mN/m, and 50–52 mN/m, respectively (Chang et al., 2022; Cui et al., 2020; Xiong et al., 2018; Yang et al., 2018). HPH treatments could destroy the hydrophobic interactions and hydrogen bonds of proteins, making protein molecules more flexible. Therefore, they can absorb to the interface much quicker (Sridharan et al., 2020). The surface tension findings correlated well with the results of foaming capability and stability.

Emulsifying capabilities and interfacial tension

Similar to the foaming capabilities, HPH treatments exhibited a positive impact on the emulsifying capacity of QPI (**Figure 10**A). The EAI was increased from ~105 m^2/g for untreated QPI to ~135 m^2/g for the 50 MPa treated sample. The similar effects of dynamic high pressure on emulsifying properties were also identified in previous reports on lentil protein (Saricaoglu, 2020), hazelnut meal protein (Saricaoglu et al., 2018), and whey protein (Dissanayake & Vasiljevic, 2009). The oil droplet size distribution of emulsions prepared by various untreated and HPH treated QPI particles are demonstrated in **Figure 10**C and values of droplet size D[4,3] are summarised in **Figure 10**D. All emulsions displayed a monomodal size distribution and the peak of emulsion shifted towards smaller size at higher pressures. To further understanding emulsifying properties of HPH treated QPI particles, the interfacial tension was determined, and it was plotted versus time as shown in **Figure 10**B. To the contrary to the surface tension results, the lag phase was not observed (**Figure 10**B inset). The differences at air-water and oil-water were also observed in albumin and could be due to the

fact that the protein surface hydrophobic groups exhibited a greater affinity to the oil phase compared to air phase (Wierenga et al., 2003). For all the QPI samples, interfacial tension decreased substantially in the first 2000 s (33.3 min) and then decreased much slowly toward 10,000 s (166.7 min), the end of the measurement. The 50 MPa treated QPI particles reached a slightly lower interfacial tension value ~18.0 mN/m compared to ~19.5 mM/m for the untreated QPI particles. All these results suggested that the HPH treatment enhanced the emulsifying performance, which agreed well with previous studies (Saricaoglu, 2020; Saricaoglu et al., 2018). The greater emulsifying properties of HPH treated QPI dispersions could be explained by partial dissociation and unfolding of protein structures, as revealed by the results of surface hydrophobicity and free SH groups (**Table 15**). It has been suggested that the proteins with higher surface hydrophobicity can reduce the interfacial tension to the greater extent and improve in emulsifying activity (Cabra et al., 2007; Kato & Nakai, 1980).

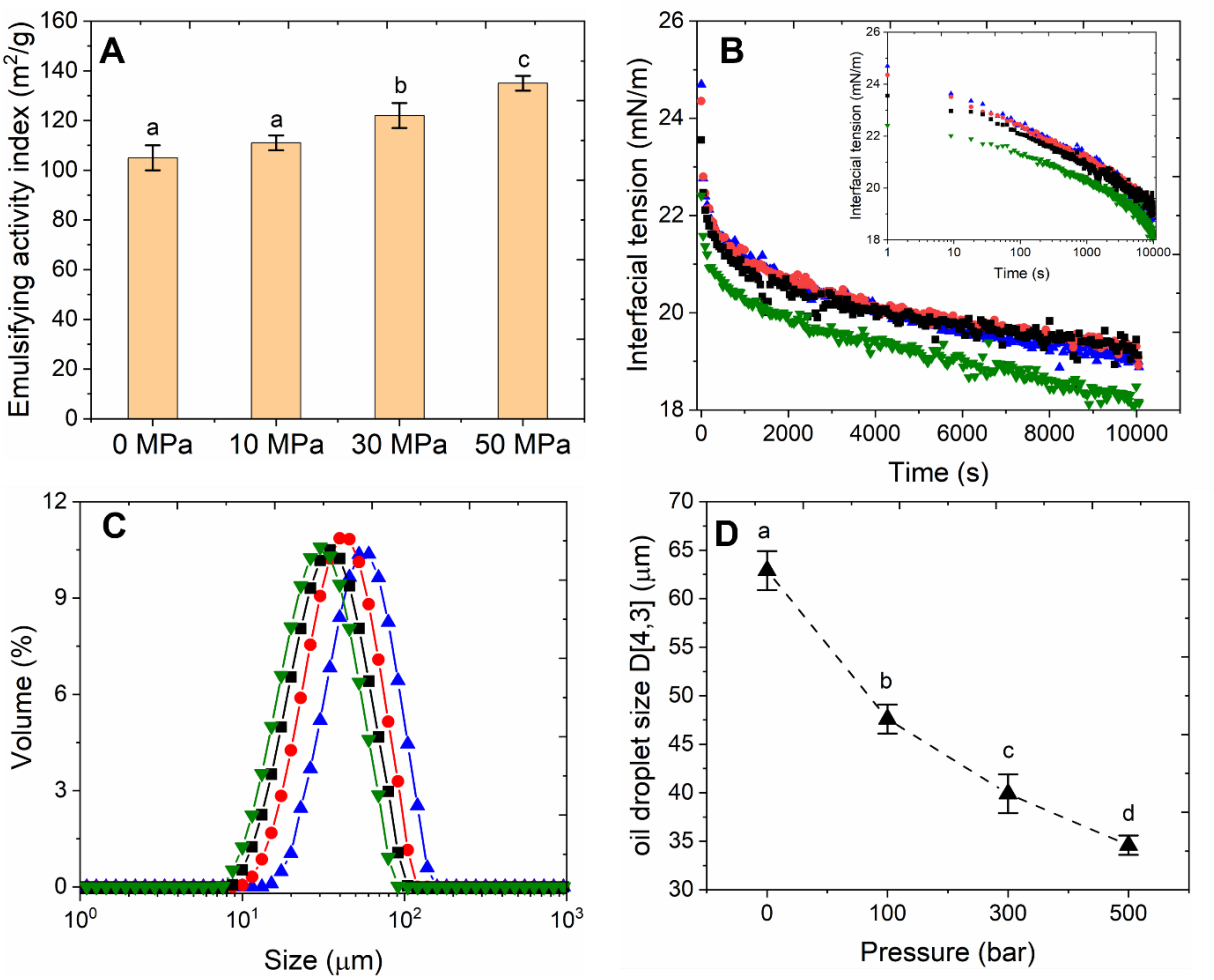

Figure 10: (A) Emulsifying activity index of untreated and HPH treated QPI suspensions (1%). (B) Time evolution of the interfacial tension for the for the adsorption of QPI (0.01 mg/mL) with different HPH treatment pressures at the oil-water interface. (C) Oil droplet size distribution of emulsions stabilised by untreated and HPH treated QPI proteins at pH 7. (D) The dependence of HPH treatment pressures on the oil droplet size of emulsions D[4,3]. (0 MPa (▲), 10 MPa (●), 30 MPa (■), 50 MPa (▼)).

The quinoa protein isolates used in the current study were extracted from aqueous solution using alkaline extraction followed by isoelectric point precipitation. Despite this method being commonly used in both laboratory and industry, the isoelectric point precipitation is often observed to induce irreversible aggregation of globulins, as observed in pea proteins (Saricaoglu, 2020), faba bean proteins (Yang et al., 2018), and quinoa proteins (Shen et al., 2021). In reconstituted plant protein dispersions, protein particles might co-exist with "free" protein molecules and an equilibrium between protein particles and protein molecules might exist (Sarkar & Dickinson, 2020). However, based on particle sizing results (**Figure 6**A)

majority of QPI particles exist as large self-assembled protein particles. Both of the protein particles and protein molecules were suggested to contribute to stabilising the emulsions (Sridharan et al., 2020). When considering the emulsifying properties of plant protein dispersions, the presence of protein particles should not be neglected. From previous studies, QPI stabilised emulsions can be regarded as Pickering type emulsions (Qin et al., 2018; Zhang et al., 2021). The size of particles is critical for the formation and characteristics of Pickering emulsions (Linke & Drusch, 2018). Large protein aggregates exhibit inferior surface properties due to their slow diffusion rate and inferior affinity to the oil-water interface as well as their prone to sedimentation under gravity (Nicorescu et al., 2008). When subjected to HPH treatments, the QPI was disintegrated into small particles with strong adsorption ability due to mechanical forces and cavitation imposed by HPH. The droplet size of emulsions stabilised by the HPH treated QPI particles was significantly smaller than that of the untreated QPI stabilised emulsions (**Figure 10**C and D). This result indicates that the HPH treatment increased the number of absorbed QPI particles at the interface of the droplets. Similar observations have been found for the Pickering emulsions stabilised by sonicated QPI particles (Qin et al., 2018; Zhang et al., 2021).

3.4. Conclusions

In this study, the effect of high pressure homogenisation (HPH) treatment on modifying the physico-chemical, microstructural, and rheological properties of QPI suspensions, was investigated. SDS-PAGE results demonstrated that neither the distribution or intensity of protein bands were altered after HPH treatment, indicating the individual protein cleavage or disruption did not occur. HPH treatment led to certain level of protein unfolding with increased exposure of hydrophobic surfaces. Particle size distribution changed from bimodal to monomodal distribution accompanied with a significant reduction of D[4,3]. The reduction of

particle size with HPH treatment facilitated particle-solvent interaction, thereby promoting the water solubility. Moreover, HPH treatment significantly improved emulsifying and forming capability of QPI suspensions, which was also confirmed with the surface tension and interfacial tension results. Small and large deformation rheology results demonstrated that the HPH treatment could promote QPI gel strength and the gels exhibited more resistance to rearrangement and fracture under large deformations. As observed by CLSM, gels formed from HPH treated QPI suspensions exhibited more denser and homogeneous protein networks. Therefore, the viscoelastic properties of QPI gels are strongly correlated to their microstructural characteristics. This works also show that HPH treatment are promising techniques in improving physico-chemical properties and techno-functional properties of QPI suspensions. It may be worth investigating the effect of HPH treatments on QPI proteins at higher treatment pressures (e.g. above 50 MPa) and at different pH. In addition, future work can be conducted to apply HPH treated QPI in several food products such as yoghurt, salad dressing, and plant based protein beverages.

4. Chapter 4: Impacts of sonication and high hydrostatic pressure on the structural and physicochemical properties of quinoa protein isolate dispersions at acidic, neutral and alkaline pHs*

Keywords: Quinoa protein isolates; Sonication; High hydrostatic pressure; Physicochemical properties

*Reprinted (adapted) with permission from Luo, L., Yang, Z., Wang, H., Ashokkumar, M., & Hemar, Y. (2022). Impacts of sonication and high hydrostatic pressure on the structural and physicochemical properties of quinoa protein isolate dispersions at acidic, neutral and alkaline pHs. *Ultrasonics Sonochemistry*, 106232. Copyright 2022 Elsevier.

4.1. Introduction

With the rapid growth of global population, last decades have seen a great increase in food protein demand (van Dijk et al., 2021). Production of plant proteins is regarded to be more sustainable due to a higher conversion rate and less resource needed compared to those from animal sources. Proteins from plants are regarded as novel and promising food ingredients and have been increasingly used to fabricating dairy and meat substitutes (McClements et al., 2019). Quinoa (*Chenopodium quinoa Willd*) is a pseudocereal that originates from South America. Quinoa has a high protein content of 13-25% (based on dry matter) in its seeds depending on varieties. The main storage proteins in quinoa seeds are 11 S globulins and 2 S albumins which accounts for ~37% and ~35% of the total proteins, respectively (Abugoch et al., 2008). Quinoa proteins have a balanced amino acid profile containing all the nine essential amino acids. Further, quinoa proteins are gluten free, which make it a nutritious protein source for Celiac disease patients, who usually have inadequate nutritional intake due to the restrictions in food choices (Miranda et al., 2014). Moreover, QPI is regarded as a less allergenic ingredient compared to traditional plant protein ingredients such as soy protein isolate (SPI) (Ran et al., 2022; Lu et al., 2022).

Despite holding a great promise as future protein ingredients, plant proteins including quinoa proteins commonly show inferior techno-functionalities (e.g., solubility) compared to milk proteins, limiting their wide applications in food products. Extensive efforts have been recently devoted to modifying plant proteins and improving their technical performances including biotransformation-enzymatic hydrolysis/crosslinking or fermentation, chemical modifications (e.g., Maillard reaction and pH-shifting) (Foegeding & Davis, 2011), as well as physical modifications (e.g., heat treatment and extrusion cooking) (Yang et al., 2022). Non-thermal processing technologies including sonication and high hydrostatic pressure (HHP) are standing

out due to relative low cost, ease of implementation, and availability at pilot and industry scale (Gharibzahedi & Smith, 2020).

HHP has been widely applied in the food industry as a non-thermal pasteurisation technique, and it has been also used to modify the structures and properties of food biomacromolecules such as proteins and starch (Yang et al., 2017). It could induce unfolding, denaturation, and gelation (when the concentration of protein exceeds the critical gelation concentration) of globular proteins such as soy protein (Speroni et al., 2009), and kidney bean protein (Ahmed et al., 2018), to name a few. For example, Ahmed et al. (2018) reported that the HHP treatment (200 to 600 MPa, 15 min) could significantly improve the water holding and gelation capacities of kidney bean protein isolates at pH 8 (Ahmed et al., 2018). Sonication is another non-thermal processing technique that are widely employed in the modification of plant proteins (Wen et al., 2019). The high shear forces, micro-jetting and shockwaves generated by the sonication cavitation collapse could lead to the disruption of large protein aggregates and the enhancement of protein solubilities (Gharibzahedi & Smith, 2020). In a recent study from Mir et al. (2019b), 8% w/v QPI dispersions were sonicated at 20 kHz, 500 W and 25% amplitude for 5, 15, 25, and 35 min, respectively. The study showed that the gelling behaviour, emulsifying capability, water solubilities are enhanced whereas the particle size and turbidity are decreased with the increase in sonication time (Mir et al., 2019b).

Sonication and HHP studies on quinoa proteins are scarce compared to other plant proteins. Further, the pH of protein dispersions which is critical to tuning their aggregation behaviours and electrostatic interactions were rarely considered in previous studies. This study is an extension of our previous HHP study of concentrated (10 w/w%) QPI (Luo et al., 2021) with more focus on a systematic comparison of sonication and HHP on microstructural

characteristics and physicochemical properties of diluted (1 w/w%) QPI dispersions at three different pHs (5, 7 and 9). For HHP treatments, an intermediate pressure (250 MPa) and the maximum pressure of the currently used HHP unit (600 MPa) was selected; while for sonication, two sonication times (5 and 15 min) were considered. The knowledge obtained from this study could provide valuable information on choosing appropriate processing techniques to modify quinoa protein isolates that meet their specific application requirements in a wide range of food products such as beverages.

4.2. Materials and methods

4.2.1. Materials

Quinoa seeds were kindly provided by Kiwi Quinoa Inc. (Taihape, New Zealand). According to the supplier, the quinoa seeds used for protein extractions contain 17.5% w/w protein, 4.5% w/w fat, 64.0% w/w carbohydrates, and 11.0% w/w dietary fibre based on a dry weight. All the chemicals including HCl, NaOH, petroleum ether, Ellman's reagent (5′, 5- dithiobis (2-nitrobenzoic acid), DTNB), 8-Anilinonaphthalene-1-sulfonic acid (ANS), and sodium azide were of analytical grade purchased from Sigma-Aldrich (St. Louis, MO, USA). Bradford reagent and bovine γ-globulin standard for determination of protein solubility and chemicals for performing SDS-PAGE (including the 4× Laemmli sample buffer, β-mercaptoethanol, 10× Tris/Glycine/SDS running buffer, Coomassie Brilliant Blue R-250 staining solution) were obtained from Bio-Rad (Hercules, CA, USA). Milli-Q water was used throughout all sample preparations.

4.2.2. Extraction of quinoa protein isolates (QPI) from quinoa seeds

The QPI was extracted from quinoa seeds using an alkaline extraction and isoelectric precipitation method (Yang et al., 2022). Briefly, quinoa flour obtained from grounding of quinoa seeds were defatted using petroleum ether. Thereafter, defatted quinoa flour was dispersed in 0.5 M NaCl solution at pH 8 under stirring for protein extraction. Starch and cell wall polysaccharides/fibres were separated from the solubilized protein fractions using centrifugation. The supernatant obtained were precipitated when the pH was adjusted to 4.5 which is close to the isoelectric point of quinoa proteins. Precipitated proteins were recovered after centrifugation and washed several times with Milli-Q water to remove salts. Finally, the precipitated proteins were redispersed in Milli-Q water containing 0.02w% sodium azide and pH was adjusted to neutral (pH ~7) before freeze-drying to powder. The protein content was ~90% based on a dry matter basis.

4.2.3. High hydrostatic pressure (HHP) treatment of QPI dispersions

A stock QPI dispersion (1.25 wt%) was prepared by the dispersion of QPI powder in Milli-Q water containing 0.02 wt% sodium azide by magnetic stirring at room temperature (~20 ℃) for ~24 h to allow full hydration. The stock solution was then divided into three aliquots and the pH was adjusted to 5, 7, and 9, using 1 M HCl and 1 M NaOH and then the dispersions were left under stirring for another ~ 12 h. The pH was regularly checked and adjusted if needed. Finally, the QPI dispersions were topped up with Milli-Q water to achieve a final QPI concentration of 1 wt%. The HHP treatment was conducted under the same conditions as in our previous study (Luo et al., 2021). In brief, QPI dispersions with different pH (~ 5 mL) were carefully transferred into LDPE plastic pouches (Thomas Scientific, USA) to avoid air bubbles. The QPI dispersions were firstly vacuum sealed with a vacuum sealer (Type C300, Multivac, Germany) and then double sealed with a food vacuum sealer (RHVS1, Russel Hobbs, New

Zealand). A Multivac high-pressure unit (HHP 002 R&D, Multivac, Wolfertschwenden, Germany) was used to conduct HHP treatments with water as the pressurizing medium. The samples were treated at 250 and 600 MPa at room temperature for 15 min. The temperature of samples was recorded throughout the HHP treatment and never exceeded 33 ℃. The pressure was released to atmospheric pressure instantaneously after the treatment is completed. The treated samples were kept sealed until further characterisations. All QPI samples were made in duplicates.

4.2.4. Sonication treatment of QPI dispersions

Sample preparations for the sonication treatment are the same as described in the section 2.3. QPI dispersions (10 mL each) were transferred to 20 mL glass vials and sonicated for 5 and 15 min, respectively in a 30s on/30s off mode using a 20 kHz ultrasonicator equipped with a 6 mm horn with a dial power of 950 W (JY92-IIN, Ningbo Scientz Biotechnology Co., Ltd, China). The actual sonication power was determined as 14.4 W using a calorimetric method by determining the increase in temperature of sonicated water with time (Contamine et al., 1995). To prevent overheating, glass vials containing samples were kept in a water-ice bath throughout the sonication treatment to maintain the temperature below 35 ℃. All QPI samples were made in duplicates.

4.2.5. Sodium dodecyl sulphate–polyacrylamide gel electrophoresis (SDS-PAGE)

Samples including the control (untreated), sonication (15 min) and HHP (600 MPa) treated were selected for SDS-PAGE analysis. The SDS-PAGE analysis was conducted under both non-reducing and reducing conditions according to Laemmli et al (1970) and Luo et al (2021)

using a commercial precast Mini-protein TGX (Tris/Glycine) gel (Bio-Rad, USA) consisting of 4% stacking gel and 15% resolving gel. The running buffer used was diluted 10 times from 10× tris/glycine/SDS running buffer with Milli-Q water (Bio-Rad). The gels were stained with Coomassie Brilliant Blue R-250 staining solution (Bio-Rad) for 60 min and destained using a destaining solution (10% Isopropanol and 10% Acetic acid glacial in Milli-Q water) under shaking. The destaining solution was changed every half hour until the gel background became transparent, the gels were stored in Milli-Q water at 4 °C. A ChemiDoc XRS imaging system (Bio-Rad, USA) was used to scan the gels. Quantification of band density was performed using the software Image Lab (Bio-Rad, USA).

4.2.6. Determination of free sulfhydryl group (SH)

Contents of free sulfhydryl group in various untreated and HHP and sonication treated QPI dispersions were determined according to previous studies (Beveridge et al., 1974). Briefly, 10 μL of Ellman's reagent (4mg/mL DTNB in Tris-glycine buffer) was mixed with 0.25 mL 1% QPI dispersions and 1.25 mL Tris-glycine buffer (0.086 M Tris, 0.09 M glycine, 0.004 M EDTA). The mixtures were vortexed for 30 s and incubated for 15 min at room temperature (~20 °C) before the absorbance measurement. The blank was prepared with the same protocol, but samples were replaced by Milli-*Q* water. The absorbance at 412 nm was measured by a UV-Vis spectrophotometer (Shimadzu 2000, Kyoto, Japan).

4.2.7. Determination of surface hydrophobicity (H_o)

Surface hydrophobicity was measured using a fluorescence spectrophotometer (RF-6000, Shimadzu, Kyoto, Japan) according to a previously reported method (Kato & Nakai, 1980) with slight modifications. Each sample was diluted to the concentrations 12.5, 25, 50, 100 and

200 µg/L in 10 mM Tris-HCl buffer (pH 7.0) separately with or without adding a fluorescence probe-8-anilino-1-naphthalene sulfonate (ANS). The reaction was conducted at 20 ℃ for 20 min in the dark. Fluorescence spectra were recorded at 470 nm (emission) and 390 nm (excitation) with a slit width of 5 nm. QPI samples in the absence of ANS was used as backgrounds. The index of surface hydrophobicity was expressed as the initial slope obtained from the linear regression analysis of the plots of fluorescence intensities versus QPI concentrations.

4.2.8. Fourier transform infrared spectra (FTIR) analysis

Sonication and HHP treated QPI samples were freeze-dried and ground to powder by a pestle and mortar. FTIR spectra was recorded using a compact ATR-FTIR spectrometer (ALPHA II, Bruker, Germany) in a range of scan between 4000 and 500 cm^{-1} at a 4 cm^{-1} resolution. A background scan (air) was conducted prior to each sample measurement. Measurements were conducted at least in duplicate and a total of 64 scans were averaged before baseline subtraction. Peak deconvolutions were conducted using the PeakFit software (Systat software Inc. USA) to obtain components of protein secondary structures.

4.2.9. Solubility determination

1% QPI samples were centrifuged at 1000×*g* for 10 min at 20 ℃ using a benchtop centrifuge (Pico17 microcentrifuge, Thermofisher scientific, USA). Thereafter, the supernatant was transferred to new Eppendorf tubes and diluted with Milli-Q water to reach the absorbance in a range from 0.2 to 0.8. The diluted supernatants (20 µL) were firstly mixed with 1.48 mL of Bradford reagent (Bio-Rad, USA) and then absorbance of each sample at 595 nm was measured

using a UV-Vis spectrophotometer (Shimadzu 2000, Kyoto, Japan). A standard curve of absorbance versus protein concentrations was made using a Bovine γ-globulin standard (Bio-Rad, USA). All measurements were conducted in triplicate. The solubility was calculated by the ratio of protein content of supernatant to the original protein concentration in the QPI suspension before centrifugation.

4.2.10.Particle size measurements of soluble proteins

The particle size (hydrodynamic diameter z-average) of various untreated and treated QPI dispersions was determined with dynamic light scattering (DLS) using ZetaSizer Nano ZS (Malvern instruments, UK) with the scattering angle of 173 ° and a fixed wavelength of 633 nm at 20 ℃. Samples were allowed to sediment on the bench overnight, then the supernatants were collected and diluted with Milli-Q water for the DLS measurements with a refractive index and viscosity of water of 1.33 and 0.89 mPa s, respectively. Each sample was measured 20 times and the z-average size is reported.

4.3. Results and discussion

4.3.1. QPI protein profiles as revealed by SDS-PAGE analysis

SDS-PAGE analysis was conducted to determine any alterations in the protein profiles after sonication or HHP treatments and results are shown in **Figure 11**. Under nonreducing conditions, untreated QPI exhibits a complex protein profile with predominant protein bands appearing at ~ 55 kDa and ~ 45 kDa; these are attributed to chenopodin or 11 S globulin (Vera et al., 2019). Smaller proteins (molecular weight smaller than 15 kDa) are suggested to be 2 S albumin (Abugoch et al., 2008). Further, untreated QPI dispersions at different pH display

similar protein profiles, which is consistent with previous SDS-PAGE studies on QPI at pH 6.5, 8.5, and 10.5 (Mäkinen et al., 2016b).

The HHP treatment (600 MPa, 15 min) induced a significant reduction in band densities of 11 S globulin at all three pHs, which could be explained by the denaturation and aggregation of 11 S globulin induced by HHP. Similar observations were found in previous HHP studies of QPI (Luo et al., 2021) and potato protein isolates (Katzav et al., 2020). It has been suggested that HHP treatment could induce unfolding of globular proteins and promote formations of protein aggregates via various non-covalent (i.e., hydrophobic interactions and hydrogen bonding) and covalent interactions (i.e., disulphide bonds) (Queirós et al., 2018; Speroni et al., 2009). Under reducing conditions (**Figure 11**B), large protein aggregates which accumulated in the loading wells during the non-reducing SDS-PAGE analysis disappeared and all the QPI dispersion exhibit similar protein profiles, which confirms the formation of disulphide bonds in HHP induced QPI aggregates. Protein bands located at ~ 37 kDa (acidic subunit) and ~25 kDa (alkaline subunit) also become more obvious under the reducing condition, suggesting two subunits of 11 S globulin are linked through disulphide bonds. In addition, the extent of 11 S globulin band fading increased with the increase in pH and the HHP treatment of QPI at pH 9 resulting in less 11 S globulin remaining in the gel (**Figure 11**C). This finding agrees well with previous studies on soy proteins (Jiang et al., 2009) and faba bean protein isolates (Alavi et al., 2021). This could be due to the oxidation of the SH groups to S-S bonds and the SH/S-S interchange reactions being much more favourable under alkaline conditions (Shimada & Cheftel, 1988).

Compared to HHP treatment, sonication treatment did not induce significant alterations to the

protein profiles at all the three pHs (**Figure 11**A and C), which agrees well with a previous sonication study of QPI (Mir et al., 2019b) confirming that sonication does not hydrolyse these proteins. However, the large molecular weight protein aggregates observed in the loading wells of lane 7 (pH 7, sonication treated 15 min) and lane 9 (pH 9, sonication treated 15 min) under non-reducing conditions as well as them vanishing in the presence of the reducing agent may indicate that sonication induced the formations of large protein aggregates via disulphide bonds (**Figure 11**). Previous studies suggested that highly reactive free radicals generated from water sonolysis could react with amino acids containing sulphur groups (Cys and Met), leading to the oxidation of free -SH groups and the formation of disulphate bonds (Vera et al., 2019). However, the fading of major QPI protein bands (i.e., 11 S globulin) is not observed. This could be due to compensation from higher solubilities and smaller particles sizes of the sonicated QPI samples, thereby increasing their solubilities in the sample buffer used in the non-reducing SDS-PAGE (Mir et al., 2019b).

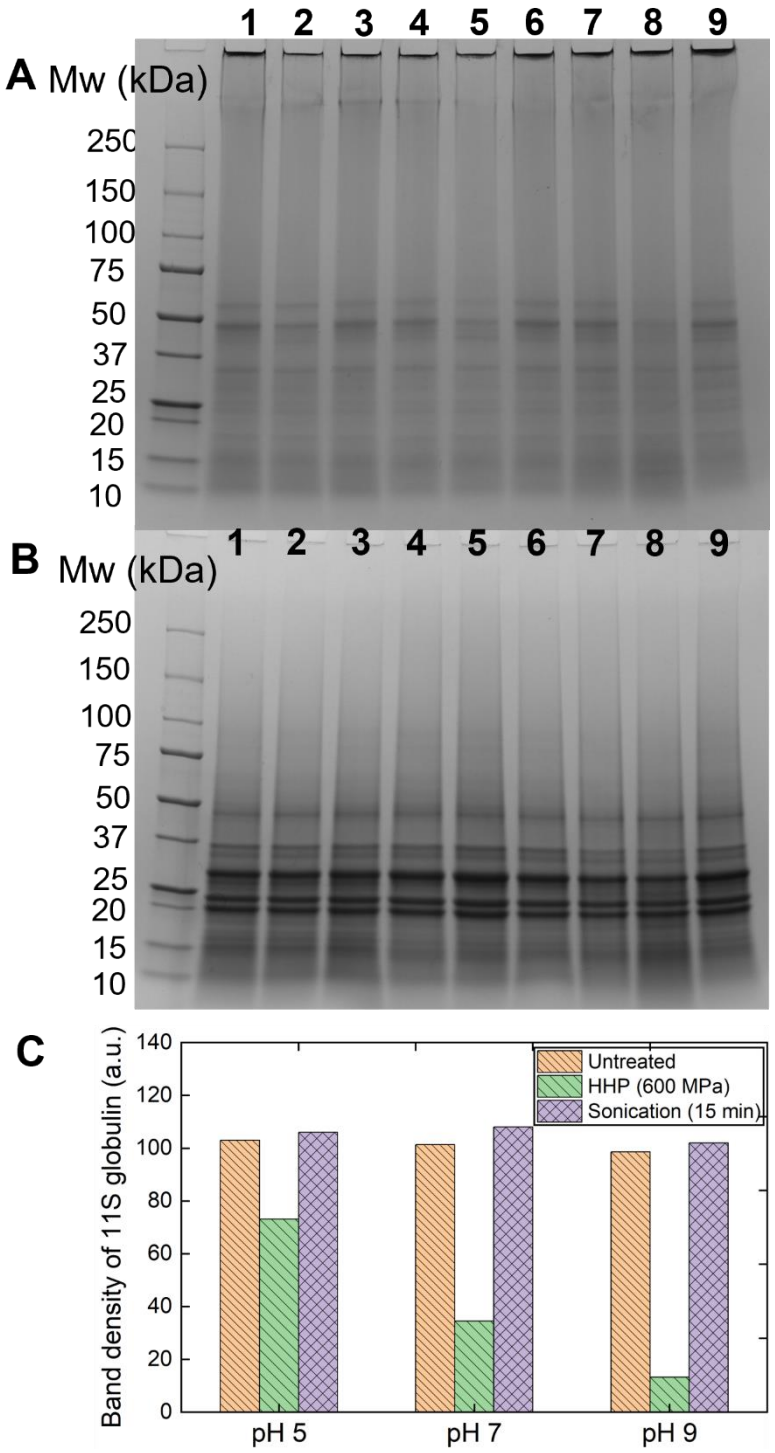

Figure 11: SDS-PAGE patterns of QPI dispersions at three pHs (5, 7, and 9) before and after HHP treatment (600 MPa, 15 min) or sonication treatment (14.4 W, 15 min) under non-reducing (A) and reducing conditions (B). Lane 1: pH 5 untreated, Lane 2: pH 5 HHP treated, Lane 3: pH 5 sonication treated, Lane 4: pH 7 untreated, Lane 5: pH 7 HHP treated, Lane 6: pH 7 sonication treated, Lane 7: pH 9 untreated, Lane 8: pH 9 HHP treated, Lane 9: pH 9 sonication treated. (C) Quantification of band densities of 11S globulins (~45 and ~55 kDa) obtained under non- reducing conditions.

4.3.2. QPI protein secondary structural changes revealed by FTIR analysis

FTIR spectra of untreated and sonication or HHP treated QPI samples are shown in **Figure 12**. All samples display characteristic absorbance features of proteins, namely the Amide I region (peak ~1630 cm^{-1}) originated from C=O stretching, or hydrogen bonding coupled with COO- group; the Amide II region (peak ~ 1520 cm^{-1}) mainly attributed to the NH bend coupled with CN stretch; and the Amide III region (peak ~1230 cm^{-1}) due to NH bend stretch coupled with CN stretch (Ahmed et al., 2018; Sow & Yang, 2015). Compared to the untreated QPI sample, the sonication or HHP treatment did not induce peak shifting in the Amide I region, however, a shift in peak ~1520 cm^{-1} (Amide II region) to higher wavenumbers can be observed in some sonication or HHP treated samples. For example, the HHP (600 MPa) treatment at pH 5 induced a shift of the Amide II peak from ~ 1510 cm^{-1} to 1525 cm^{-1}. Similarly, the sonication treatment (5 min) at pH 9 induced a shift of the Amide II peak from ~ 1518 cm^{-1} to 1532 cm^{-1}. A similar shift in the Amide II peak was reported in a previous FTIR study of kidney bean protein isolate after HHP treatment (600 MPa. 15 min) (Ahmed et al., 2018) and it has been suggested to occur due to the unfolding of the protein tertiary structure (Tang & Ma, 2009). The red shift (an increase in the wavenumber of amide II band peaks is also observed in a recent sonication study (600-2000 W, 5-30 min) of walnut protein isolates, which could be attributed to the change in interactions between protein molecules and structural unfolding due to ultrasonication (Zhao et al., 2022a).

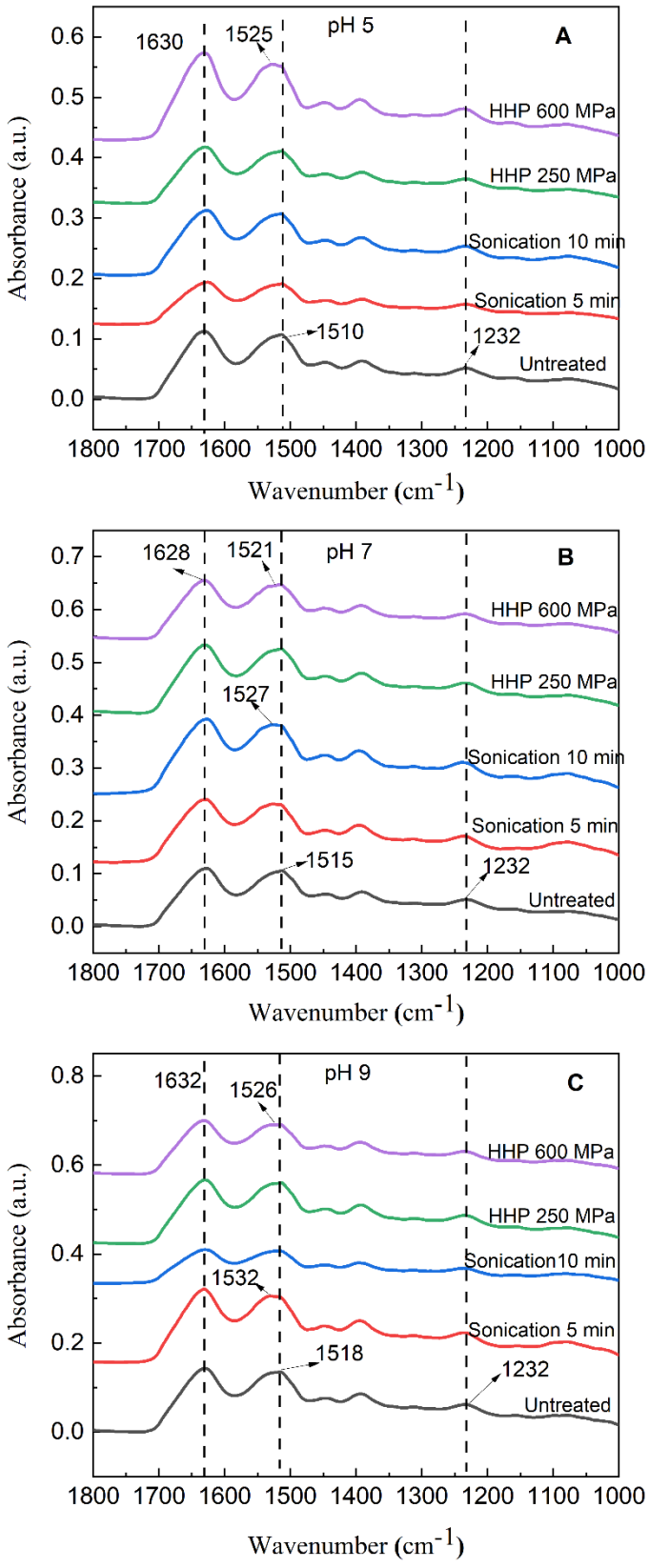

Figure 12: FTIR spectra of untreated and sonication or HHP treated QPI samples at pH 5 (A), pH 7 (B), and pH 9 (C). The spectra were vertically shifted to avoid overlap.

In order to better understand the impact of sonication or HHP treatment on the secondary structures of QPI, the deconvolution of the amide I region (1590 cm^{-1} to 1710 cm^{-1}) was conducted, and the percentage of each structural component (α-helix, β-turn, β-sheet, and random coil) is illustrated in **Figure 13**. In general, changes of all the secondary structures have similar trends at three pHs: percentages of disordered secondary structures (β-turn and random coil) increased after the sonication/HHP treatment, whereas a decrease in ordered secondary structures (α-helix and β-sheet) was observed in the sonication and HHP treated samples. This indicated that both sonication and HHP treatments could induce the unfolding of protein structures, in agreement with previous studies (Elahi & Mu, 2017; Hu et al., 2013). However, changes in secondary structures of QPI are more prominent in the sonication treated samples particularly at pH 9. For example, the content of β-sheet at pH 9 is decreased from ~38.9 % (untreated) to ~29.7% after the sonication treatment for 15 min, while the HHP treatment (600 MPa, 15 min) only leads to a reduction of ~ 36.6 %. Changes in other secondary structures follow a similar trend.

It has been suggested that cavities in proteins and hydrogen bonds are the most compressible parts of proteins, and pressurisation could induce the collapse of the cavities due to water penetrations and decreasing the distance between hydrogen bonds (Akasaka, 2006). These effects enhance intermolecular interactions but destabilise the protein tertiary structures, leading to a partial or complete unfolding of proteins (Queirós et al., 2018). Under sonication treatment, proteins unfolding, weakening of non-covalent interactions and cleavages of disulfide bonds could also occur as a result of strong shear cavitational forces and micro-streaming generated during ultrasonication (Gharibzahedi & Smith, 2020). Using circular dichroism to probe the secondary structures of quinoa proteins, Li et al. (2018) found that the content of α-helix and random coil significantly decreased and increased, respectively, after a sonication treatment at

HHP treatment. In another sonication study on soybean proteins, Hu et al. (2013) reported that the percentage of β-sheet is reduced from 60% to 38.2% while the percentage of random coil increased from 32.3% to 38.9%. In a HHP study of patatin, Elahi et al. (2017) found that the percentage of α-helix progressively decreased from 24.2% (untreated) to 4.1 (550 MPa) while the content of random coil increased from 30.3% to 37.2%. Different extents of changes in secondary structures could be due to the differences in plant proteins and different treatment conditions used in these studies.

Further, at the same pH, sonication treatment induced much more significant alterations in protein secondary structures than the HHP treatment, particularly at higher pHs (7 and 9). This could be due to the effects of high shear forces, microstreaming, and microjetting exerted by the cavitation during the sonication treatment. Further, the high pH could increase electrostatic repulsions between protein molecules and enhance interactions between proteins and water molecules, thus promoting the unfolding of protein structures and extension of protein chains. The synergistic effect of ultrasonication and high pH on unfolding of plant proteins have been well documented on pea proteins (Jiang et al., 2017) and barley proteins (Silventoinen & Sozer, 2020), for examples. It has been suggested that the change in protein secondary structures is commonly accompanied with the exposure of embedded hydrophobic regions (Sun et al., 2013). Therefore, the contents of free SH groups and surface hydrophobicity of QPI is further investigated in the following sections.

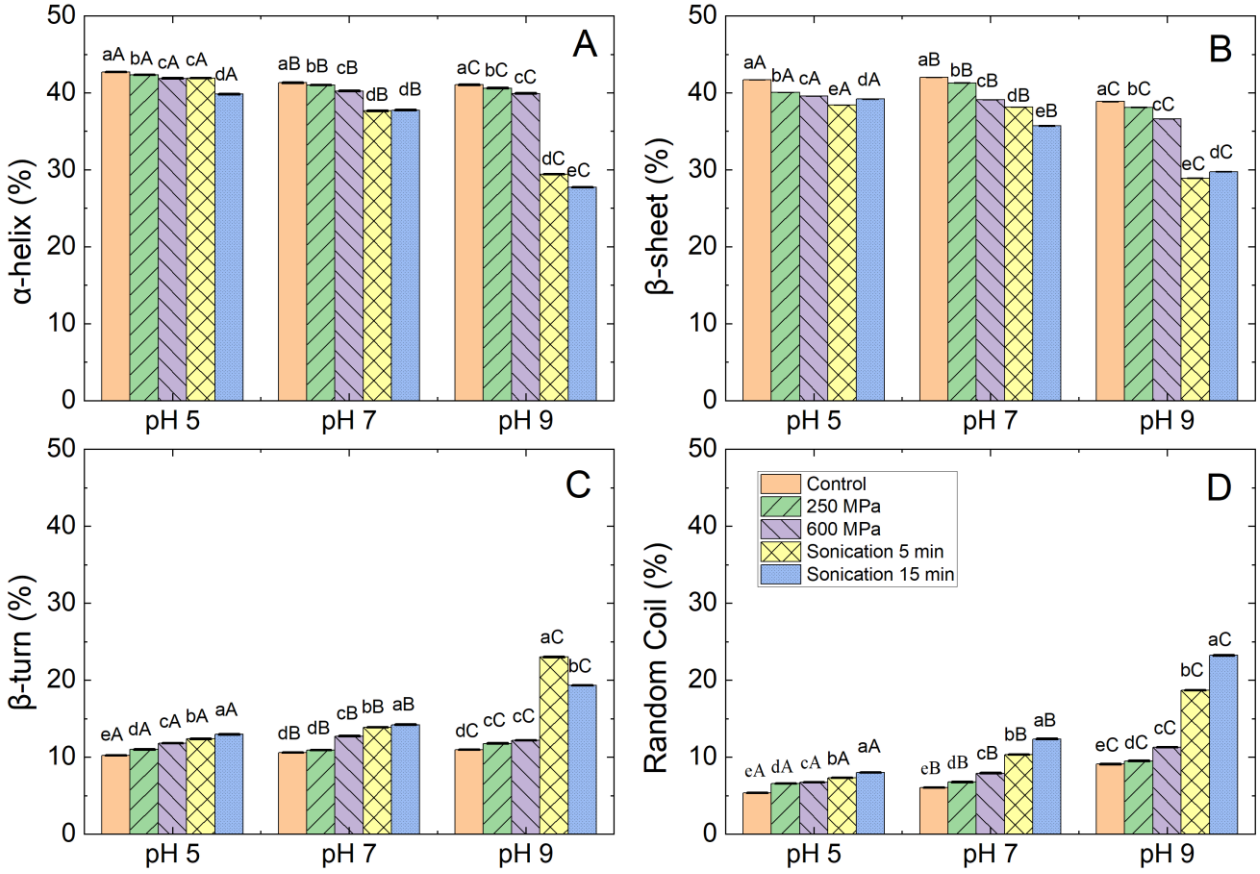

Figure 13: Percentages of the secondary structure (α-helix (A), β-sheet (B), β-turn (C), and random coil (D)) in untreated and HHP or sonication treated QPI dispersions at pH 5, 7, and 9. Mean values between samples at same treatment with different uppercase letters (A, B, C) are significantly different. Mean values between samples at same pH with different lowercase letters (a, b, c) are significantly different.

4.3.3. Determination of free SH groups and surface hydrophobicity

The content of free SH groups and surface hydrophobicity of untreated and the sonication /HHP treated QPI samples is shown in **Figure 14**. For the untreated QPI samples, higher pHs (7 and 9) resulted in a significant increase in the free SH content, which could be due to diminished protein-protein attractions and greater extents of structural unfolding as supported by FTIR (Jiang et al., 2009). At all pHs, the content of free SH groups and surface hydrophobicity are increased after the sonication treatment. For example, the content of free SH group is increased from ~22 µmol/g (untreated) to ~28 µmol/g (sonication, 10 min) at pH 9. The increase of SH content and surface hydrophobicity might be attributed to the exposure of embedded SH and

other hydrophobic groups to the surface of QPI molecules, the enhanced solubility, or the cleavages of S-S bonds induced by sonication (Hu et al., 2013; Jiang et al., 2017). Similar observations have been made in previous sonication studies of various plant protein samples including QPI (Li et al., 2018), soy protein isolates (Hu et al., 2013), and pea proteins (Jiang et al., 2017). It is worth noting that the oxidation of free SH groups by the free radicals during the sonication and the formation of S-S bonds via SH/SS interchange reactions under alkaline conditions might also occur (Jiang et al., 2009), but probably to a smaller extent, so that the exposure of embedded SH and hydrophobic groups is dominated leading to the overall increase of free SH content.

Contrary to sonication treatment, HHP treatment induced a decrease in the free SH content at all three pHs. At pH 5 and 7, the free SH content progressively decreased when the pressure is decreased from 250 MPa to 600 MPa. For example, the content of free SH group decreased from ~ 7.7 µmol/g (untreated) to ~6.1 µmol/g (600 MPa, 15 min) and ~22.2 µmol/g (untreated) to ~8.3 µmol/g (600 MPa, 15 min) at pH 7 and pH 9, respectively. This might be due to the formations of S-S linkages via SH/SS interchange reactions and protein aggregation (Elahi & Mu, 2017). This observation is also supported by the SDS-PAGE results that 11S globulin participated in the formations of large protein aggregates via S-S bonds (**Figure 11**). The aggregation of proteins induced by HHP treatment is also reflected in the decrease in the surface hydrophobicity (**Figure 14**B). The index of surface hydrophobicity is decreased from ~35299 (untreated) to ~121888 (600 MPa, 15 min), ~283940 (untreated) to ~257824 (600 MPa, 15 min), and ~172962 (untreated) to ~126646 (600 MPa, 15 min) at pH 5, pH7, and pH 9, respectively. Aggregation of unfolded protein leads to the formation of protein aggregates with large molecular weight and subsequent decrease of the surface hydrophobicity (Hu et al., 2013). Further, the decrease in the surface hydrophobicity is most significant at pH 5 because the

electrostatic repulsions between proteins are minimized at the isoelectric point, thus the most extensive protein aggregation is expected at this pH. This observation agrees well with our previous study on HHP treatment of 10 wt% QPI (Luo et al., 2021).

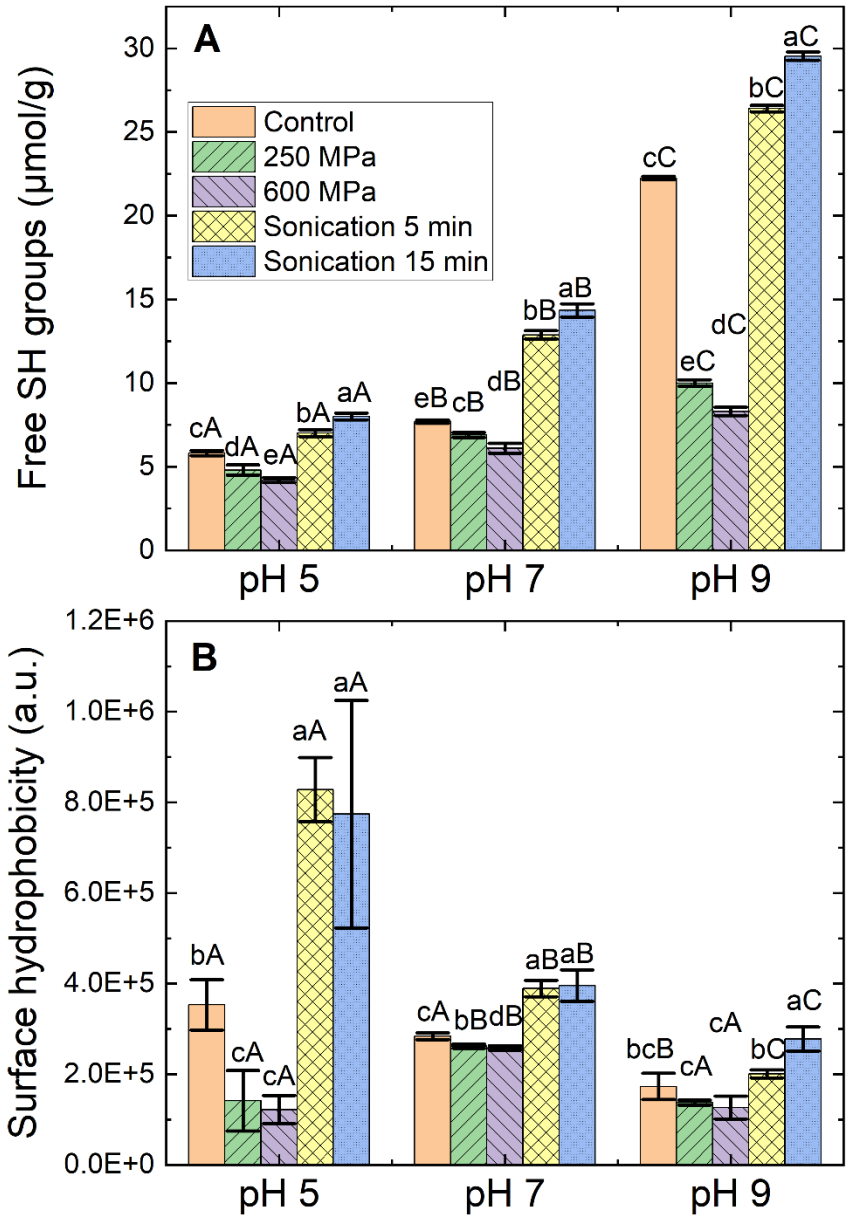

Figure 14: Free sulfhydryl (SH) groups content (A) and surface hydrophobicity (B) of untreated and sonication or HHP treated QPI dispersions. Mean values between samples at same treatment with different uppercase letters (A, B, C) are significantly different. Mean values between samples at same pH with different lowercase letters (a, b, c) are significantly different.

In a HHP study of patatin, Elahi et al. (2017) found that the content of free SH groups and

surface hydrophobicity is firstly increased from atmospheric to 350 MPa and 450 MPa, respectively, and then decreased when the pressure is further increased to 550 MPa (Elahi & Mu, 2017). A similar trend has been reported in a HHP study of soy protein isolate, but the maximum of the free SH group content was reached at 300 MPa before decreasing when the pressure is increased up to 550 MPa (Li et al., 2012). The authors attributed this to the initial unfolding of proteins at intermediate pressures followed by the subsequent protein aggregation and reassociation at higher pressures. In another HHP study of soy protein isolates, Torrezan, Tham, Bell, Frazier and Cristianini (2007) reported that free SH contents are lower in all HHP (198-702 MPa) treated samples (in comparison with the untreated one). The discrepancy between our findings and previous studies could be due to different HHP treatment conditions (pressure, time, and temperature) and different structures of these plant proteins.

4.3.4. Protein solubilities and particles sizes as affected by the sonication or HHP treatment

The solubility and particle size of various untreated and sonication/HHP treated QPI dispersions are shown in **Figure 15**. Among the untreated samples, the QPI dispersion at pH 5 shows the lowest solubility (~ 4%) and largest particle size (~1200 nm), while at pH 9 the solubility markedly increased to (~33%) with a small reduction in the particle size to ~800 nm. This finding is consistent with previous studies that proteins typically exhibit minimum solubility and largest particle size at or close to their isoelectric point (Shen et al., 2021). The sonication treatment induced a significant increase in solubility at pH 7 and pH 9, while the change of solubility is marginal at pH 5. Comparing with the untreated sample, sonication treated for 15 min increased the solubilities to ~45% and ~82% at pH 7 and pH 9, respectively. Similar observations have been found in the sonication studies of QPI (Mir et al., 2019b; Vera et al., 2019), soy protein isolate (Hu et al., 2013), and canola protein isolate (Flores-Jiménez et al., 2022). Various extents of increase in solubilities of proteins have been reported in previous

studies, which depends on the sonication conditions and sample characteristics. However, it is generally believed that protein interactions (e.g., hydrophobic interactions and hydrogen bonding) can be disrupted by the sonication treatment, leading to smaller particle sizes, large surface areas for water accessibility, and higher solubilities. This is confirmed with the particle size results showing that the particle size is decreased from ~750 nm (untreated) to ~ 210 nm (sonication, 15 min) at pH 7, and from ~800 nm (untreated) to ~160 nm (sonication 15 min) at pH 9. The unfolding of proteins and the loss of their internal native structure were also confirmed with FTIR analysis. The change in particle size and solubility by sonication treatment is not obvious at pH 5, which could be due to strong electrostatic attractions close to its isoelectric point (pH ~4.5). It has been suggested that turbulent flow and high shear force exerted by ultrasound cavitations could facilitate creating large interfacial area between air and water thereby disrupting hydrogen bonds and hydrophobic interactions of the protein molecules. Thus techno-functional properties of proteins such as solubilities and some physicochemical characteristics, such as particle size, can be affected (Akharume et al., 2021; Nazari et al., 2018; Wen et al., 2019).

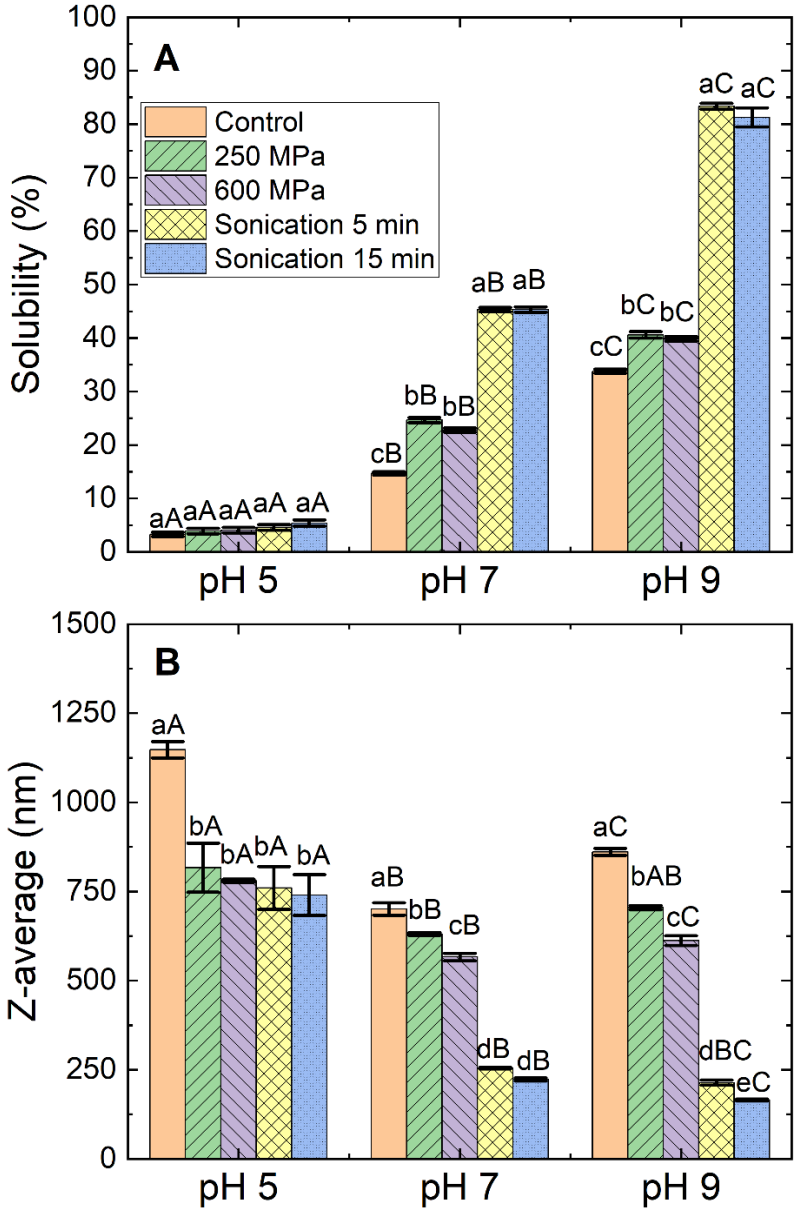

Figure 15: Solubility and particle size (Z-average) of untreated and sonication or HHP treated QPI dispersions. Mean values between samples at same treatment with different uppercase letters (A, B, C) are significantly different. Mean values between samples at same pH with different lowercase letters (a, b, c) are significantly different.

Contrary to sonication treatment, the solubility of QPI increased only slightly after HHP (600 MPa) treatment at pH 7 and pH 9. The solubility increased from ~14.7% (untreated) to ~22.8% (600 MPa, 15 min) and ~33.8% (untreated) to ~39.8% (600 MPa, 15 min) at pH 7 and pH 9, respectively. However it did not induce changes in solubility at pH 5 similarly to sonication treatment. A similar observation was reported in a previous HHP study of soy protein isolates, where solubilities at pH 3 and pH 8 increased up to 400 MPa (Puppo et al., 2004). This could

be due to the conversion of insoluble aggregates to soluble ones because of their smaller particle size through the newly formed S-S bonds as revealed by the SDS-PAGE and free SH groups analysis (Yin et al., 2008). This is also consistent with the particle size reduction observed for all three pHs. It has been suggested that the HHP could disrupt weak interactions in proteins such as hydrogen bonds and Van der Waals force (Puppo et al., 2004). The extent of protein unfolding and aggregation due to HHP treatment will be determinant for the particle size and solubility of the QPI dispersion. The mechanisms of the effect of HHP on protein modifications depends on the extent of volume change of the protein molecules in solution, which leads to disruption, denaturation, and aggregation. According to Le Chatelier's principle a decrease in protein volume occurs by increased pressure and vice versa (Messens et al., 1997). The volume change in proteins under HHP typically consists of the compression of protein cavities and disruptions of the non-covalent interactions (e.g. hydrophobic interactions and electrostatic interactions) as well as alterations in protein-solvent interactions (Galazka et al., 2000). These changes in molecular structures and interactions could lead to alterations in the physicochemical and techno-functional properties of proteins (Huang et al., 2021).

4.4. Conclusions

In summary, this study shows that sonication and HHP treatments have different influences on microstructural characteristics and physicochemical properties of QPI dispersions, and these influences are pH dependent. Sonication treatment significantly reduce the particle size and improve the solubility of QPI at pH 7 and pH 9 without significantly affecting the protein profiles as revealed by SDS-PAGE. Due to the substantial protein aggregation at pH 5 (close to the isoelectric point of QPI), the changes in particle size and solubility are marginal. Further, the sonication treatment induced the exposure of interior SH and/or hydrophobic groups via proteins unfolding which is reflected in the increase in free SH content and surface

hydrophobicity. In contrast, HHP treatment induced significant changes in the QPI protein profiles where 11 S globulins tend to form aggregates via S-S bonds especially at pH 9. This is also supported by a decrease in the free SH content and surface hydrophobicity after the HHP treatment. FTIR revealed that both HHP and sonication treatments induce an increase in the disordered secondary structure (β-sheet and random coil) resulting from the transformations from the ordered secondary structures (α-helix and β-turn). In addition, other than pH, some other process parameters such as ultrasonication power/pulses/times, the level/duration of applied pressure, the treatment temperature, as well as the presence of other food constituents and additives (e.g., salts and polysaccharides) may also have an impact on QPI dispersions being treated (Akharume et al., 2021). Further research is needed to clarify the effect of these different parameters. Finally, this study demonstrated that tailored QPI properties can be achieved by selecting different processing techniques and different pHs. Further studies can be conducted to reveal the effects of sonication and HHP on techno-functional properties (e.g., gelation, emulsifying, and foaming) of the treated QPI dispersions.

5. Chapter 5: Impact of high hydrostatic pressure on the gelation behaviour and microstructure of quinoa protein isolate dispersions*

Keywords: High hydrostatic pressure processing; Quinoa protein isolates; Viscosity, Gelation;

Microstructure

5.1. Introduction

Recently, the consumption of plant-based foods has increased substantially, and a wide range of plant-based food products including meat substitutes and dairy alternatives are being developed (Mäkinen et al., 2016). Plant proteins have started to become a novel and promising alternative protein to partially replace dairy and animal-derived proteins in food and pharmaceutical applications (Le Roux et al., 2020). It is believed that the fabrication of plant protein is much more sustainable than those of dairy and animal proteins, thus providing a promising solution to feed the rapidly growing world population and address some of the environmental challenges (Sá et al., 2020).

Quinoa (*Chenopodium Willd*.) is an important protein source in the countries of its origin (South America) and has recently gained increasing popularity in the west (Ruiz et al., 2016). Quinoa seeds contain 12–23 g/100 g protein on a dry weight basis depending on the variety and exhibit a well-balanced essential amino acid profile (Abugoch et al., 2008). The 11S globulin (50–60 kDa) and 2S albumin (<15 kDa) are the major storage proteins in the quinoa seeds, constituting approximately 37 and 35 g/100 g of the total seed proteins (Ruiz et al., 2016). Quinoa protein isolate (QPI) has demonstrated excellent gelation, emulsifying, and foaming abilities than other plant proteins (Shen et al., 2021). Therefore, QPI has potential applications as a versatile food ingredient for various food products, such as vegan yoghurt, baking, meat analogues, and extruded products.

Gelation is considered as one of the most critical technical functionalities of proteins because it is central to various applications in the food, cosmetic, and nutraceutical industries (Katzav et al., 2020). For example, the gel formation capabilities of proteins play important roles in the determination of textural properties, organoleptic perceptions, and digestion behavior of

yoghurt, cheese, tofu-like products, and meat substitutes (Luo et al., 2017). In the case of globular proteins such as QPI and whey proteins, heat-induced gelation is one of the most extensively used gelation routes (Katzav et al., 2020; Nicolai, 2019). During heat treatment, protein starts to denature and unfold, which results in the progressive exposure of the hydrophobic groups that were originally buried inside of the protein. This leads to the generation of protein aggregates. When the concentration of protein exceeds the minimum concentration required for gelation, the gelation occurs where an interconnected and three-dimensional protein network with water entrapped inside the network is formed (Marangoni et al., 2000). The mechanical properties and microstructural characteristics of protein gels are strongly dependent on both the polypeptides' nature and the gelation conditions (Phan-Xuan et al., 2013).

In recent years, nonthermal food processing technologies, such as high hydrostatic pressure (HHP) processing, have received massive attention from both industry and academia and have been applied extensively to modify the molecular structures, physicochemical properties, and technical functionalities of food biopolymers (Yang et al., 2017). In the case of globular proteins, HHP is usually employed to induce gelation as an alternative to thermal treatment. Previous studies showed that HHP treatment could induce the denaturation and gelation of various dairy and plant sourced proteins (Katzav et al., 2020; Ngarize et al., 2005). For instance, the application of HHP (400 MPa, 30 min) results in the formation of whey protein concentrate (WPC) gels. The HHP-formed WPC gels have relatively weaker mechanical strength than the thermally obtained gel (Van Camp & Huyghebaert, 1995). In addition, the effects of both heat and HHP treatments on the gelation behavior of proteins are shown to be related to pH. Katzav et al. (2020) reported that heat treatment (90 °C, 30 min) of potato protein isolate at pH 7 and pH 3 results in the formation of gels, while HHP treatment (300–500 MPa, 30 min) allows gel

formation only at pH 3 when the treatment temperature exceeds 30 °C. However, to the best of our knowledge, HHP induced alterations in the rheological properties and microstructural characteristics of QPI dispersions at different pHs, and its comparisons with heat treatment have not been investigated yet.

The objective of this study is to compare the effect of HHP treatment (100, 250, 400, and 600 MPa) and thermal treatment (81 ± 2 °C, 30 min) on the protein aggregation, flow behavior, viscoelasticity, and microstructural characteristics of QPI dispersions at pH 5, 7, and 9. The different pHs were selected to modulate electrostatic interactions between proteins. At pH 5, which is close to the isoelectric point (pH 4.5–5.0) of 11S globulin, the major protein in QPI (Shen et al., 2021), the proteins exhibit zero net charges and thus minimal repulsions. On the other hand, at a pH that is far from the isoelectric point, such as pH 9, the electrostatic repulsion is dominant resulting in a higher solubility. This work aims to establish a fundamental knowledge of the relationship between the microstructural changes and the resulting functional properties of QPI solution when treated by HHP. This can provide a theoretical-based technical guidance to the food industry to ensure optimal conditions for the production of high-quality quinoa protein-based products. We believe that the knowledge gained from this study can be extended to future HHP applications in other emerging protein-based systems such as pea, faba bean, and algae proteins.

5.2. Materials and methods

5.2.1. Materials

Quinoa seeds were kindly provided by Kiwi Quinoa Inc. (Taihape, New Zealand). All chemicals including HCl, NaOH, petroleum ether, and sodium azide were obtained from Sigma-Aldrich, and they were of analytical grade. All samples were prepared using Milli-*Q*

water.

5.2.2. Preparation of QPIs

Raw quinoa seeds were fully washed with Milli-*Q* water three times to remove saponins (El Hazzam et al., 2020) and air-dried. Subsequently, they were ground using a coffee grinder (Coffee and Spice Grinder, Breville, NZ) and passed through a 500 μm sieve (Endecotts, UK). For defatting, quinoa fine flour was stirred overnight with petroleum ether (1:10 w/w). The solvent was replaced the next day, and the mixture was stirred for another 60 min. The suspension was left in the fume hood for 30 min to allow the flour to sediment. Thereafter, the supernatant was poured out, and the sediment was spread onto a plastic tray and air-dried in the fume hood for 6 h. The defatted quinoa flour was soaked into 0.5 M NaCl solution containing 0.02 w/w % sodium azide with a ratio of quinoa flour to NaCl solution of 1:10 (w/w). The mixture was then adjusted to pH 8 with 1 M NaOH under magnetic stirring. The mixture was adjusted to pH 8 every hour for 3 h and then was continuously stirred overnight. After that, the mixture was centrifuged at 10 000 g at 20 °C (6–16 KS with rotor 12 356, Sigma, Germany) for 15 min, and the supernatant was collected. These steps were repeated at least twice until the supernatant presented a low turbidity. Afterward, the pH of the supernatant was adjusted to 4.5 using 1 M HCl every hour for 2 h followed by centrifuging at 10 000 g at 20 °C for 15 min, and the sediment was collected. 150 g of Milli-*Q* water was added to the sediment and centrifuged under the same conditions at least twice to wash the precipitate until the electrical conductivity became lower than 80 μS/cm. The precipitate was then resolubilized in Milli-*Q* water containing 0.02 w/w % sodium azide and neutralized to pH 7 with 1 M NaOH overnight. QPI dispersions were then frozen for 24 h in a −20 °C freezer before being freeze-dried with a Labconco freeze dryer (model 7753034, Labconco, USA) for 4 days and ground to powders with a pestle and mortar. Finally, the QPI powder was transferred to a plastic bottle and sealed

by avoiding sunlight at 20 °C for further uses (Zhang et al., 2021). The compositional analysis of QPI was done at the Nutrition Laboratory of Massey University. The protein, fat, ash, and moisture contents of the QPI powder were 91.6, 2.9, 2.8, and 2.7%, respectively.

5.2.3. HHP processing

A stock QPI dispersion (12.5 wt %) containing 0.04 wt % sodium azide was prepared by suspending the QPI powder in Milli-*Q* water under magnetic stirring at 20 °C for 24 h to enable protein hydration and solubilization. The QPI dispersions (10 wt %) at different pHs (5, 7, and 9) were then prepared by mixing appropriate amounts of the QPI stock solutions, 1 M NaOH or 1 M HCl, and water. Thereafter, the mixtures were magnetically stirred for another 12 h, and the pH was regularly checked and adjusted if needed. 5 mL of QPI dispersions were transferred into LDPE plastic bags (Thomas Scientific, USA). Air bubbles in the bags were carefully removed by squeezing the bags, and the samples were double-sealed with a food vacuum sealer (RHVS1, Russel Hobbs, New Zealand). HHP treatment was conducted using a multivac high-pressure unit (HHP 002 R&D, Multivac, Wolfertschwenden, Germany) with water as the pressurizing medium. The samples were pressurized at pressures of 100, 250, 400, and 600 MPa for 15 min at an initial temperature of 20 °C. The maximum temperature reached during the HHP treatment was 33 °C. The pressure was released instantaneously when the treatment was completed, for example, it took approximately 10 s to bring down the pressure from 600 MPa to atmospheric pressure. Samples which did not undergo any HHP treatment (kept at the atmospheric pressure) were considered as controls.

5.2.4. Thermally induced QPI gelation

Similar sample preparation procedures were followed as described in Section 5.2.2. For thermally induced gelation, the QPI dispersions were transferred into an oven (OGH 60,

Thermofisher Scientific, USA) preset at 88 °C in order to achieve an internal temperature of 81 ± 2 °C. It took approximately 20 min for the sample to reach this temperature, and the sample was kept at this temperature for another 30 min. Before analysis, all thermally prepared gels were left on the bench for ~2 h to cool down to room temperature (~20 °C). Previous studies showed that heat treatment under these conditions induced a substantial QPI gelation and network formation (Ruiz et al., 2016).

5.2.5. Rheological measurements

The rheological measurements were conducted using a stress-controlled rheometer (DHR-3, TA instruments, USA) equipped with a stainless steel parallel plate geometry (diameter 40 mm and gap 0.5 mm). All measurements were conducted at a constant temperature of 20 °C and in duplicate. The viscosity measurement was conducted as follows. First, aliquots of samples were carefully loaded onto the bottom plate of the rheometer and then allowed to rest with no shear for 5 min to allow temperature equilibrium. After that, a thixotropic loop test was performed by increasing the shear rate from 0.1 to 1000 s^{-1} (up measurement) and then decreased from 1000 to 0.1 s^{-1} (down measurement). The extent of thixotropy was estimated by calculating the area between the two viscosity versus shear rate curves (up and down) using Origin Pro software (version 2021b, OriginLabs, MA, USA) (Liu et al., 2019).

Dynamic oscillatory rheological measurements were also conducted to probe the viscoelasticity of QPI dispersions treated by HHP or heating. First, a frequency sweep measurement was performed by varying the frequency from 0.1 to 10 Hz at a fixed strain amplitude of 1%. At the end of the frequency sweep, a strain sweep was performed at a constant frequency of 1 Hz, and the strain amplitude was varied from 0.01 to 10 000%.

5.2.6. Confocal laser scanning microscopy

Sample preparations for the confocal laser scanning microscopy (CLSM) observations were similar to those described in Sections 5.2.2 and 5.2.3. Briefly, to the QPI dispersions, several drops of 1% fast green (Sigma-Aldrich, USA) were added and then vortex-mixed for 10 s at 20 °C. Afterward, aliquots of each sample were added into a glass slide with a cavity and covered with a coverslip. Nail polish was used to seal the coverslip edges to prevent water evaporation (Wang et al., 2019). The QPI samples were observed with a confocal laser scanning microscope (Leica TCS SP5, Leica Microsystems, Wetzlar, Germany) equipped with an oil immersed 100× objective lens at a wavelength of 630 nm. All images were processed using Image J software (version 1.51 k, NIH, MD, USA).

5.2.7. Sodium dodecyl sulphate–polyacrylamide gel electrophoresis

Sodium dodecyl sulphate–polyacrylamide gel electrophoresis (SDS–PAGE) was performed under reducing and nonreducing conditions to study the difference in protein compositions among control, 600 MPa HPP-treated, and heat-treated samples at pH 5, 7, and 9. All samples were diluted to 0.14 w/v % with 1 w/v % SDS solution and incubated overnight at 20 °C. 25 µL of the diluted samples were mixed with 8.75 µL of 4 times concentrated Laemmli sample buffer and 1.25 µL of β-mercaptoethanol or Milli-*Q* water under reducing or nonreducing conditions, respectively. All samples were vortexed, and the reduced samples were boiled for 10 min. 10 µL of nontreated QPI solution and samples were injected into the wells of a commercial precast Mini-protein TGX (Tris/Glycine) gel (Bio-Rad, USA) consisting of 4% stacking gel and 15% resolving gel. The electrophoresis was performed at 100 V for ~1.5 h using a PowerPac Basic (Bio-Rad, USA). A running buffer was obtained by the dilution of 10× tris/glycine/SDS running buffer with Milli-*Q* water (Bio-Rad, USA). Coomassie Brilliant Blue R-250 staining solution (Bio-Rad, USA) was used to stain the gels for 45 min on a shaker and

destained every 0.5 h until the background became clear. The gels were soaked and stored in Milli-*Q* water before scanning. The gels were scanned using a ChemiDoc touch imaging system (Bio-Rad, USA). The bands were compared to a protein marker with Mw ranging from 10 to 250 kDa (Precision Plus Protein Dual Xtra Standards, Catalog # 161–0377, Bio-Rad, USA), and densitometric analysis of gels was conducted using Image Lab software (version 6.1, Bio-Rad, USA).

5.3. Results and discussion

5.3.1. Effect of heat or HHP treatments on the microstructures of QPI dispersions

Confocal micrographs of QPI dispersions before and after heat or HHP treatment at different pH levels are shown in **Figure 16**. Proteins stained with Fast Green appear as green, while the voids in between the protein particles appear in dark. It can be seen that the untreated QPI dispersion at pH 5 has much larger protein particles due to protein aggregation near the isoelectric point of 11S globulin (pI ~ 4.5). Significant structural alterations can be identified when the samples were subjected to HHP or heat treatment. At pH 5, few large protein aggregates (>20 μm) started to form at 100 MPa, and they grow to large clusters at 250 MPa with a heterogenous structure. When the pressure is further increased to 400 and 600 MPa, those protein clusters are further interconnected to form a compact three-dimensional protein network. It is expected that the formation of a well spanned network with compact microstructures would result in greater gel strength (Ngarize et al., 2005). Working on HHP-induced peanut protein isolate gels (Zhao et al., 2018a), the authors also observed that a coarse and large aggregated microstructure was formed by the application of 550 MPa compared to lower pressure levels. Compared to the samples at pH 5, HHP treatments at pH 7 and 9 induced much less significant microstructural changes, and prominent protein aggregation only

occurred at much higher pressures (>400 MPa). In addition, the protein aggregate size is much smaller at pH 9 compared to pH 7. This can be explained by the higher net charge and greater electrostatic repulsions at pH 9, being away from the isoelectric point of QPI (~pH 4.5), which increase protein solubility and suppress aggregation (Petruccelli & Añón, 1996). Compared to HHP treatment, heat-induced gels at all pHs exhibited a relatively homogeneous network structure formed by small aggregates and small pores. Similar observations had been found in heat-induced QPI gels (Kaspchak et al., 2017; Ruiz et al., 2016) and whey protein isolate (WPI) gels (Devi et al., 2014). Differences in microstructures of protein gels formed by heat or HHP treatment had been observed in previous studies on WPC, WPI (Kanno et al., 1998), and soy protein isolate (SPI) (Saowapark et al., 2008). Despite both heat and HHP treatment being known to induce protein gelation through protein unfolding and denaturation, the exact mechanism and extent of protein denaturation could be different (Katzav et al., 2020). In addition, the impact of heat and HHP treatment on the forces involved in the formation of network such as hydrogen bond, hydrophobic and electrostatic interactions, and disulfide bonds could vary (Kanno et al., 1998). This could contribute to different gel structures. The differences in disulfide bond formation and protein profile changes between heat and HHP treatment will be discussed in Section 5.3.4.

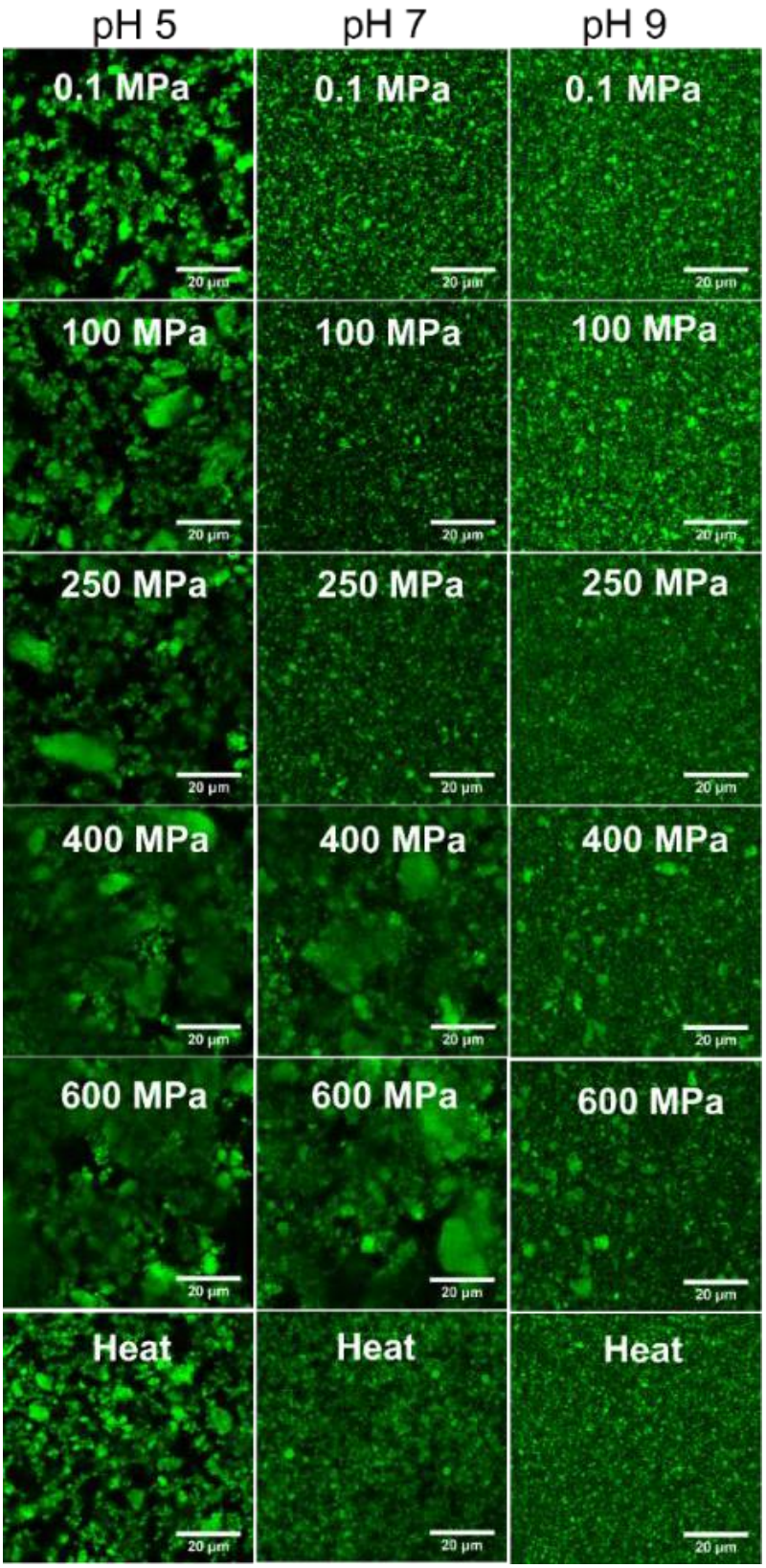

Figure 16: Confocal micrographs of QPI dispersions at three pHs (5, 7, and 9) before and after thermal treatment (81 ± 2 °C, holding time 30 min) and HHP treatments (100, 250, 400, and 600 MPa) for 15 min each.

5.3.2. Effect of heat or HHP treatments on the viscosity of QPI dispersions

Flow curves of the untreated as well as heat- and HHP-treated QPI dispersions at pH 5, 7, and 9 are shown in **Figure 17**A–C, respectively. At pH 5, all samples display shear-thinning behavior where the viscosity decreases with the shear rate increase. For untreated and 100 and 250 MPa-treated QPI dispersions, a plateau viscosity of ~0.8 Pa·s was observed at a very low shear rate (<1 s^{-1}). For the sample treated with >400 MPa or for the heat-treated sample, the viscosity significantly increased, and it steeply decreased with increasing shear rate, particularly at a shear rate below 10 s^{-1} in the up measurements. This is due to the interconnected protein network formation as revealed by CLSM (**Figure 16**). At pH 7 and pH 9, the flow behavior transited from a Newtonian fluid at lower pressures (≤250 MPa) to a shear-thinning fluid at higher pressures (≥400 MPa) or when heat-treated. Also, it can be seen that the decrease of viscosity with the shear rate is much steeper at pH 5 than at pH 7 and 9. The shear thinning behavior is due to the presence of large protein aggregate particles, especially at pH 5. When the samples were subjected to shear, hydrodynamic forces are generated which result in the disruption of the protein aggregates. Consequently, the viscosity decreased with the shear rate. Similar shear-thinning behavior had been observed in starch aggregate suspensions (Kang et al., 2016) and protein dispersions (Tung, 1978).

The “up” and “down” viscosity sweep measurements displayed a hysteresis loop indicating that these samples are thixotropic, meaning that their flow behavior is time-dependent. The extent of thixotropy can be quantified by calculating the area S between the up and down curves (hysteresis), and the larger the area (S value), the stronger the thixotropic behavior (Armelin et al., 2006). The hysteresis loop areas calculated from all QPI samples are listed in **Table 16**. It can be seen that the area varies significantly between the different QPI samples. At all pHs, the hysteresis area significantly increased with the increase in the applied pressure. Further, at the

same pressure, the area is the highest at pH 5 and substantially decreased at pH 7 and is the lowest at pH 9. For example, at 600 MPa, the area considerably decreased from 26682.9 ± 225.2 to 21.5 ± 1.3 when the pH was varied from 5 to 9. Comparing the hysteresis area results with the CLSM observations, it can be inferred that the QPI samples having large aggregates show stronger thixotropic behavior. Previous studies demonstrated that the hysteresis area is proportional to the energy required to disrupt the sample internal structures responsible for the time-dependent flow (Dankar et al., 2018). Thus, it is expected that QPI dispersions with large protein aggregates required higher energy to destroy the internal structure, thus exhibiting a larger hysteresis. This finding is in agreement with the steady shear viscosity behavior and the microstructural observations. For example, the 600 MPa-treated QPI dispersion at pH 5, which showed the largest loop area (**Table 16**), is also the one exhibiting the largest protein aggregates (**Figure 16**) and the highest viscosity (**Figure 17**). Similar observations were also reported in previous studies on WPI-stabilized emulsions, where emulsions having the largest oil droplet size and the strongest gel network displayed the largest hysteresis loop area (Liu et al., 2019).

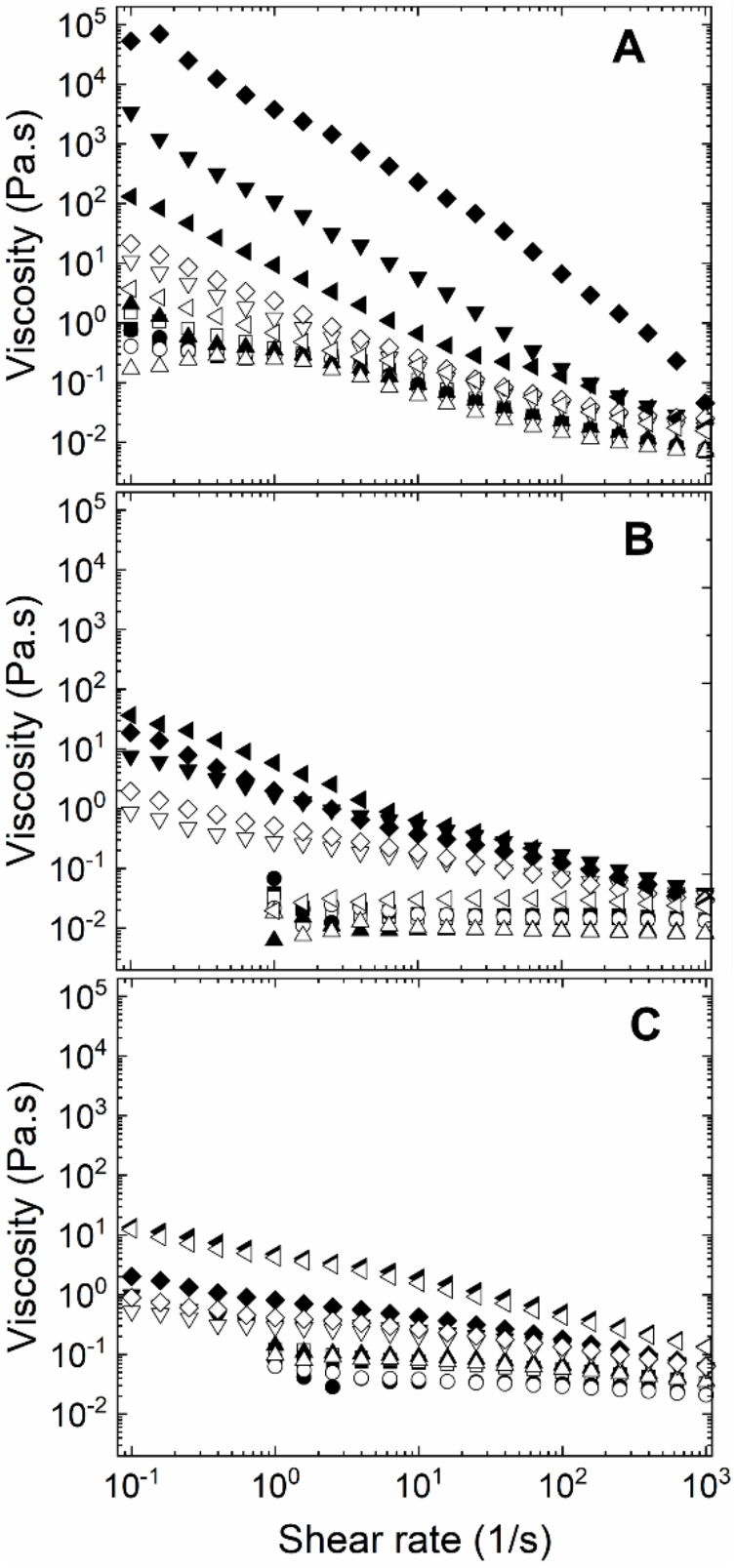

Figure 17: Viscosity as a function of shear rate for HHP and thermally treated QPI dispersions at (A) pH 5, (B) pH 7, and (C) pH 9. Symbols are nontreated (■); 100 MPa (●); 250 MPa (▲); 400 MPa (▼); 600 MPa (◆); thermally treated (◀). Solid and open symbols indicate the "up" and "down" measurements, respectively.

Table 16: Thixotropic hysteresis loop area of heat- and HHP-treated QPI dispersions obtained from the "up" and "down" viscosity measurements

Samples	Hysteresis loop area (Pa)
pH 5, untreated	n.d. (not determined)
pH 5, 100 MPa	n.d.
pH 5, 250 MPa	4.8 ± 0.4
pH 5, 400 MPa	1917.9 ± 1232.3
pH 5, 600 MPa	26682.9 ± 225.2
pH 5, heated	78.1 ± 4.7
pH 7, untreated	n.d.
pH 7, 100 MPa	n.d.
pH 7, 250 MPa	2.8 ± 2.3
pH 7, 400 MPa	44.4 ± 1.5
pH 7, 600 MPa	45.1 ± 0.0
pH 7, heated	78.4 ± 8.3
pH 9, untreated	n.d.
pH 9, 100 MPa	n.d.
pH 9, 250 MPa	3.3 ± 0.8
pH 9, 400 MPa	8.0 ± 2.2
pH 9, 600 MPa	21.5 ± 1.3
pH 9, heated	29.2 ± 4.6

In order to better compare the flow behaviors of QPI dispersions subjected to heat or HHP treatment at different pHs, the viscosities at different constant shear rates are plotted in **Figure 18**. For all shear rates and at all pH levels, the viscosity of QPI dispersions was not considerably affected when the pressure is ≤250 MPa. The viscosity significantly increased at 400 MPa and reached a maximum at 600 MPa. These trends are more prominent at low (0.1 s^{-1}) and intermediate shear rates (1 s^{-1}) than at high shear rates (10 and 100 s^{-1}). At pH 5, the highest viscosity was achieved at 600 MPa, while the heat treatment gives the highest viscosity at pH 7 and 9.

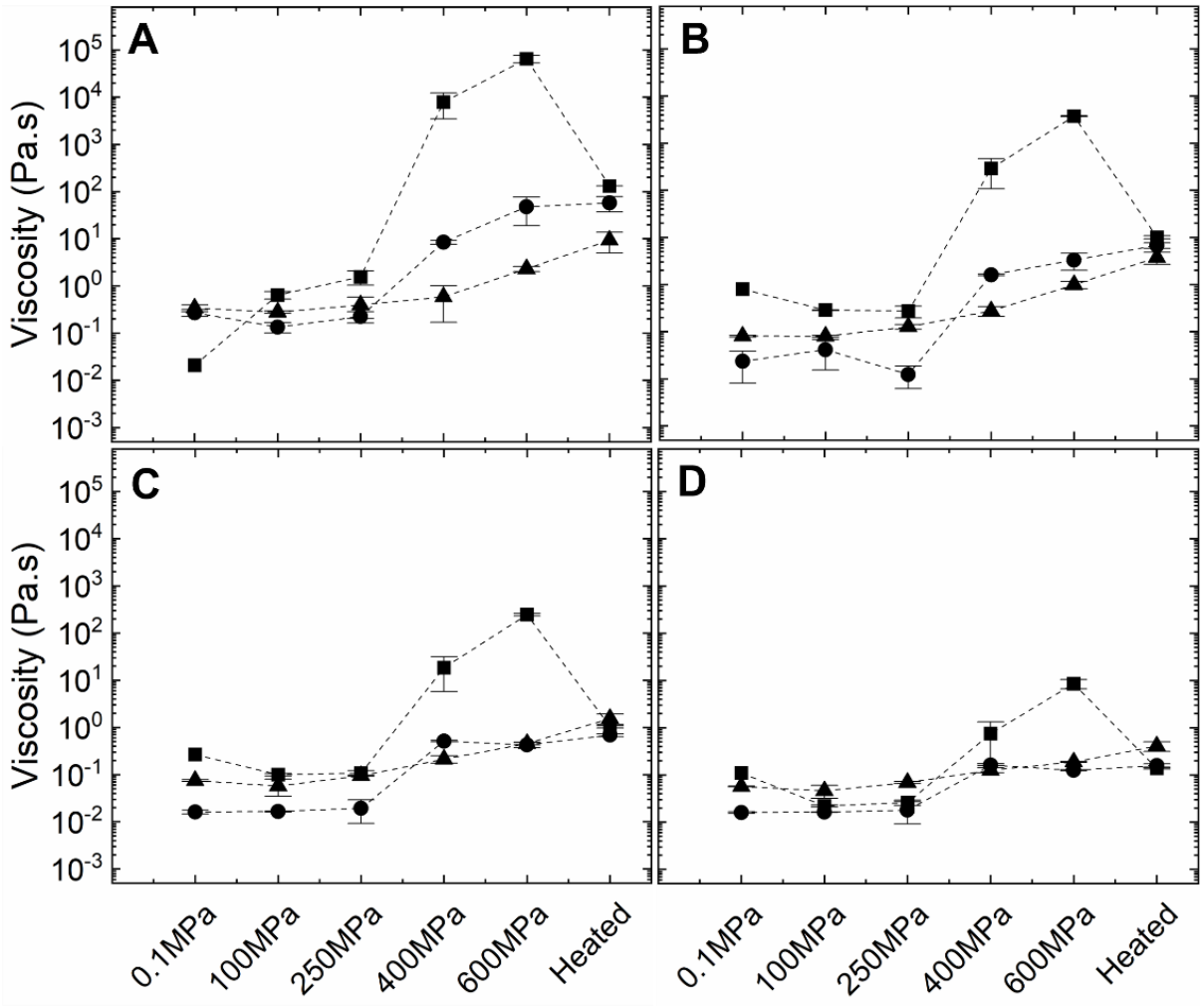

Figure 18: Viscosity at different shear rates as a function of HHP treatment or heat treatment for 10 wt % QPI dispersions. Shear rates were (A) 0.1, (B) 1, (C) 10, and (D) 100 s−1. pH levels are pH 5 (■), pH 7 (●), and pH 9 (▲). Error bars represent standard deviations.

5.3.3. Dynamic oscillatory viscoelasticity of heat- and HHP-induced gels

The small and large deformation rheological behaviors of 10 w/w % heat- and HHP-treated QPI solutions at different pHs were probed by the frequency sweep and strain sweep tests, and the results are shown in **Figure 19**. The storage modulus G' and loss modulus G'' represent the elastic and viscous attributes of the samples, respectively. The frequency sweep measurements were conducted at a constant strain of 1%, which is well within the linear viscoelastic region (LVR). The dependence of G' and G'' on the frequency for all QPI samples are presented in **Figure 19**A,C,E. At all pH levels, for untreated and 100 MPa-treated samples, both G' and G''

are very low (0.01−0.5 Pa), indicating that there are no gel formations (results not shown). However, for both heat- and HHP-treated QPI samples (above 250 MPa), G' is larger than G'' over the whole frequency range, and both are nearly not varied with frequency, suggesting that those samples can be considered as gels (Ross-Murphy, 1995). The complex modulus G^* at 1 Hz, which is contributed from both G' and G'' at this frequency, is presented in **Figure 20**A to enable better comparisons between the different samples. Generally, G^* follows the same trend as the viscosity. Stronger gels are formed when the pressure is increased. For instance, at pH 5, the value of G^* sharply increased from ~2.0 Pa at 250 MPa to ~95700 Pa at 600 MPa. Heat- or pressure-induced gelation had been observed in many globular protein systems. Working on the HHP- and heat-induced gelation of cowpea proteins (12 w/w %, pH 7), Peyrano et al. (2021) found that G' was higher than G'' when samples were treated at 400 MPa and the samples behaved as a gel at 600 MPa; heat treatment at 70 or 90 °C for 20 min resulted in a stiffer gel than HHP-induced ones (Peyrano et al., 2021). In another study working on the HHP treatment of SPI (10 w/v %, pH 8), Speroni et al. (2009) observed a liquidlike behavior ($G'' > G'$) of the SPI dispersion transiting to a solid-like characteristic ($G' > G''$) at 600 MPa. Similar findings have also been reported on WPC and WPI (Kanno et al., 1998), where a significant gel formation was observed when the pressure is above 400 MPa. Previous studies demonstrated that the gelation of globular proteins induced by either heat or HHP treatment is influenced by intrinsic factors including the nature and concentration of the proteins and extrinsic factors including temperature, pressure, treatment time, pH, and ionic strength (Nicolai, 2019). Therefore, direct comparison of gel strength among different proteins and treatment conditions is not always straightforward.

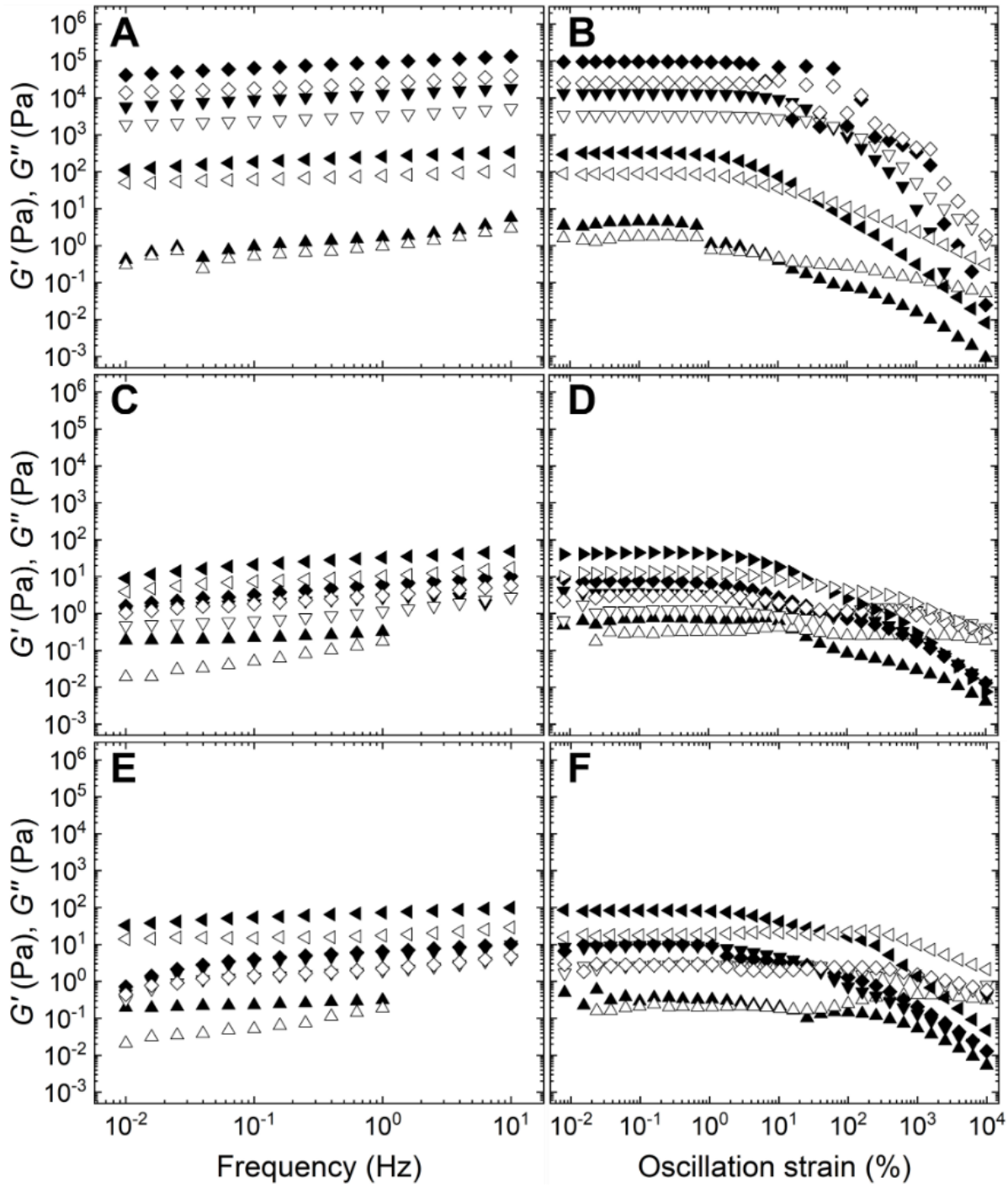

Figure 19: Storage modulus (G') and loss modulus (G'') as a function of frequency (A,C,E) and strain amplitude (B,D,F). pHs are (A,B) pH 5; (C,D) pH7; (E,F) pH 9. Symbols are 250 (▲); 400 (▼); 600 MPa (◆); heat treated (◀). Solid and open symbols represent G' and G'', respectively.

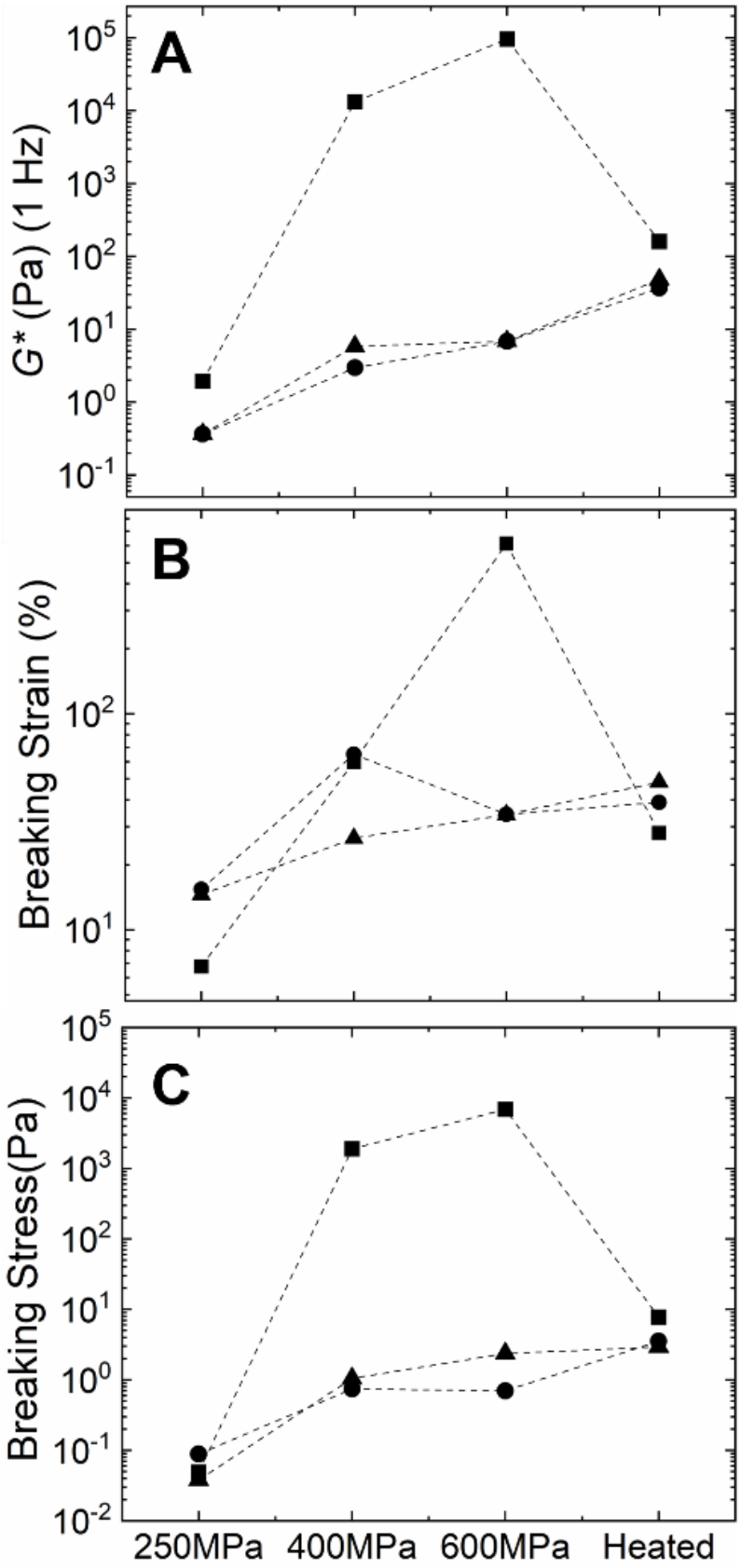

Figure 20: (A) Complex modulus *G** at 1 Hz, (B) breaking strain (%), and (C) breaking stress (Pa) for different HHP- or heat-treated QPI samples. pHs are 5 (■), 7 (●), and 9 (▲)

For both heat- and HHP-treated gels, the gels that were made at pH 5 showed a much higher G^* value when compared to those at pH 7 and 9. For instance, the value of G^* was ~95 700, ~7.0, and ~6.5 Pa for 600 MPa-treated QPI dispersions at pH 5, 7, and 9, respectively. pH affects the conformation and structure of proteins substantially by modulating the ionization of charged amino acid side chains (Dumetz et al., 2008). The surface charge distributions greatly influence the protein–protein and protein–solvent interactions (Oncley et al., 1952). As the pH is close to the isoelectric point, the surface charge is minimized and protein–protein repulsions are suppressed, thus promoting protein aggregation (Mäkinen et al., 2016). In the present work, a significant stiffer gel was obtained at pH 5 regardless of the treatment conditions, which supports the importance of the electrostatic interactions in the gel network formation. Interestingly, at pH 5, 600 MPa-treated QPI dispersion resulted in a much stiffer gel than the heat-treated ones. This is consistent with CLSM observations where the 600 MPa sample exhibited significant protein aggregation and network formation compared to the heat-treated sample (**Figure 16**), while at pH 7 and 9, QPI gels induced by heat treatment are slightly stiffer than those induced by 600 MPa. According to the Le Chatelier principle, pressure elevation will lead to a volume reduction through reactions or interactions facilitating a smaller volume (Heremans, 1982). At pH 5, the total volume of the proteins in the QPI solution is decreased by reducing the surface charges and protein–solvent interactions. Therefore, it is expected that pressure-induced gelation would be promoted better under this condition, resulting in the highest gel strength. It is worth noting that spontaneous syneresis or water loss was observed for the QPI gels formed at pH 5 and 7 after HHP treatment at 400 and 600 MPa. This indicates that at pH 5 and 7, protein–protein interaction is promoted and is accompanied by a decrease of protein–water association, resulting in a compact microstructure with a low water content and leading to high values of the G' and G'' of the gels obtained at pH 5 and 400 and 600 MPa HHP treatments. In the case of heat treatment, the gels induced at pH 5 are also stiffer than

those obtained at pH 7 and 9, which is consistent with the recent work by Tanger et al. (2022) who found that pea protein isolate gelation at 95 °C resulted in a much stiffer gel at pH 4.5 than at pH 7 and 9 (Tanger et al., 2022).

For a large deformation rheology, G' and G'' as a function of applied strain is illustrated in **Figure 19**B,D,F. All samples exhibit qualitatively similar behavior, and G' and G'' are independent of the applied strain until reaching a critical strain value, which is defined as the LVR region. Beyond this point, G' and G'' start to deviate from the plateau and decrease significantly with a further increase in the applied strain. Finally, the crossover of G' and G'' occurs, and beyond this point, G'' starts to dominate G', suggesting that the gel network is disrupted. The strain and stress corresponding to this yield point ($G' = G''$) are named the breaking strain and breaking stress, respectively. To examine the large deformation rheological behaviors among the different heat- or HHP-treated QPI gels, the breaking strain (%) and breaking stress (Pa) for the different samples are shown in **Figure 20**B,C, respectively. Generally, both the breaking strain and breaking stress increased with the increase in pressures in a pH-dependent manner, following a similar trend to G^*. The larger value of breaking strain and breaking stress is observed at pH 5, indicating that the gels are more resistant to break down under large deformation. In summary, the large deformation rheological behavior is in good agreement with the viscoelastic properties under small deformation.

5.3.4. Effect of heat or HHP treatments on the protein profiles of QPI dispersions

The nonreducing and reducing SDS–PAGE profiles of QPI dispersions at the three pHs (5, 7, and 9) as affected by heat or HHP treatments are shown in **Figure 21**. The presence of SDS destroys noncovalent interactions and suppresses hydrophobic interactions, allowing the

observation of dissociated protein subunits (Kanno et al., 1998). It can be seen from **Figure 21**A that untreated QPI exhibited a complex protein profile containing protein bands with varying molecular weights from less than 15 kDa to more than 250 kDa. Similar protein profiles had been found in previous SDS–PAGE studies of QPI obtained from similar alkaline extractions (Shen et al., 2021). Two major protein clusters can be identified: protein bands at ~45 and 55 kDa represent subunits constituting the 11S globulin hexamer through noncovalent interactions, while the bands below 15 kDa were assigned as 2S albumin (Brinegar et al., 1996). In the case of untreated QPI, there was no significant difference in protein profiles among different pHs, which agrees with previous studies on QPI at pH 6.5, 8.5, and 10.5 (Mäkinen et al., 2016) and potato protein isolate at pH 3 and 7 (Katzav et al., 2020).

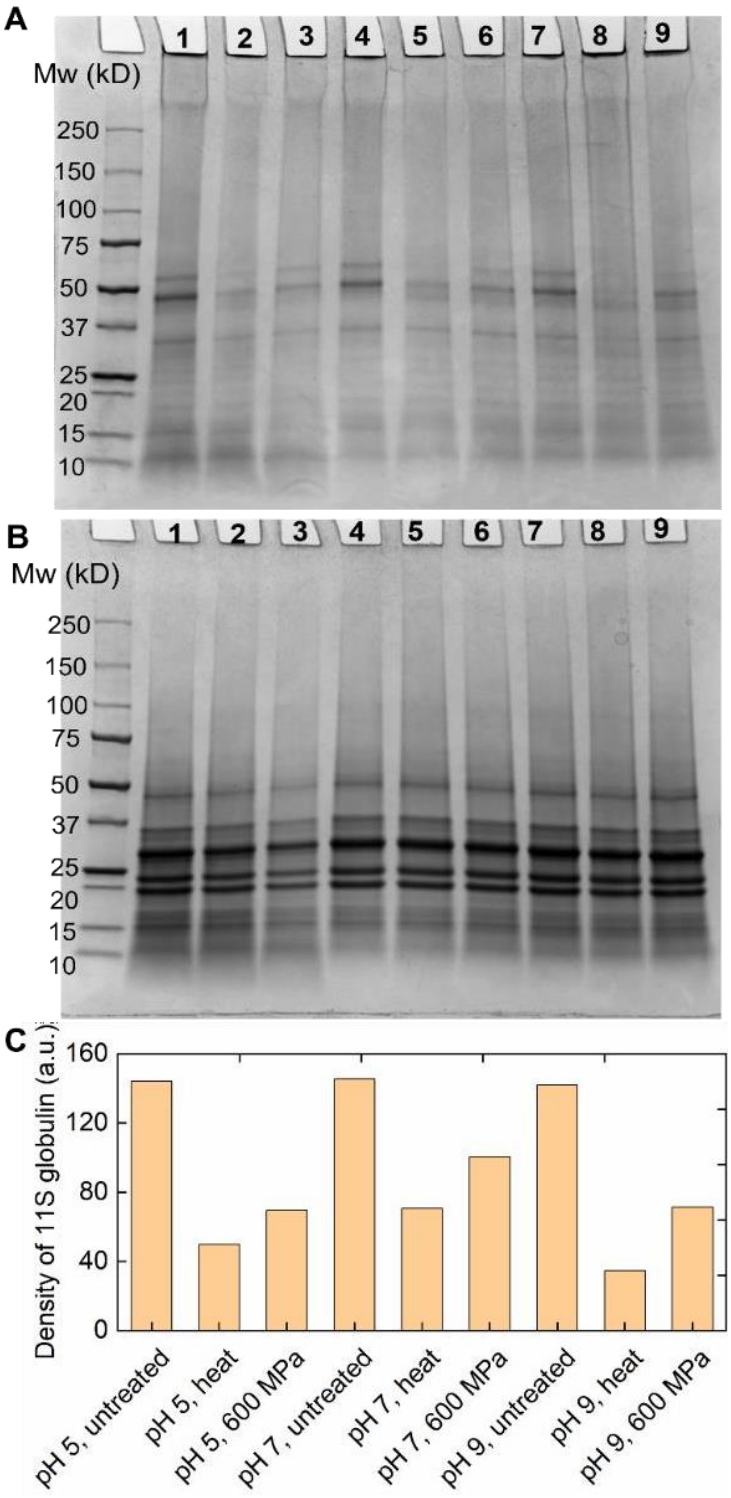

Figure 21: SDS–PAGE profiles of QPI dispersions at three pHs (5, 7, and 9) before and after thermal treatment (81 ± 2 °C, holding 30 min) or HHP treatments (600 MPa, 15 min) under nonreducing (A) and reducing (B) conditions. Lane 1: pH 5 untreated, Lane 2: pH 5 thermally treated, Lane 3: pH 5 HHP treated, Lane 4: pH 7 untreated, Lane 5: pH 7 thermally treated, Lane 6: pH 7 HHP treated, Lane 7: pH 9 untreated, Lane 8: pH 9 thermally treated, and Lane 9: pH 9 HHP treated. (C) Densitometric analysis of 11S globulin protein bands (~45 and ~55 kDa) obtained under nonreducing condition.

At all pHs, application of heat or HHP treatments induced a significant reduction in the band intensity of 11S globulin (**Figure 21**A), which could be due to the formation of large protein aggregates through intermolecular disulfide bonds. Similar observations were found in heat-treated QPI (Mäkinen et al., 2016) as well as HHP-treated potato protein isolate (Katzav et al., 2020). For instance, under nonreducing conditions, Mäkinen et al. (2016) observed that the 11S globulin band had faded significantly after heating in boiling water for 5 min, and the disappearance of the band was completed after 15 min of heating at pH 6.5 and 10.5. It is worth noting that the large protein aggregates (M_w > 1000 kDa) that are formed after heat or HHP treatments (**Figure 16**) could not enter into the gel to be detected by SDS–PAGE (Utsumi et al., 1984).

To better compare the heat- and HHP-induced aggregation of QPI at different pHs, intensities of the major protein band-11S globulin were determined, and the results are presented in **Figure 21**C. At all pHs, heat treatment resulted in a greater reduction in the band intensity compared to that of 600 MPa treatment. This finding indicated that heat treatment may cause more extensive intermolecular disulfide bond formation. Previous studies indicated that the impact of heat and HHP treatment on the extent of protein aggregation is strongly related to the severity of the treatment conditions (temperature, pressure level, and time) and the types of proteins (Speroni et al., 2009). Furthermore, it can be observed that the 11S globulin band intensity is the lowest for the heat-treated QPI at pH 9. This could be attributed to the fact that the reactivity of SH groups, which facilitates both the oxidation of SH groups to S–S bonds and the SH/S–S interchange reactions, is considerably promoted under alkaline conditions (Shimada & Cheftel, 1988). It is critical to note that during the heat and HHP treatments, the protein may undergo unfolding which gives rise to the exposure of the hydrophobic sites, free sulfhydryl groups, and charged amino acids (Zhao et al., 2018a). Therefore, the final gel

formation involves both noncovalent (e.g., hydrophobic and electrostatic interactions, hydrogen bonding) and covalent (e.g. disulfide bonding) interactions (Sun & Arntfield, 2012). These protein aggregates would not be expected to be fully shown during electrophoresis as noncovalent bonds are broken down in the presence of SDS (Mäkinen et al., 2016). As a consequence, the extent of 11S globulin aggregation (**Figure 21**C) as revealed by nonreducing SDS–PAGE can be only partially correlated with the viscosity or viscoelasticity of the QPI gels.

Under reducing conditions, both untreated and heat- or HHP-treated QPI at pH 5, 7, and 9 displayed similar characteristics (**Figure 21**B). This observation is consistent with a pervious report on the SDS–PAGE study of HHP-treated sweet potato protein isolate at pH 3, 6, and 9 (Zhao et al., 2018a). For all samples, the large protein aggregates accumulated in the gel wells of the nonreducing SDS–PAGE gel (**Figure 21**A) disappeared in the presence of β-mercaptoethanol, suggesting that they were stabilized by disulfide bonds. Moreover, intensive protein bands at 25–37 kDa and 15–25 KDa appeared, which represent acidic and alkaline subunits of the 11S globulins that were associated through disulfide bonds (Brinegar et al., 1996; Shen et al., 2021). In the case of 600 MPa-treated QPI at pH 5, a decrease in intensities of all bands is observed, which is likely the result of extensive aggregation and lower solubility of the protein aggregates (Katzav et al., 2020). In the case of HHP-treated SPI, Speroni et al. (2009) found that the greater the applied pressure, the higher the amount of protein substance that did not migrate into the gel because of the presence of aggregates with a large molecular weight.

In summary, the findings of this study indicate that both pressure and heat treatment can induce the formation of QPI gels under the conditions of protein concentration, pH, and extent of

pressure and heat treatments considered here. The gel strength and microstructural characteristics are strongly dependent on the pH and pressure levels. At all pHs, an increase in pressure results in higher viscosity and stronger shear thinning and thixotropic behavior, and the gel is formed when the pressure is greater than 250 MPa. Pressurized or heat-treated QPI dispersion close to its isoelectric point (pH ~ 5) lead to the formation of a stiff gel with a compact and well-spanned three-dimensional network. HHP treatment at 600 MPa and pH 5 results in a stiffer gel than the heat-treated one, and it was the inverse at pH 7 and pH 9, where heat treatment resulted in stiffer gels. The 11S globulin participated substantially in heat- or HHP-induced aggregation and gelation, where the intermolecular disulfide bonding is likely to play an important role. At all pHs, heat treatment induced a greater extent of 11S globulin cross-linking than HHP treatment at 600 MPa. Nevertheless, further studies are underway to understand the effect of HHP and heat treatment on the extent of QPI protein denaturation, secondary structural changes, and noncovalent interactions that stabilize the gels. Finally, HHP treatment provides great potential in incorporating thermolabile food compounds and nutraceuticals into the quinoa protein gel matrix while imparting sought-after textural characteristics to the product.

6. Chapter 6: Conclusion and future work

In summary, this thesis includes the extraction, modifications and physicochemical characterisations of QPI. QPI was firstly extracted from quinoa seeds using alkaline extractions followed by the isoelectric point precipitation. Then the 5% w/w QPI suspension was subjected to HPH treatment at 0-50 MPa at pH 7, and the structural, physicochemical and techno-functional properties were characterised before and after treatments. In another study, the structural, physicochemical and techno-functional property changes were determined for diluted (1% w/w) QPI treated with HHP (0-600 MPa for 15 min) and HIUS (14.4 W, 10mL for 0-15 min). Finally, HHP (0-600 MPa for 15 min) and heat (81 ± 2 °C for 30 min) treatments were performed on concentrated (10% w/w) QPI suspensions at pH 5, 7 and 9 to investigate the gelation properties of QPI.

In terms of microstructural changes, SDS-PAGE and FTIR were performed to probe the changes in the primary and secondary structures, respectively, while surface hydrophobicity and free SH contents were determined to reveal the changes in the tertiary structure of treated QPI. As shown in the SDS-PAGE results, only HHP-treated QPI suspensions formed large aggregates via S-S bonds formed between 11S globulins. There were no significant changes observed in the primary structure of QPI after HPH and HIUS treatment. The secondary structure of HPH-treated QPI presented no significant changes in comparison to the native QPI, while the HIUS and HHP-treated QPI presented higher degrees of disordered secondary structures with increasing treatment time and pressure. Furthermore, QPI was unfolded after HPH and HIUS treatments but aggregated under HHP treatments as revealed by the results of free SH content and surface hydrophobicity.

The particle size and solubility of QPI were determined after all three treatments. Apart from

HIUS and HHP treated samples at pH 5, all other samples (including HIUS and HHP samples at pH 7 and 9, and all HPH samples at pH 7) were found to have smaller particle sizes and higher solubilities than the untreated QPI. Moreover, the emulsifying and foaming capacities of QPI dispersions were improved after the HPH treatment, together with the decrease in surface and interfacial tensions.

The thermally induced HPH-treated 5% w/w QPI gels exhibited a 2-fold increase in the complex modulus compared to the native QPI gels prepared under the same conditions. Meanwhile, the HPH-treated QPI gels showed denser and more homogeneous structures than the native QPI gels. When comparing the HHP and thermally induced 10% w/w QPI gels, both the HHP treatment at 250-600 MPa and the heat treatment (81 ± 2 °C) formed gels at pH 5, 7 and 9. The gels formed by HHP and heat treatment both exhibited the highest gel strength at pH 5 and the G^* of HHP-induced gels was 1000-fold greater than that of the heat-induced gel. However, stiffer gels were formed by the heat treatment than HHP at pH 7 and pH 9. Heat-induced gels showed more compact and homogeneous structures under all pHs and pressure levels as observed by CLSM. Finally, the findings of this thesis showed that the physicochemical and techno-functional properties of QPI dispersions can be tailored by applying thermal and different non-thermal processing techniques with various processing conditions (pH, time and power/pressure).

Based on the findings of this thesis, some future work directions are proposed below:

- *To investigate the effects of HIUS and HHP processing on other techno-functional properties of QPI.*

Effects of HIUS and HHP treatment on other techno-functional properties of QPI such as gelation, emulsification, foaming, water and oil holding capabilities should be studied in the

future. In this thesis, only gelation properties of QPI after HHP and heat treatment were studied. However, it is expected that other non-thermal processing techniques such as HIUS could also affect the gelation properties of QPI by reducing particle sizes and improving solubilities.

- *To study the effects of pH on physicochemical and techno-functional properties of QPI dispersions at higher HPH pressures (e.g., above 50 MPa).*

It has been demonstrated in this thesis that the effects of HUIS and HHP on the physicochemical properties of QPI are pH dependent. Therefore, it is expected that the effect of HPH treatment would also be highly related to the pH of QPI dispersions. Furthermore, previous studies suggested that the level of pressure is also a critical processing parameter in the HPH treatment. For example, a previous study found that 1% kidney bean protein formed soluble aggregates at 60 MPa but the aggregates were broken down when the pressure was further increased to 90-120 MPa (Guo et al., 2021). Therefore, it is expected that HPH treatment at higher pressures could induce further changes in the physicochemical properties of QPI.

- *To employ other non-thermal processing technologies on QPI dispersions.*

Effects of other non-thermal treatments such as pulsed electric field (PEF) on the microstructure and physicochemical properties of QPI could be studied. Previous PEF studies showed that radicals were generated from polar amino acids, which can result in the unfolding and aggregation of proteins (Barbhuiya et al., 2021; Liu et al., 2011). Moreover, various interactions between protein molecules such as disulfide bonds, hydrogen bonding, electrostatic forces and hydrophobic interactions could be disrupted under the PEF treatment, thus altering the functional properties (Barbhuiya et al., 2021). Therefore, it is worth investigating the effect of PEF on changes in QPI.

- *To study the effect of salt additions on HHP-induced QPI gels.*

Effects of salt (Sodium chloride and Calcium chloride) additions in heat-induced QPI gels have been studied in a previous study (Yang et al., 2022), where increasing NaCl from 0 to 200 mM accelerated and the gel formation and led to a stronger gel. However, the effects of salt addition in HHP-induced QPI gels are still unknown and further study is required.

- *To study the effects of HHP on defatted quinoa flour suspensions.*

The effects of HHP on QPI have been studied in this thesis. However, complex food systems containing both proteins and polysaccharides (such as starch) usually appear in real food products. For example, flour of grains is commonly used in food formulations of bakery products. Quinoa flour which contains rich nutrients beyond proteins such as dietary fibres, minerals, and starch is a promising food ingredient. To promote the usage of quinoa flour in food formulations, the effects of non-thermal processing technologies on modifications of quinoa flour should be also studied. The structural and property changes of quinoa flour could be determined and compared with that of QPI.

7. References

Abugoch, L. E., Romero, N., Tapia, C. A., Silva, J., & Rivera, M. (2008). Study of some physicochemical and functional properties of quinoa (*Chenopodium quinoa* Willd) protein isolates. *Journal of Agricultural and Food Chemistry*, *56*(12), 4745-4750.

Aganovic, K., Bindrich, U., & Heinz, V. (2018). Ultra-high pressure homogenisation process for production of reduced fat mayonnaise with similar rheological characteristics as its full fat counterpart. *Innovative Food Science & Emerging Technologies*, *45*, 208-214.

Ahmed, J., Al-Ruwaih, N., Mulla, M., & Rahman, M. H. (2018). Effect of high pressure treatment on functional, rheological and structural properties of kidney bean protein isolate. *LWT*, *91*, 191-197.

Ahmed, J., Mulla, M., Al-Ruwaih, N., & Arfat, Y. A. (2019). Effect of high-pressure treatment prior to enzymatic hydrolysis on rheological, thermal, and antioxidant properties of lentil protein isolate. *Legume Science*, *1*(1), e10.

Ahn, J. M., Kassees, K., Lee, T. K., Manandhar, B., & Yousif, A. M. (2017). Strategy and tactics for designing analogs biochemical characterization of the large molecules. In S. Chackalamannil, D. Rotella, & S. E. Ward (Eds.), *Comprehensive Medicinal Chemistry III* (pp. 66-115). Elsevier.

Akasaka, K. (2006). Probing conformational fluctuation of proteins by pressure perturbation. *Chemical Reviews*, *106*(5), 1814-1835.

Akharume, F. U., Aluko, R. E., & Adedeji, A. A. (2021). Modification of plant proteins for improved functionality: A review. *Comprehensive Reviews in Food Science and Food Safety*, *20*(1), 198-224.

Alam, S.; Kaur, J.; Khaira, H.; Gupta, K. (2015). Extrusion and extruded products: Changes in quality attributes as affected by extrusion process parameters: A Review. *Crit. Rev. Food Sci. Nutr*., *56*, 445–473.

Alavi, F., Chen, L., & Emam-Djomeh, Z. (2021). Effect of ultrasound-assisted alkaline treatment on functional property modifications of faba bean protein. *Food Chemistry*, *354*, 129494.

Ando, H., Chen, Y.C., Tang, H., Shimizu, M., Watanabe, K., & Mitsunaga, T. (2002). Food components in fractions of quinoa seed. *Food Science and Technology Research*, *8*(1), 80-84.

Antosiewicz, J. M., & Shugar, D. (2016). UV-Vis spectroscopy of tyrosine side-groups in studies of protein structure. Part 1: basic principles and properties of tyrosine chromophore. *Biophysical Reviews*, *8*(2), 151-161.

Armelin, E., Martí, M., Rudé, E., Labanda, J., Llorens, J., & Alemán, C. (2006). A simple model to describe the thixotropic behavior of paints. *Progress in Organic Coatings*, *57*(3), 229-235.

Aschemann-Witzel, J., Gantriis, R. F., Fraga, P., & Perez-Cueto, F. J. A. (2021). Plant-based food and protein trend from a business perspective: markets, consumers, and the challenges and opportunities in the future. *Critical Reviews in Food Science and Nutrition*, *61*(18), 3119-3128.

Assatory, A., Vitelli, M., Rajabzadeh, A. R., & Legge, R. L. (2019). Dry fractionation methods for plant protein, starch and fiber enrichment: A review. *Trends in Food Science & Technology*, *86*, 340-351.

Bader, R., & Henneker, W. (1965). The ionic bond. *Journal of the American Chemical Society*, *87*(14), 3063-3068.

Barbhuiya, R. I., Singha, P., & Singh, S. K. (2021). A comprehensive review on impact of non-thermal processing on the structural changes of food components. *Food Research International*, *149*, 110647.

Barbosa-Cánovas, G. V., & Rodríguez, J. J. (2002). Update on nonthermal food processing technologies: Pulsed electric field, high hydrostatic pressure, irradiation and ultrasound. *Food Australia*, *54*(11), 513-520.

Barr, C. D., Giacin, J. R. and Hernandez, R. J. (2000), A determination of solubility coefficient values determined by gravimetric and isostatic permeability techniques. *Packag. Technol. Sci.*, *13*, 157-167.

Bazile, D., Fuentes, F., & Mujica, A. (2013). Historical perspectives and domestication of quinoa. In A. Bhargava & S. Srivastava (Eds.), *Quinoa-Botany, Production and Uses*. CABI Publisher.

Bello-Pérez, L. A., & Paredes-López, O. (1994). Starch and amylopectin - rheological behavior of gels. *Starch - Stärke*, *46*(11), 411-413.

Beveridge, T., Toma, S. J., & Nakai, S. (1974). Determination of SH- and SS-groups in some food proteins using Ellman's reagent. *Journal of Food Science*, *39*(1), 49-51.

Bi, C., Wang, P., Sun, D., Yan, Z., Liu, Y., Huang, Z., & Gao, F. (2020). Effect of high-pressure homogenization on gelling and rheological properties of soybean protein isolate emulsion gel. *Journal of Food Engineering*, *277*, 109923.

Boye, J. I., Aksay, S., Roufik, S., Ribéreau, S., Mondor, M., Farnworth, E., & Rajamohamed, S. H. (2010). Comparison of the functional properties of pea, chickpea and lentil protein concentrates processed using ultrafiltration and isoelectric precipitation techniques. *Food Research International*, *43*(2), 537-546.

Bradford, M. L., & Thodos, G. (1966). Solubility parameters of hydrocarbons. *The Canadian Journal of Chemical Engineering*, *44*(6), 345-348.

Bradford, M. M. (1976). A rapid and sensitive method for the quantitation of microgram quantities of protein utilizing the principle of protein-dye binding. *Analytical Biochemistry*, *72*(1–2), 248–254.

Brady, K., Ho, C. T., Rosen, R. T., Sang, S., & Karwe, M. V. (2007). Effects of processing on the nutraceutical profile of quinoa. *Food Chemistry*, *100*(3), 1209-1216.

Brinegar, C., & Goundan, S. (1993). Isolation and characterization of chenopodin, the 11S seed storage protein of quinoa (*Chenopodium quinoa*). *Journal of Agricultural and Food Chemistry*, *41*(2), 182-185.

Brinegar, C., Sine, B., & Nwokocha, L. (1996). High-cysteine 2S seed storage proteins from quinoa (*Chenopodium quinoa*). *Journal of Agricultural and Food Chemistry*, *44*(7), 1621-1623.

Brishti, F. H., Chay, S. Y., Muhammad, K., Ismail-Fitry, M. R., Zarei, M., & Saari, N. (2021). Texturized mung bean protein as a sustainable food source: Effects of extrusion on its physical, textural and protein quality. *Innovative Food Science & Emerging Technologies*, *67*, 102591.

Brosnan, M. E., & Brosnan, J. T. (2020). Histidine metabolism and function. *The Journal of Nutrition*, *150*(Supplement_1), 2570S-2575S.

Bruin, A. D. (1964). Investigation of the food value of quinua and cañihua seed. *Journal of Food Science*, *29*(6), 872-876.

Cabra, V., Arreguin, R., Vazquez-Duhalt, R., & Farres, A. (2007). Effect of alkaline deamidation on the structure, surface hydrophobicity, and emulsifying properties of the Z19 alpha-zein. *Journal of Agricultural and Food Chemistry*, *55*(2), 439-445.

Capraro, J., De Benedetti, S., Di Dio, M., Bona, E., Abate, A., Corsetto, P. A., & Scarafoni, A. (2020). Characterization of Chenopodin isoforms from quinoa seeds and assessment of their potential anti-inflammatory activity in Caco-2 cells. *Biomolecules*, *10*(5), 795.

Chang, L., Lan, Y., Bandillo, N., Ohm, J.B., Chen, B., & Rao, J. (2022). Plant proteins from green pea and chickpea: Extraction, fractionation, structural characterization and functional properties. *Food Hydrocolloids*, *123*, 107165.

Chao, D., Jung, S., & Aluko, R. E. (2018). Physicochemical and functional properties of high pressure-treated isolated pea protein. *Innovative Food Science & Emerging Technologies*, *45*, 179-185.

Chauhan, G., Eskin, N., & Tkachuk, R. (1992). Nutrients and antinutrients in quinoa seed. *Cereal Chem*, *69*(1), 85-88.

Chen, D., Pang, X., Zhao, J., Gao, L., Liao, X., Wu, J., & Li, Q. (2015). Comparing the effects of high hydrostatic pressure and high temperature short time on papaya beverage. *Innovative Food Science & Emerging Technologies*, *32*, 16-28.

Chen, Y., Sheng, L., Gouda, M., & Ma, M. (2019). Impact of ultrasound treatment on the foaming and physicochemical properties of egg white during cold storage. *LWT*, *113*, 108303.

Cheng, J., Li, Z., Wang, J., Zhu, Z., Yi, J., Chen, B., & Cui, L. (2022). Structural characteristics of pea protein isolate (PPI) modified by high-pressure homogenization and its relation to the packaging properties of PPI edible film. *Food Chemistry*, *388*, 132974.

Collar, C., & Angioloni, A. (2014). Pseudocereals and teff in complex breadmaking matrices: Impact on lipid dynamics. *Journal of Cereal Science*, *59*(2), 145-154.

Comuzzo, P., & Calligaris, S. (2019). Potential applications of high pressure homogenization in winemaking: a review. *Beverages*, *5*(3), 56.

Condés, M. C., Speroni, F., Mauri, A., & Añón, M. C. (2012). Physicochemical and structural properties of amaranth protein isolates treated with high pressure. *Innovative Food Science & Emerging Technologies*, *14*, 11-17.

Constantino, A. B. T., & Garcia-Rojas, E. E. (2020). Modifications of physicochemical and functional properties of amaranth protein isolate (*Amaranthus cruentus* BRS Alegria) treated with high-intensity ultrasound. *Journal of Cereal Science*, *95*, 103076.

Contamine, R. F., Wilhelm, A. M., Berlan, J., & Delmas, H. (1995). Power measurement in sonochemistry. *Ultrasonics Sonochemistry*, *2*(1), S43-S47.

Contreras-Jimenez, B., Torres-Vargas, O. L., & Rodriguez-Garcia, M. E. (2019). Physicochemical characterization of quinoa (*Chenopodium quinoa*) flour and isolated starch. *Food Chemistry*,

298, 124982.

Cruz, N. S., Capellas, M., Jaramillo, D. P., Trujillo, A. J., Guamis, B., & Ferragut, V. (2009). Soymilk treated by ultra high-pressure homogenization: Acid coagulation properties and characteristics of a soy-yogurt product. *Food Hydrocolloids*, *23*(2), 490-496.

Cui, L., Bandillo, N., Wang, Y., Ohm, J. B., Chen, B., & Rao, J. (2020). Functionality and structure of yellow pea protein isolate as affected by cultivars and extraction pH. *Food Hydrocolloids*, *108*, 106008.

Dakhili, S., Abdolalizadeh, L., Hosseini, S. M., Shojaee-Aliabadi, S., & Mirmoghtadaie, L. (2019). Quinoa protein: Composition, structure and functional properties. *Food Chemistry*, *299*, 125161.

Daliri, H., Ahmadi, R., Pezeshki, A., Hamishehkar, H., Mohammadi, M., Beyrami, H., . . . Ghorbani, M. (2021). Quinoa bioactive protein hydrolysate produced by pancreatin enzyme - functional and antioxidant properties. *LWT*, *150*, 111853.

Dankar, I., Haddarah, A., El Omar, F., Sepulcre, F., & Pujolà, M. (2018). Assessing the microstructural and rheological changes induced by food additives on potato puree. *Food Chemistry*, *240*, 304-313.

Day, L., Cakebread, J. A., & Loveday, S. M. (2022). Food proteins from animals and plants: differences in the nutritional and functional properties. *Trends in Food Science & Technology*, *119*, 428-442.

DeJong, G., & Koppelman, S. (2002). Transglutaminase catalyzed reactions: Impact on food applications. *Journal of Food Science*, *67*(8), 2798-2806.

Dekkers, B. L., Boom, R. M., & van der Goot, A. J. (2018). Structuring processes for meat analogues. *Trends in Food Science & Technology*, *81*, 25-36.

Devi, A. F., Buckow, R., Hemar, Y., & Kasapis, S. (2014). Modification of the structural and rheological properties of whey protein/gelatin mixtures through high pressure processing. *Food Chemistry*, *156*, 243-249.

Dini, A., Rastrelli, L., Saturnino, P., & Schettino, O. (1992). A compositional study of *Chenopodium quinoa* seeds. *Food / Nahrung*, *36*(4), 400-404.

Dissanayake, M., & Vasiljevic, T. (2009). Functional properties of whey proteins affected by heat treatment and hydrodynamic high-pressure shearing. *Journal of Dairy Science*, *92*(4), 1387-1397.

Dong, X., Zhao, M., Yang, B. A. O., Yang, X., Shi, J., & Jiang, Y. (2011). Effect of high-pressure homogenization on the functional property of peanut protein. *Journal of Food Process Engineering*, *34*(6), 2191-2204.

dos Santos Aguilar, J. G., Cristianini, M., & Sato, H. H. (2018). Modification of enzymes by use of high-pressure homogenization. *Food Research International*, *109*, 120-125.

Drzewiecki, J., Leticia Martinez-Ayala, A., Lozano-Grande, M. A., Leontowicz, H., Leontowicz, M., Jastrzebski, Z., . . . Gorinstein, S. (2018). In vitro screening of bioactive compounds in some gluten-free plants. *Applied Biochemistry and Biotechnology*, *186*(4), 847-860.

Dumetz, A. C., Chockla, A. M., Kaler, E. W., & Lenhoff, A. M. (2008). Effects of pH on protein–protein interactions and implications for protein phase behavior. *Biochimica et Biophysica Acta (BBA)-Proteins and Proteomics*, *1784*(4), 600-610.

Dumont, C., Bourgeois, S., Fessi, H., & Jannin, V. (2018). Lipid-based nanosuspensions for oral delivery of peptides, a critical review. *International Journal of Pharmaceutics*, *541*(1), 117-135.

El Hazzam, K., Hafsa, J., Sobeh, M., Mhada, M., Taourirte, M., El Kacimi, K., & Yasri, A. (2020). An insight into saponins from quinoa (*Chenopodium quinoa* Willd): A review. *Molecules*, *25*(5), 1059.

Elahi, R., & Mu, T. H. (2017). High hydrostatic pressure (HHP)-induced structural modification of patatin and its antioxidant activities. *Molecules*, *22*(3), 438.

Elsohaimy, S. A., Refaay, T. M., & Zaytoun, M. A. M. (2015). Physicochemical and functional properties of quinoa protein isolate. *Annals of Agricultural Sciences*, *60*(2), 297-305.

Escamilla-García, M., Delgado-Sánchez, L. F., Ríos-Romo, R. A., García-Almendárez, B. E., Calderón-Domínguez, G., Méndez-Méndez, J. V., . . . Regalado-González, C. (2019). Effect of transglutaminase cross-linking in protein isolates from a mixture of two quinoa varieties with chitosan on the physicochemical properties of edible films. *Coatings*, *9*(11), 736.

Fang, Z., Cai, X., Wu, J., Zhang, L., Fang, Y., & Wang, S. (2021). Effect of simultaneous treatment combining ultrasonication and pH-shifting on SPI in the formation of nanoparticles and encapsulating resveratrol. *Food Hydrocolloids*, *111*, 106250.

Fayaz, G., Plazzotta, S., Calligaris, S., Manzocco, L., & Nicoli, M. C. (2019). Impact of high pressure homogenization on physical properties, extraction yield and biopolymer structure of soybean okara. *LWT-Food Science and Technology*, *113*, 108324.

Figueroa-González, J. J., Lobato-Calleros, C., Vernon-Carter, E. J., Aguirre-Mandujano, E., Alvarez-Ramirez, J., & Martínez-Velasco, A. (2022). Modifying the structure, physicochemical properties, and foaming ability of amaranth protein by dual pH-shifting and ultrasound treatments. *LWT*, *153*, 112561.

Flores-Jiménez, N. T., Ulloa, J. A., Urías-Silvas, J. E., Ramírez-Ramírez, J. C., Bautista-Rosales, P. U., & Gutiérrez-Leyva, R. (2022). Influence of high-intensity ultrasound on physicochemical and functional properties of a guamuchil *Pithecellobium dulce* (Roxb.) seed protein isolate. *Ultrasonics Sonochemistry*, *84*, 105976.

Foegeding, E. A., & Davis, J. P. (2011). Food protein functionality: A comprehensive approach. *Food Hydrocolloids*, *25*(8), 1853-1864.

Galante, M., De Flaviis, R., Boeris, V., & Spelzini, D. (2020). Effects of the enzymatic hydrolysis treatment on functional and antioxidant properties of quinoa protein acid-induced gels. *LWT*, *118*, 108845.

Galazka, V. B., Dickinson, E., & Ledward, D. A. (2000). Influence of high pressure processing on protein solutions and emulsions. *Current Opinion in Colloid & Interface Science*, *5*(3-4), 182-187.

Gao, K., Zha, F., Yang, Z., Rao, J., & Chen, B. (2022). Structure characteristics and functionality of water-soluble fraction from high-intensity ultrasound treated pea protein isolate. *Food Hydrocolloids*, *125*, 107409.

Gharibzahedi, S. M. T., & Smith, B. (2020). The functional modification of legume proteins by ultrasonication: A review. *Trends in Food Science & Technology, 98*, 107-116.

Guo, Z., Huang, Z., Guo, Y., Li, B., Yu, W., Zhou, L., . . . Wang, Z. (2021). Effects of high-pressure homogenization on structural and emulsifying properties of thermally soluble aggregated kidney bean (*Phaseolus vulgaris L.*) proteins. *Food Hydrocolloids, 119*, 106835.

Hager, A. S., Wolter, A., Jacob, F., Zannini, E., & Arendt, E. K. (2012). Nutritional properties and ultra-structure of commercial gluten free flours from different botanical sources compared to wheat flours. *Journal of Cereal Science, 56*(2), 239-247.

He, X. H., Liu, H. Z., Liu, L., Zhao, G. L., Wang, Q., & Chen, Q. L. (2014). Effects of high pressure on the physicochemical and functional properties of peanut protein isolates. *Food Hydrocolloids, 36*, 123-129.

Heremans, K. (1982). High pressure effects on proteins and other biomolecules. *Annual Review of Biophysics and Bioengineering, 11*(1), 1-21.

Hopwood, C. J., Bleidorn, W., Schwaba, T., & Chen, S. (2020). Health, environmental, and animal rights motives for vegetarian eating. *PLOS One, 15*(4), e0230609.

Hu, C., Xiong, Z., Xiong, H., Chen, L., & Zhang, Z. (2021). Effects of dynamic high-pressure microfluidization treatment on the functional and structural properties of potato protein isolate and its complex with chitosan. *Food Research International, 140*, 109868.

Hu, H., Wu, J., Li-Chan, E. C. Y., Zhu, L., Zhang, F., Xu, X., . . . Pan, S. (2013). Effects of ultrasound on structural and physical properties of soy protein isolate (SPI) dispersions. *Food Hydrocolloids, 30*(2), 647-655.

Huang, H. W., Hsu, C. P., & Wang, C. Y. (2020). Healthy expectations of high hydrostatic pressure treatment in food processing industry. *Journal of Food and Drug Analysis, 28*(1), 1-13.

Huang, K., Liu, Y., Zhang, Y., Cao, H., Luo, D., Yi, C., & Guan, X. (2022). Formulation of plant-based yoghurt from soybean and quinoa and evaluation of physicochemical, rheological, sensory and functional properties. *Food Bioscience, 49*, 101831.

Huang, M., Mao, Y., Li, H., & Yang, H. (2021). Kappa-carrageenan enhances the gelation and structural changes of egg yolk via electrostatic interactions with yolk protein. *Food Chemistry, 360*, 129972.

Iwasaki, T., Noshiroya, K., Saitoh, N., Okano, K., & Yamamoto, K. (2006). Studies of the effect of hydrostatic pressure pretreatment on thermal gelation of chicken myofibrils and pork meat patty. *Food Chemistry, 95*(3), 474-483.

Izzetti, R., Vitali, S., Aringhieri, G., Nisi, M., Oranges, T., Dini, V., ... & Gabriele, M. (2021). Ultra-high frequency ultrasound, a promising diagnostic technique: Review of the literature and single-center experience. *Canadian Association of Radiologists Journal*, 72(3), 418-431.

Jeske, S., Zannini, E., & Arendt, E. K. (2018). Past, present and future: the strength of plant-based dairy substitutes based on gluten-free raw materials. *Food Research International, 110*, 42-51.

Jiang, J., Chen, J., & Xiong, Y. L. (2009). Structural and emulsifying properties of soy protein isolate subjected to acid and alkaline pH-shifting processes. *Journal of Agricultural and Food Chemistry, 57*(16), 7576-7583.

Jiang, L., Wang, J., Li, Y., Wang, Z., Liang, J., Wang, R., . . . Zhang, M. (2014). Effects of ultrasound on the structure and physical properties of black bean protein isolates. *Food Research International*, *62*, 595-601.

Jiang, S., Ding, J., Andrade, J., Rababah, T. M., Almajwal, A., Abulmeaty, M. M., & Feng, H. (2017). Modifying the physicochemical properties of pea protein by pH-shifting and ultrasound combined treatments. *Ultrasonics Sonochemistry*, *38*, 835-842.

Kang, N., Zuo, Y., Hilliou, L., Ashokkumar, M., & Hemar, Y. (2016). Viscosity and hydrodynamic radius relationship of high-power ultrasound depolymerised starch pastes with different amylose content. *Food Hydrocolloids*, *52*, 183-191.

Kang, Z. L., Bai, R., Lu, F., Zhang, T., Gao, Z. S., Zhao, S. M., . . . Ma, H. J. (2022). Effects of high pressure homogenization on the solubility, foaming, and gel properties of soy 11S globulin. *Food Hydrocolloids*, *124*, 107261.

Kanno, C., Mu, T. H., Hagiwara, T., Ametani, M., & Azuma, N. (1998). Gel formation from industrial milk whey proteins under hydrostatic pressure: effect of hydrostatic pressure and protein concentration. *Journal of Agricultural and Food Chemistry*, *46*(2), 417-424.

Karaca, A. C., Low, N., & Nickerson, M. (2011). Emulsifying properties of canola and flaxseed protein isolates produced by isoelectric precipitation and salt extraction. *Food Research International*, *44*(9), 2991-2998.

Karaman, S., & Ozcan, T. (2021). Determination of gelation properties and bio-therapeutic potential of black carrot fibre- enriched functional yoghurt produced using pectin and gum arabic as prebiotic. *International Journal of Dairy Technology*, *74*(3), 505-517.

Kaspchak, E., Schuler de Oliveira, M. A., Simas, F. F., Cavicchiolo Franco, C. R., Meira Silveira, J. L., Mafra, M. R., & Igarashi-Mafra, L. (2017). Determination of heat-set gelation capacity of a quinoa protein isolate (*Chenopodium quinoa*) by dynamic oscillatory rheological analysis. *Food Chemistry*, *232*, 263-271.

Kato, A., & Nakai, S. (1980). Hydrophobicity determined by a fluorescence probe method and its correlation with surface properties of proteins. *Biochimica et Biophysica Acta (BBA) - Protein Structure*, *624*(1), 13-20.

Katzav, H., Chirug, L., Okun, Z., Davidovich-Pinhas, M., & Shpigelman, A. (2020). Comparison of thermal and high-pressure gelation of potato protein isolates. *Foods*, *9*(8), 1041.

Kaur, N., Chugh, V., & Gupta, A. K. (2014). Essential fatty acids as functional components of foods - a review. *Journal of Food Science and Technology*, *51*(10), 2289-2303.

Kchaou, H., Benbettaieb, N., Jridi, M., Nasri, M., & Debeaufort, F. (2019). Influence of Maillard reaction and temperature on functional, structure and bioactive properties of fish gelatin films. *Food Hydrocolloids*, *97*, 105196.

Keerati-u-rai, M., & Corredig, M. (2009). Effect of dynamic high pressure homogenization on the aggregation state of soy protein. *Journal of Agricultural and Food Chemistry*, *57*(9), 3556-3562.

Khan, N. M., Mu, T. H., Sun, H. N., Zhang, M., & Chen, J. W. (2015). Effects of high hydrostatic pressure on secondary structure and emulsifying behavior of sweet potato protein. *High*

Pressure Research, *35*(2), 189-202.

Khatkar, A. B., Kaur, A., & Khatkar, S. K. (2020). Restructuring of soy protein employing ultrasound: Effect on hydration, gelation, thermal, in-vitro protein digestibility and structural attributes. *LWT*, *132*, 109781.

Kornet, R., Shek, C., Venema, P., Jan van der Goot, A., Meinders, M., & van der Linden, E. (2021). Substitution of whey protein by pea protein is facilitated by specific fractionation routes. *Food Hydrocolloids*, *117*, 106691.

Kozioł, M. J. (1992). Chemical composition and nutritional evaluation of quinoa (*Chenopodium quinoa* Willd.). *Journal of Food Composition and Analysis*, *5*(1), 35-68.

Laemmli, U. K. (1970). Cleavage of structural proteins during the assembly of the head of bacteriophage T4. *Nature*, *227*(5259), 680-685.

Lai, Q. D., Huynh, T. T. L., Doan, N. T. T., & Nguyen, H. D. (2022). Particle size distribution and homogenisation efficiency in high-pressure homogenisation of wheat germ oil-water system. *International Journal of Food Science & Technology*, *57*(7), 4337-4346.

Le Roux, L., Mejean, S., Chacon, R., Lopez, C., Dupont, D., Deglaire, A., . . . Jeantet, R. (2020). Plant proteins partially replacing dairy proteins greatly influence infant formula functionalities. *LWT*, *120*, 108891.

Levy, R., Okun, Z., Davidovich-Pinhas, M., & Shpigelman, A. (2021). Utilization of high-pressure homogenization of potato protein isolate for the production of dairy-free yogurt-like fermented product. *Food Hydrocolloids*, *113*, 106442.

Levy, R., Okun, Z., & Shpigelman, A. (2021). High-pressure homogenization: Principles and applications beyond microbial inactivation. *Food Engineering Reviews*, *13*(3), 490-508.

Li, H., Zhu, K., Zhou, H., & Peng, W. (2012). Effects of high hydrostatic pressure treatment on allergenicity and structural properties of soybean protein isolate for infant formula. *Food Chemistry*, *132*(2), 808-814.

Li, L., Zhou, Y., Teng, F., Zhang, S., Qi, B., Wu, C., . . . Li, Y. (2020). Application of ultrasound treatment for modulating the structural, functional and rheological properties of black bean protein isolates. *International Journal of Food Science & Technology*, *55*(4), 1637-1647.

Li, X., Da, S., Li, C., Xue, F., & Zang, T. (2018). Effects of high-intensity ultrasound pretreatment with different levels of power output on the antioxidant properties of alcalase hydrolyzates from Quinoa (*Chenopodium quinoa* Willd.) protein isolate. *Cereal Chemistry*, *95*(4), 518-526.

Lima, G. P. P., Vianello, F., Corrêa, C. R., Campos, R. A. d. S., & Borguini, M. G. (2014). Polyphenols in fruits and vegetables and its effect on human health. *Food and Nutrition Sciences*, 1065-1082.

Linke, C., & Drusch, S. (2018). Pickering emulsions in foods - opportunities and limitations. *Critical Reviews in Food Science and Nutrition*, *58*(12), 1971-1985.

Liu, Y., Zhang, W., Wang, K., Bao, Y., Regenstein, J. M., & Zhou, P. (2019). Fabrication of gel-like emulsions with whey protein isolate using microfluidization: Rheological properties and 3D printing performance. *Food and Bioprocess Technology*, *12*(12), 1967-1979.

Liu, Y. Y., Zeng, X. A., Deng, Z., Yu, S. J., & Yamasaki, S. (2011). Effect of pulsed electric field on the secondary structure and thermal properties of soy protein isolate. *European Food Research and Technology*, *233*(5), 841-850.

Lomelí-Martín, A., Martínez, L. M., Welti-Chanes, J., & Escobedo-Avellaneda, Z. (2021). Induced changes in aroma compounds of foods treated with high hydrostatic pressure: A review. *Foods*, *10*(4), 878.

López-Castejón, M. L., Bengoechea, C., Díaz-Franco, J., & Carrera, C. (2020). Interfacial and emulsifying properties of quinoa protein concentrates. *Food Biophysics*, *15*(1), 122-132.

Lozober, H. S., Okun, Z., & Shpigelman, A. (2021). The impact of high-pressure homogenization on thermal gelation of *Arthrospira platensis* (*Spirulina*) protein concentrate. *Innovative Food Science & Emerging Technologies*, *74*, 102857.

Lu, Z., Lee, P. R., & Yang, H. (2022). Chickpea flour and soy protein isolate interacted with κ-carrageenan via electrostatic interactions to form egg omelets analogue. *Food Hydrocolloids*, *130*, 107691.

Lullien-Pellerin, V., & Balny, C. (2002). High-pressure as a tool to study some proteins' properties: Conformational modification, activity and oligomeric dissociation. *Innovative Food Science & Emerging Technologies*, *3*(3), 209-221.

Lundgren, M. (2011). Composition of fractions from air-classified wheat flour. Second cycle, A1E. Uppsala: SLU, Dept. of Food Science

Luo, L., Zhang, R., Palmer, J., Hemar, Y., & Yang, Z. (2021). Impact of high hydrostatic pressure on the gelation behavior and microstructure of quinoa protein isolate dispersions. *ACS Food Science & Technology*, *1*(11), 2144-2151.

Luo, Q., Borst, J. W., Westphal, A. H., Boom, R. M., & Janssen, A. E. (2017). Pepsin diffusivity in whey protein gels and its effect on gastric digestion. *Food Hydrocolloids*, *66*, 318-325.

MacDonald, I. F., Marsh, B. D., & Ashare, E. (1969). Rheological behavior for large amplitude oscillatory motion. *Chemical Engineering Science*, *24*(10), 1615-1625.

Mackie, A. R., Gunning, A. P., Wilde, P. J., & Morris, V. J. (2000). Competitive displacement of beta-lactoglobulin from the air/water interface by sodium dodecyl sulfate. *Langmuir*, *16*(21), 8176-8181.

MacRitchie, F. (1989). Protein adsorption desorption at fluid interfaces. *Colloids and Surfaces*, *41*(1-2), 25-34.

Maguire, C. M., Rösslein, M., Wick, P., & Prina-Mello, A. (2018). Characterisation of particles in solution – a perspective on light scattering and comparative technologies. *Science and Technology of Advanced Materials*, *19*(1), 732-745.

Mäkinen, O. E., Wanhalinna, V., Zannini, E., & Arendt, E. K. (2016a). Foods for special dietary needs: Non-dairy plant-based milk substitutes and fermented dairy-type products. *Critical Reviews in Food Science and Nutrition*, *56*(3), 339-349.

Mäkinen, O. E., Zannini, E., Koehler, P., & Arendt, E. K. (2016b). Heat-denaturation and aggregation of quinoa (*Chenopodium quinoa*) globulins as affected by the pH value. *Food Chemistry*, *196*, 17-24.

Malek, M. N. F. A., Hussin, N. M., Embong, N. H., Bhuyar, P., Rahim, M. H. A., Govindan, N., & Maniam, G. P. (2020). Ultrasonication: A process intensification tool for methyl ester synthesis: A mini review. *Biomass Conversion and Biorefinery*, 1-11.

Manassero, C. A., Vaudagna, S. R., Añón, M. C., & Speroni, F. (2015). High hydrostatic pressure improves protein solubility and dispersion stability of mineral-added soybean protein isolate. *Food Hydrocolloids, 43*, 629-635.

Marangoni, A., Barbut, S., McGauley, S., Marcone, M., & Narine, S. (2000). On the structure of particulate gels - the case of salt-induced cold gelation of heat-denatured whey protein isolate. *Food Hydrocolloids, 14*(1), 61-74.

McClements, D. J., Newman, E., & McClements, I. F. (2019). Plant-based milks: A review of the science underpinning their design, fabrication, and performance. *Comprehensive Reviews in Food Science and Food Safety, 18*(6), 2047-2067.

Melchior, S., Moretton, M., Calligaris, S., Manzocco, L., & Nicoli, M. C. (2022). High pressure homogenization shapes the techno-functionalities and digestibility of pea proteins. *Food and Bioproducts Processing, 131*, 77-85.

Messens, W., Van Camp, J., & Huyghebaert, A. (1997). The use of high pressure to modify the functionality of food proteins. *Trends in Food Science & Technology, 8*(4), 107-112.

Mession, J. L., Sok, N., Assifaoui, A., & Saurel, R. (2013). Thermal denaturation of pea globulins (*Pisum sativum L.*)-molecular interactions leading to heat-induced protein aggregation. *Journal of Agricultural and Food Chemistry, 61*(6), 1196-1204.

Mir, N. A., Riar, C. S., & Singh, S. (2019a). Physicochemical, molecular and thermal properties of high-intensity ultrasound (HIUS) treated protein isolates from album (*Chenopodium album*) seed. *Food Hydrocolloids, 96*, 433-441.

Mir, N. A., Riar, C. S., & Singh, S. (2019b). Structural modification of quinoa seed protein isolates (QPIs) by variable time sonification for improving its physicochemical and functional characteristics. *Ultrasonics Sonochemistry, 58*, 104700.

Miranda, J., Lasa, A., Bustamante, M. A., Churruca, I., & Simon, E. (2014). Nutritional differences between a gluten-free diet and a diet containing equivalent products with gluten. *Plant Foods for Human Nutrition, 69*(2), 182-187.

Mirmoghtadaie, L., Aliabadi, S. S., & Hosseini, S. M. (2016). Recent approaches in physical modification of protein functionality. *Food Chemistry, 199*, 619-627.

Nascimento, A. C., Mota, C., Coelho, I., Gueifão, S., Santos, M., Matos, A. S., . . . Castanheira, I. (2014). Characterisation of nutrient profile of quinoa (*Chenopodium quinoa*), amaranth (*Amaranthus caudatus*), and purple corn (*Zea mays* L.) consumed in the north of Argentina: proximates, minerals and trace elements. *Food Chemistry, 148*, 420-426.

Nasrabadi, M. N., Doost, A. S., & Mezzenga, R. (2021). Modification approaches of plant-based proteins to improve their techno-functionality and use in food products. *Food Hydrocolloids, 118*, 106789.

Nazari, B., Mohammadifar, M. A., Shojaee-Aliabadi, S., Feizollahi, E., & Mirmoghtadaie, L. (2018). Effect of ultrasound treatments on functional properties and structure of millet protein

concentrate.*Ultrasonics Sonochemistry*,*41*, 382-388.

Ngarize, S., Adams, A., & Howell, N. (2005). A comparative study of heat and high pressure induced gels of whey and egg albumen proteins and their binary mixtures. *Food Hydrocolloids*, *19*(6), 984-996.

Nicolai, T. (2019). Gelation of food protein-protein mixtures. *Advances in Colloid and Interface Science*, *270*, 147-164.

Nicolai, T., & Chassenieux, C. (2019). Heat-induced gelation of plant globulins. *Current Opinion in Food Science*, *27*, 18-22.

Nicorescu, I., Loisel, C., Vial, C., Riaublanc, A., Djelveh, G., Cuvelier, G., & Legrand, J. (2008). Combined effect of dynamic heat treatment and ionic strength on the properties of whey protein foams - part II. *Food Research International*, *41*(10), 980-988.

Nowak, V., Du, J., & Charrondière, U. R. (2016). Assessment of the nutritional composition of quinoa (*Chenopodium quinoa* Willd.). *Food Chemistry*, *193*, 47-54.

O'Donnell, C., Tiwari, B., Bourke, P., & Cullen, P. (2010). Effect of ultrasonic processing on food enzymes of industrial importance. *Trends in Food Science & Technology*, *21*(7), 358-367.

Ogungbenle, H. N. (2003). Nutritional evaluation and functional properties of quinoa (*Chenopodium quinoa*) flour. *International Journal of Food Sciences and Nutrition*, *54*(2), 153-158.

Oncley, J., Ellenbogen, E., Gitlin, D., & Gurd, F. (1952). Protein–protein interactions. *The Journal of Physical Chemistry*, *56*(1), 85-92.

Oomah, B. D., Mazza, G., & Cui, W. (1994). Optimization of protein extraction from flaxseed meal. *Food Research International*, *27*(4), 355-361.

Panyam, D., & Kilara, A. (1996). Enhancing the functionality of food proteins by enzymatic modification. *Trends in Food Science & Technology*, *7*(4), 120-125.

Patist, A., & Bates, D. (2008). Ultrasonic innovations in the food industry: from the laboratory to commercial production. *Innovative Food Science & Emerging Technologies*, *9*(2), 147-154.

Pearce, K. N., & Kinsella, J. E. (1978). Emulsifying properties of proteins: evaluation of a turbidimetric technique. *Journal of Agricultural and Food Chemistry*, *26*(3), 716-723.

Pelgrom, P. J. M., Boom, R. M., & Schutyser, M. A. I. (2015). Method development to increase protein enrichment during dry fractionation of starch-rich legumes. *Food and Bioprocess Technology*, *8*(7), 1495-1502.

Pelgrom, P. J. M., Vissers, A. M., Boom, R. M., & Schutyser, M. A. I. (2013). Dry fractionation for production of functional pea protein concentrates. *Food Research International*, *53*(1), 232-239.

Petruccelli, S., & Añón, M. C. (1996). pH-induced modifications in the thermal stability of soybean protein isolates. *Journal of Agricultural and Food Chemistry*, *44*(10), 3005-3009.

Peyrano, F., de Lamballerie, M., Avanza, M. V., & Speroni, F. (2021). Gelation of cowpea proteins induced by high hydrostatic pressure. *Food Hydrocolloids*, *111*, 106191.

Peyrano, F., Speroni, F., & Avanza, M. V. (2016). Physicochemical and functional properties of cowpea protein isolates treated with temperature or high hydrostatic pressure. *Innovative Food Science & Emerging Technologies*, *33*, 38-46.

Phan-Xuan, T., Durand, D., Nicolai, T., Donato, L., Schmitt, C., & Bovetto, L. (2013). Tuning the structure of protein particles and gels with calcium or sodium ions. *Biomacromolecules*, *14*(6), 1980-1989.

Písaříková, B., Kráčmar, S., & Herzig, I. (2005). Amino acid contents and biological value of protein in various amaranth species. *Czech Journal of Animal Science*, *50*(4), 169-174.

Porretta, S., Birzi, A., Ghizzoni, C., & Vicini, E. (1995). Effects of ultra-high hydrostatic pressure treatments on the quality of tomato juice. *Food Chemistry*, *52*(1), 35-41.

Prego, I., Maldonado, S., & Otegui, M. (1998). Seed structure and localization of reserves in *Chenopodium quinoa*. *Annals of Botany*, *82*(4), 481-488.

Pulvento, C., Riccardi, M., Lavini, A., Iafelice, G., Marconi, E., & d'Andria, R. (2012). Yield and quality characteristics of quinoa grown in open field under different saline and non-saline irrigation regimes. *Journal of Agronomy and Crop Science*, *198*(4), 254-263.

Puppo, C., Chapleau, N., Speroni, F., de Lamballerie-Anton, M., Michel, F., Añón, C., & Anton, M. (2004). Physicochemical modifications of high-pressure-treated soybean protein isolates. *Journal of Agricultural and Food Chemistry*, *52*(6), 1564-1571.

Qamar, S., Bhandari, B., & Prakash, S. (2019). Effect of different homogenisation methods and UHT processing on the stability of pea protein emulsion. *Food Research International*, *116*, 1374-1385.

Qin, X. S., Luo, Z. G., & Peng, X. C. (2018). Fabrication and characterization of quinoa protein nanoparticle-stabilized food-grade Pickering emulsions with ultrasound treatment: Interfacial adsorption/arrangement properties. *Journal of Agricultural and Food Chemistry*, *66*(17), 4449-4457.

Queirós, R. P., Saraiva, J. A., & da Silva, J. A. L. (2018). Tailoring structure and technological properties of plant proteins using high hydrostatic pressure. *Critical Reviews in Food Science and Nutrition*, *58*(9), 1538-1556.

Ran, X., Yang, Z., Chen, Y., & Yang, H. (2022). Konjac glucomannan decreases metabolite release of a plant-based fishball analogue during in vitro digestion by affecting amino acid and carbohydrate metabolic pathways. *Food Hydrocolloids*, *129*, 107623.

Ridout, C. L., Price, K. R., Dupont, M. S., Parker, M. L., & Fenwick, G. R. (1991). Quinoa saponins - analysis and preliminary investigations into the effects of reduction by processing. *Journal of the Science of Food and Agriculture*, *54*(2), 165-176.

Rocchetti, G., Miragoli, F., Zacconi, C., Lucini, L., & Rebecchi, A. (2019). Impact of cooking and fermentation by lactic acid bacteria on phenolic profile of quinoa and buckwheat seeds. *Food Research International*, *119*, 886-894.

Romero, A., Beaumal, V., David-Briand, E., Cordobes, F., Guerrero, A., & Anton, M. (2012). Interfacial and emulsifying behaviour of rice protein concentrate. *Food Hydrocolloids*, *29*(1), 1-8.

Rose, W. C., Haines, W., Warner, D., & Johnson, J. (1976). Amino acid requirements of man. *Nutr Rev*, *34*, 307-309.

Ross-Murphy, S. B. (1995). Rheological characterisation of gels 1. *Journal of Texture Studies*, *26*(4), 391-400.

Ruales, J., Grijalva, Y. d., Lopez-Jaramillo, P., & Nair, B. M. (2002). The nutritional quality of an infant food from quinoa and its effect on the plasma level of insulin-like growth factor-1 (IGF-1) in undernourished children. *International Journal of Food Sciences and Nutrition*, *53*(2), 143-154.

Ruiz, G. A., Xiao, W., van Boekel, M., Minor, M., & Stieger, M. (2016). Effect of extraction pH on heat-induced aggregation, gelation and microstructure of protein isolate from quinoa (*Chenopodium quinoa* Willd). *Food Chemistry*, *209*, 203-210.

Rullier, B., Novales, B., & Axelos, M. A. V. (2008). Effect of protein aggregates on foaming properties of beta-lactoglobulin. *Colloids and Surfaces a-Physicochemical and Engineering Aspects*, *330*(2-3), 96-102.

Sá, A. G. A., Moreno, Y. M. F., & Carciofi, B. A. M. (2020). Plant proteins as high-quality nutritional source for human diet. *Trends in Food Science & Technology*, *97*, 170-184.

Sagis, L. M. C., & Yang, J. (2022). Protein-stabilized interfaces in multiphase food: Comparing structure-function relations of plant-based and animal-based proteins. *Current Opinion in Food Science*, *43*, 53-60.

Sajedi, M., Nasirpour, A., Keramat, J., & Desobry, S. (2014). Effect of modified whey protein concentrate on physical properties and stability of whipped cream. *Food Hydrocolloids*, *36*, 93-101.

Saowapark, S., Apichartsrangkoon, A., & Bell, A. E. (2008). Viscoelastic properties of high pressure and heat induced tofu gels. *Food Chemistry*, *107*(3), 984-989.

Saricaoglu, F. T. (2020). Application of high-pressure homogenization (HPH) to modify functional, structural and rheological properties of lentil (*Lens culinaris*) proteins. *International Journal of Biological Macromolecules*, *144*, 760-769.

Saricaoglu, F. T., Gul, O., Besir, A., & Atalar, I. (2018). Effect of high pressure homogenization (HPH) on functional and rheological properties of hazelnut meal proteins obtained from hazelnut oil industry by-products. *Journal of Food Engineering*, *233*, 98-108.

Sarkar, A., & Dickinson, E. (2020). Sustainable food-grade Pickering emulsions stabilized by plant-based particles. *Current Opinion in Colloid & Interface Science*, *49*, 69-81.

Sato, A., Matsumiya, K., Kosugi, T., Kubouchi, H., & Matsumura, Y. (2022). Effects of different gases on foaming properties of protein dispersions prepared with whipped cream dispenser. *Journal of Food Engineering*, *314*, 110764.

Schabes, F. I., & Sigstad, E. E. (2005). Calorimetric studies of quinoa (*Chenopodium quinoa* Willd.) seed germination under saline stress conditions. *Thermochimica Acta*, *428*(1), 71-75.

Schoenfeld, B. J., & Aragon, A. A. (2018). How much protein can the body use in a single meal for muscle-building? Implications for daily protein distribution. *Journal of the International Society of Sports Nutrition*, *15*(1), 10.

Sen, D., & Kahveci, D. (2020). Production of a protein concentrate from hazelnut meal obtained as a hazelnut oil industry by-product and its application in a functional beverage. *Waste and Biomass Valorization*, *11*(10), 5099-5107.

Shen, X., Fang, T., Gao, F., & Guo, M. (2017). Effects of ultrasound treatment on physicochemical and emulsifying properties of whey proteins pre- and post-thermal aggregation. *Food Hydrocolloids*, *63*, 668-676.

Shen, Y., Hong, S., Singh, G., Koppel, K., & Li, Y. (2022). Improving functional properties of pea protein through "green" modifications using enzymes and polysaccharides. *Food Chemistry*, *385*, 132687.

Shen, Y., Tang, X., & Li, Y. (2021). Drying methods affect physicochemical and functional properties of quinoa protein isolate. *Food Chemistry*, *339*, 127823.

Shimada, K., & Cheftel, J. C. (1988). Texture characteristics, protein solubility, and sulfhydryl group/disulfide bond contents of heat-induced gels of whey protein isolate. *Journal of Agricultural and Food Chemistry*, *36*(5), 1018-1025.

Silva, J. V. C., Cochereau, R., Schmitt, C., Chassenieux, C., & Nicolai, T. (2019). Heat-induced gelation of mixtures of micellar caseins and plant proteins in aqueous solution. *Food Research International*, *116*, 1135-1143.

Silventoinen, P., & Sozer, N. (2020). Impact of ultrasound treatment and pH-shifting on physicochemical properties of protein-enriched barley fraction and barley protein Isolate. *Foods*, *9*(8), 1055.

Song, C. L., & Zhao, X. H. (2014). Structure and property modification of an oligochitosan-glycosylated and crosslinked soybean protein generated by microbial transglutaminase. *Food Chemistry*, *163*, 114-119.

Soria, A. C., & Villamiel, M. (2010). Effect of ultrasound on the technological properties and bioactivity of food: A review. *Trends in Food Science & Technology*, *21*(7), 323-331.

Sow, L. C., & Yang, H. (2015). Effects of salt and sugar addition on the physicochemical properties and nanostructure of fish gelatin. *Food Hydrocolloids*, *45*, 72-82.

Speroni, F., Beaumal, V., de Lamballerie, M., Anton, M., Añón, M., & Puppo, M. (2009). Gelation of soybean proteins induced by sequential high-pressure and thermal treatments. *Food Hydrocolloids*, *23*(5), 1433-1442.

Sridharan, S., Meinders, M. B. J., Bitter, J. H., & Nikiforidis, C. V. (2020). On the emulsifying properties of self-assembled pea protein particles. *Langmuir*, *36*(41), 12221-12229.

Steffolani, M. E., Villacorta, P., Morales-Soriano, E. R., Repo-Carrasco, R., León, A. E., & Pérez, G. T. (2016). Physicochemical and functional characterization of protein isolated from different quinoa varieties (*Chenopodium quinoa* Willd.). *Cereal Chemistry*, *93*(3), 275-281.

Stone, A. K., Karalash, A., Tyler, R. T., Warkentin, T. D., & Nickerson, M. T. (2015). Functional attributes of pea protein isolates prepared using different extraction methods and cultivars. *Food Research International*, *76*, 31-38.

Sun, B., Li, Z., Huang, Y., Liu, L., Gu, X., Gao, Y., . . . Xia, X. (2022). High-pressure homogenisation - Lactobacillus induced changes in the properties and structure of soymilk protein gels. *International Journal of Food Science & Technology*, *57*(10), 6852-6866.

Sun, C., Dai, L., Liu, F., & Gao, Y. (2016). Simultaneous treatment of heat and high pressure homogenization of zein in ethanol–water solution: Physical, structural, thermal and morphological characteristics. *Innovative Food Science & Emerging Technologies*, *34*, 161-170.

Sun, W., Zhou, F., Sun, D.-W., & Zhao, M. (2013). Effect of oxidation on the emulsifying properties of myofibrillar proteins. *Food and Bioprocess Technology*, *6*(7), 1703-1712.

Sun, X. D., & Arntfield, S. D. (2010). Gelation properties of salt-extracted pea protein induced by heat treatment. *Food Research International*, *43*(2), 509-515.

Sun, X. D., & Arntfield, S. D. (2012). Molecular forces involved in heat-induced pea protein gelation: Effects of various reagents on the rheological properties of salt-extracted pea protein gels. *Food Hydrocolloids*, *28*(2), 325-332.

Tabtabaei, S., Jafari, M., Rajabzadeh, A. R., & Legge, R. L. (2016). Solvent-free production of protein-enriched fractions from navy bean flour using a triboelectrification-based approach. *Journal of Food Engineering*, *174*, 21-28.

Tan, M., Xu, J., Gao, H., Yu, Z., Liang, J., Mu, D., . . . Zheng, Z. (2021). Effects of combined high hydrostatic pressure and pH-shifting pretreatment on the structure and emulsifying properties of soy protein isolates. *Journal of Food Engineering*, *306*, 110622.

Tan, M. C., Chin, N. L., Yusof, Y. A., Taip, F. S., & Abdullah, J. (2014). Gel strength and stability characterization of ultrasound treated whey protein foams. *Agriculture and Agricultural Science Procedia*, *2*, 144-149.

Tang, C. H., & Ma, C. Y. (2009). Effect of high pressure treatment on aggregation and structural properties of soy protein isolate. *LWT-Food Science and Technology*, *42*(2), 606-611.

Tanger, C., Müller, M., Andlinger, D., & Kulozik, U. (2022). Influence of pH and ionic strength on the thermal gelation behaviour of pea protein. *Food Hydrocolloids*, *123*, 106903.

Tapiero, H., Mathé, G., Couvreur, P., & Tew, K. D. (2002). I. Arginine. *Biomedicine & Pharmacotherapy*, *56*(9), 439-445.

Teng, C., Xing, B., Fan, X., Zhang, B., Li, Y., & Ren, G. (2021). Effects of Maillard reaction on the properties and anti-inflammatory, anti-proliferative activity in vitro of quinoa protein isolates. *Industrial Crops and Products*, *174*, 114165.

Thiebaud, M., Dumay, E., Picart, L., Guiraud, J., & Cheftel, J. (2003). High-pressure homogenisation of raw bovine milk. Effects on fat globule size distribution and microbial inactivation. *International Dairy Journal*, *13*(6), 427-439.

Torrezan, R., Tham, W. P., Bell, A. E., Frazier, R. A., & Cristianini, M. (2007). Effects of high pressure on functional properties of soy protein. *Food Chemistry*, *104*(1), 140-147.

Tung, M. A. (1978). Rheology of protein dispersions. *Journal of Texture Studies*, *9*(1-2), 3-31.

Utsumi, S., Damodaran, S., & Kinsella, J. E. (1984). Heat-induced interactions between soybean proteins: Preferential association of 11S basic subunits and. beta. subunits of 7S. *Journal of Agricultural and Food Chemistry*, *32*(6), 1406-1412.

Van Camp, J., & Huyghebaert, A. (1995). A comparative rheological study of heat and high pressure induced whey protein gels. *Food Chemistry, 54*(4), 357-364.

Van der Plancken, I., Van Loey, A., & Hendrickx, M. E. (2007). Foaming properties of egg white proteins affected by heat or high pressure treatment. *Journal of Food Engineering, 78*(4), 1410-1426.

van Dijk, M., Morley, T., Rau, M. L., & Saghai, Y. (2021). A meta-analysis of projected global food demand and population at risk of hunger for the period 2010–2050. *Nature Food, 2*(7), 494-501.

Vera, A., Valenzuela, M. A., Yazdani-Pedram, M., Tapia, C., & Abugoch, L. (2019). Conformational and physicochemical properties of quinoa proteins affected by different conditions of high-intensity ultrasound treatments. *Ultrasonics Sonochemistry, 51,* 186-196.

Vilcacundo, R., Martinez-Villaluenga, C., & Hernandez-Ledesma, B. (2017). Release of dipeptidyl peptidase IV, alpha-amylase and alpha-glucosidase inhibitory peptides from quinoa (*Chenopodium quinoa* Willd.) during in vitro simulated gastrointestinal digestion. *Journal of Functional Foods, 35,* 531-539.

Visser, S., Slangen, C. J., & Rollema, H. S. (1991). Phenotyping of bovine milk proteins by reversed-phase high-performance liquid chromatography. *Journal of Chromatography A, 548,* 361-370.

Volkenstein, M. V. (1965). Coding of polar and non-polar amino-acids. *Nature, 207*(4994), 294-295.

Wang, C., Tian, Z., Chen, L., Temelli, F., Liu, H., & Wang, Y. (2010). Functionality of barley proteins extracted and fractionated by alkaline and alcohol methods. *Cereal Chemistry, 87*(6), 597-606.

Wang, J., Smits, E., Boom, R. M., & Schutyser, M. A. I. (2015). Arabinoxylans concentrates from wheat bran by electrostatic separation. *Journal of Food Engineering, 155,* 29-36.

Wang, X., Zhao, R., & Yuan, W. (2020). Composition and secondary structure of proteins isolated from six different quinoa varieties from China. *Journal of Cereal Science, 95,* 103036.

Wang, Y., Eastwood, B., Yang, Z., de Campo, L., Knott, R., Prosser, C., . . . Hemar, Y. (2019). Rheological and structural characterization of acidified skim milks and infant formulae made from cow and goat milk. *Food Hydrocolloids, 96,* 161-170.

Wen, C., Zhang, J., Yao, H., Zhou, J., Duan, Y., Zhang, H., & Ma, H. (2019). Advances in renewable plant-derived protein source: The structure, physicochemical properties affected by ultrasonication. *Ultrasonics Sonochemistry, 53,* 83-98.

Wierenga, P. A., Meinders, M. B. J., Egmond, M. R., Voragen, F., & de Jongh, H. H. J. (2003). Protein exposed hydrophobicity reduces the kinetic barrier for adsorption of ovalbumin to the air-water interface. *Langmuir, 19*(21), 8964-8970.

Wood, S., Lawson, L., Fairbanks, D. J., Robison, L., & Andersen, W. (1993). Seed lipid content and fatty acid composition of three quinoa cultivars. *Journal of Food Composition and Analysis, 6*(1), 41-44.

Wright, K. H., Pike, O. A., Fairbanks, D. J., & Huber, C. S. (2002). Composition of atriplex hortensis, sweet and bitter *Chenopodium quinoa* Seeds. *Journal of Food Science, 67*(4), 1383-1385.

Xiong, T., Xiong, W., Ge, M., Xia, J., Li, B., & Chen, Y. (2018). Effect of high intensity ultrasound on

structure and foaming properties of pea protein isolate. *Food Research International*, *109*, 260-267.

Xiong, X., Ho, M. T., Bhandari, B., & Bansal, N. (2020). Foaming properties of milk protein dispersions at different protein content and casein to whey protein ratios. *International Dairy Journal*, *109*, 104758.

Yang, H., Yang, S., Kong, J., Dong, A., & Yu, S. (2015). Obtaining information about protein secondary structures in aqueous solution using Fourier transform IR spectroscopy. *Nature Protocols*, *10*(3), 382-396.

Yang, J., Liu, G., Zeng, H., & Chen, L. (2018). Effects of high pressure homogenization on faba bean protein aggregation in relation to solubility and interfacial properties. *Food Hydrocolloids*, *83*, 275-286.

Yang, J., & Sagis, L. M. C. (2021). Interfacial behavior of plant proteins - novel sources and extraction methods. *Current Opinion in Colloid & Interface Science*, *56*, 101499.

Yang, J., Zamani, S., Liang, L., & Chen, L. (2021). Extraction methods significantly impact pea protein composition, structure and gelling properties. *Food Hydrocolloids*, *117*, 106678.

Yang, Z., Chaib, S., Gu, Q., & Hemar, Y. (2017). Impact of pressure on physicochemical properties of starch dispersions. *Food Hydrocolloids*, *68*, 164-177.

Yang, Z., Chaieb, S., Hemar, Y., de Campo, L., Rehm, C., & McGillivray, D. J. (2015). Investigating linear and nonlinear viscoelastic behaviour and microstructures of gelatin-multiwalled carbon nanotube composites. *Rsc Advances*, *5*(130), 107916-107926.

Yang, Z., de Campo, L., Gilbert, E. P., Knott, R., Cheng, L., Storer, B., . . . Hemar, Y. (2022). Effect of NaCl and $CaCl_2$ concentration on the rheological and structural characteristics of thermally-induced quinoa protein gels. *Food Hydrocolloids*, *124*, 107350.

Yin, S. W., Tang, C. H., Wen, Q. B., Yang, X. Q., & Li, L. (2008). Functional properties and in vitro trypsin digestibility of red kidney bean (*Phaseolus vulgaris* L.) protein isolate: Effect of high-pressure treatment. *Food Chemistry*, *110*(4), 938-945.

Yordanov, D., & Angelova, G. V. (2010). High pressure processing for foods preserving. *Biotechnology & Biotechnological Equipment*, *24*, 1940-1945.

Zannini, E., Jeske, S., Lynch, K. M., & Arendt, E. K. (2018). Development of novel quinoa-based yoghurt fermented with dextran producer *Weissella cibaria* MG1. *International Journal of Food Microbiology*, *268*, 19-26.

Zhang, H., Chen, G., Liu, M., Mei, X., Yu, Q., & Kan, J. (2020). Effects of multi-frequency ultrasound on physicochemical properties, structural characteristics of gluten protein and the quality of noodle. *Ultrasonics Sonochemistry*, *67*, 105135.

Zhang, J., Li, M., Cheng, J., Zhang, X., Li, K., Li, B., . . . Liu, X. (2021). Viscozyme L hydrolysis and *Lactobacillus* fermentation increase the phenolic compound content and antioxidant properties of aqueous solutions of quinoa pretreated by steaming with α-amylase. *Journal of Food Science*, *86*(5), 1726-1736.

Zhang, L., Pan, Z., Shen, K., Cai, X., Zheng, B., & Miao, S. (2018). Influence of ultrasound-assisted alkali treatment on the structural properties and functionalities of rice protein. *Journal of Cereal*

Science, *79*, 204-209.

Zhang, R., Cheng, L., Luo, L., Hemar, Y., & Yang, Z. (2021). Formation and characterisation of high-internal-phase emulsions stabilised by high-pressure homogenised quinoa protein isolate. *Colloids and Surfaces a-Physicochemical and Engineering Aspects*, *631*, 127688.

Zhang, X., Zuo, Z., Ma, W., Yu, P., Li, T., & Wang, L. (2021). Assemble behavior of ultrasound-induced quinoa protein nanoparticles and their roles on rheological properties and stability of high internal phase emulsions. *Food Hydrocolloids*, *117*, 106748.

Zhao, F., Zhai, X., Liu, X., Lian, M., Liang, G., Cui, J., . . . Wang, W. (2022a). Effects of high-intensity ultrasound pretreatment on structure, properties, and enzymolysis of walnut protein isolate. Molecules, 27(1), 208.

Zhao, J., Zhou, T., Zhang, Y., Ni, Y., & Li, Q. (2015). Optimization of arachin extraction from defatted peanut (Arachis hypogaea) cakes and effects of ultra-high pressure (UHP) treatment on physiochemical properties of arachin. *Food and Bioproducts Processing*, *95*, 38-46.

Zhao, S., Huang, Y., McClements, D. J., Liu, X., Wang, P., & Liu, F. (2022b). Improving pea protein functionality by combining high-pressure homogenization with an ultrasound-assisted Maillard reaction. *Food Hydrocolloids*, *126*, 107441.

Zhao, Y. Y., Cao, F. H., Li, X. J., Mu, D. D., Zhong, X. Y., Jiang, S. T., . . . Luo, S. Z. (2020). Effects of different salts on the gelation behaviour and mechanical properties of citric acid-induced tofu. *International Journal of Food Science & Technology*, *55*(2), 785-794.

Zhao, Z. K., Mu, T. H., Zhang, M., & Richel, A. (2018a). Chemical forces, structure, and gelation properties of sweet potato protein as affected by pH and high hydrostatic pressure. *Food and Bioprocess Technology*, *11*(9), 1719-1732.

Zhao, Z. K., Mu, T. H., Zhang, M., & Richel, A. (2018b). Effect of salts combined with high hydrostatic pressure on structure and gelation properties of sweet potato protein. *LWT*, *93*, 36-44.

Zhao, Z. (2019). Effects of high hydrostatic pressure on structure and gelation properties of sweet potato protein.

Zheng, L., Regenstein, J. M., Zhou, L., & Wang, Z. (2022). Soy protein isolates: A review of their composition, aggregation, and gelation. *Comprehensive Reviews in Food Science and Food Safety*, *21*(2), 1940-1957.

Zheng, Y., Wang, X., Zhuang, Y., Li, Y., Tian, H., Shi, P., & Li, G. (2019). Isolation of novel ACE-inhibitory and antioxidant peptides from quinoa bran albumin assisted with an in silico approach: characterization, in vivo antihypertension, and molecular docking. *Molecules*, *24*(24), 4562.

Zhou, M., Liu, J., Zhou, Y., Huang, X., Liu, F., Pan, S., & Hu, H. (2016). Effect of high intensity ultrasound on physicochemical and functional properties of soybean glycinin at different ionic strengths. *Innovative Food Science & Emerging Technologies*, *34*, 205-213.

Zhou, Y., Ouyang, B., Du, L., Wei, Y., Zhou, X., Xiao, Y., & Wang, Y. (2022). Effects of ultra-high-pressure treatment on the structural and functional properties of buckwheat 13S globulin. *Food Science and Human Wellness*, *11*(4), 895-903.

Zhu, P., Huang, W., Guo, X., & Chen, L. (2021). Strong and elastic pea protein hydrogels formed through pH-shifting method. *Food Hydrocolloids*, *117*, 106705.

Zhu, Z., Zhu, W., Yi, J., Liu, N., Cao, Y., Lu, J., . . . McClements, D. J. (2018). Effects of sonication on the physicochemical and functional properties of walnut protein isolate. *Food Research International*, *106*, 853-861.

Zink, J., Wyrobnik, T., Prinz, T., & Schmid, M. (2016). Physical, chemical and biochemical modifications of protein-based films and coatings: An extensive review. *International Journal of Molecular Sciences*, *17*(9), 1376.

Zuo, Z., Zhang, X., Li, T., Zhou, J., Yang, Y., Bian, X., & Wang, L. (2022). High internal phase emulsions stabilized solely by sonicated quinoa protein isolate at various pH values and concentrations. *Food Chemistry*, *378*, 132011.

8. Appendices

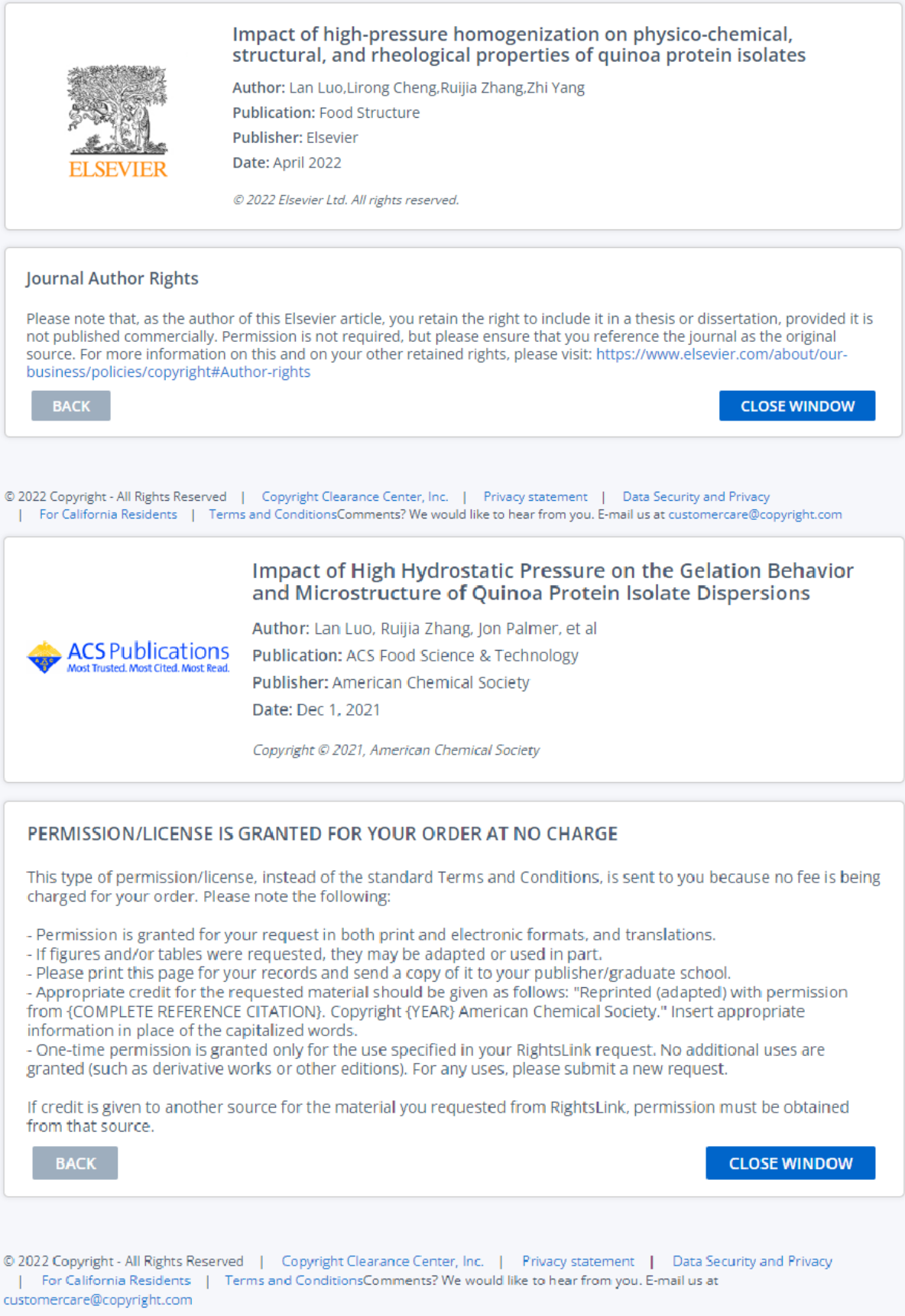

Impact of high-pressure homogenization on physico-chemical, structural, and rheological properties of quinoa protein isolates

Author: Lan Luo,Lirong Cheng,Ruijia Zhang,Zhi Yang
Publication: Food Structure
Publisher: Elsevier
Date: April 2022

© 2022 Elsevier Ltd. All rights reserved.

Journal Author Rights

Please note that, as the author of this Elsevier article, you retain the right to include it in a thesis or dissertation, provided it is not published commercially. Permission is not required, but please ensure that you reference the journal as the original source. For more information on this and on your other retained rights, please visit: https://www.elsevier.com/about/our-business/policies/copyright#Author-rights

BACK CLOSE WINDOW

© 2022 Copyright - All Rights Reserved | Copyright Clearance Center, Inc. | Privacy statement | Data Security and Privacy | For California Residents | Terms and ConditionsComments? We would like to hear from you. E-mail us at customercare@copyright.com

Impact of High Hydrostatic Pressure on the Gelation Behavior and Microstructure of Quinoa Protein Isolate Dispersions

Author: Lan Luo, Ruijia Zhang, Jon Palmer, et al
Publication: ACS Food Science & Technology
Publisher: American Chemical Society
Date: Dec 1, 2021

Copyright © 2021, American Chemical Society

PERMISSION/LICENSE IS GRANTED FOR YOUR ORDER AT NO CHARGE

This type of permission/license, instead of the standard Terms and Conditions, is sent to you because no fee is being charged for your order. Please note the following:

- Permission is granted for your request in both print and electronic formats, and translations.
- If figures and/or tables were requested, they may be adapted or used in part.
- Please print this page for your records and send a copy of it to your publisher/graduate school.
- Appropriate credit for the requested material should be given as follows: "Reprinted (adapted) with permission from {COMPLETE REFERENCE CITATION}. Copyright {YEAR} American Chemical Society." Insert appropriate information in place of the capitalized words.
- One-time permission is granted only for the use specified in your RightsLink request. No additional uses are granted (such as derivative works or other editions). For any uses, please submit a new request.

If credit is given to another source for the material you requested from RightsLink, permission must be obtained from that source.

BACK CLOSE WINDOW

© 2022 Copyright - All Rights Reserved | Copyright Clearance Center, Inc. | Privacy statement | Data Security and Privacy | For California Residents | Terms and ConditionsComments? We would like to hear from you. E-mail us at customercare@copyright.com

Impacts of sonication and high hydrostatic pressure on the structural and physicochemical properties of quinoa protein isolate dispersions at acidic, neutral and alkaline pHs

Author: Lan Luo,Zhi Yang,Haifeng Wang,Muthupandian Ashokkumar,Yacine Hemar

Publication: Ultrasonics Sonochemistry

Publisher: Elsevier

Date: December 2022

Journal Author Rights

BACK CLOSE WINDOW